BULLETIN (New Series) OF THE
AMERICAN MATHEMATICAL SOCIETY
Volume 51, Number 3, July 2014, Pages 373–445
S 0273-0979(2014)01437-5
Article electronically published on April 1, 2014

BICENTENNIAL OF THE GREAT PONCELET THEOREM (1813–2013): CURRENT ADVANCES

VLADIMIR DRAGOVIĆ AND MILENA RADNOVIĆ

Abstract. We present very recent results related to the Poncelet Theorem on the occasion of its bicentennial. We are telling the story of one of the most beautiful theorems of geometry, recalling for general mathematical audiences the dramatic historic circumstances which led to its discovery, a glimpse of its intrinsic appeal, and the importance of its relationship to dynamics of billiards within confocal conics. We focus on the three main issues: A) The case of pseudo-Euclidean spaces, for which we present a recent notion of relativistic quadrics and apply it to the description of periodic trajectories of billiards within quadrics. B) The relationship between so-called billiard algebra and the foundations of modern discrete differential geometry which leads to double-reflection nets. C) We present a new class of dynamical systems—pseudo-integrable billiards generated by a boundary composed of several arcs of confocal conics having nonconvex angles. The dynamics of such billiards have several extraordinary properties, which are related to interval exchange transformations and which generate families of flows that are minimal but not uniquely ergodic. This type of dynamics provides a novel type of Poncelet porisms—the local ones.

Contents

Received by the editors November 1, 2012, and in revised form, March 25, 2013.
2010 *Mathematics Subject Classification.* Primary 37J35, 14H70, 37A05.
Key words and phrases. Poncelet Theorem, periodic billiard trajectories, pencils of quadrics, relativistic quadrics, integrable line congruences, double reflection nets, pseudo-integrable billiards, interval exchange transformations.
The research which led to this paper was partially supported by the Serbian Ministry of Education and Science (Project no. 174020: *Geometry and Topology of Manifolds and Integrable Dynamical Systems*).

1. Introduction and history

On November 18th, 1812, near Smolensk, Russia, a young French officer serving as a battery commander was wounded and his horse was killed under him. This was the last day of the battle of Krasnoi, when the French III Corps of Marshal Ney clashed with three corps commanded by general Count Miloradovich of the Russian Army. Napoleon's army was heavily defeated and many thousands of his men were left during the withdrawal and imprisoned. A day after the battle, the officer was found by Russian soldiers.

During his subsequent imprisonment in Saratov, which lasted from April 1813 until June 1814, while recovering from an illness, he recalled the fundamental principles of geometry to which he had been introduced during his studies at the École Polytechnique. Without literature, he not only recollected what he had learned from his professors Monge, Carnot, and Brianchon, but also went on to develop projective geometry, in particular the properties of conics. The young officer's name was Jean-Victor Poncelet. The notes he made in the prison, called *Cahiers de Saratov*[1] contained one of deepest, most beautiful, and most important theorems of projective geometry—the Great Poncelet Theorem; see [1869].

The first published proof of the Great Poncelet Theorem appeared in Poncelet's famous work, *Traité des propriétés projectives des figures*, in 1822 [Pon1822]. The complete *Cahiers de Saratov* were published many decades later, in 1862, as [Pon1862]. Meanwhile, Poncelet became a professor of Mechanics at the Sorbonne and at the Collège de France, the general of a brigade, the governor of the École Polytechnique, the commander of the National Guard of the Department of the Seine, an elected member of the Constitutional Assembly, and the President of the Scientific Commission for the English exhibition of 1851. Poncelet was also a Grand Officer of the Legion of Honour, a Chevalier of the Prussian order, a corresponding member of the academies of Sankt Petersburg, Turin, Berlin, and a foreign member of the Royal Society of London.

It is interesting to mention that, in Chebyshev's report on his business trip to France [Tch1852], Poncelet is described "as a well-known scientist in practical mechanics".

[1]Saratov notebooks

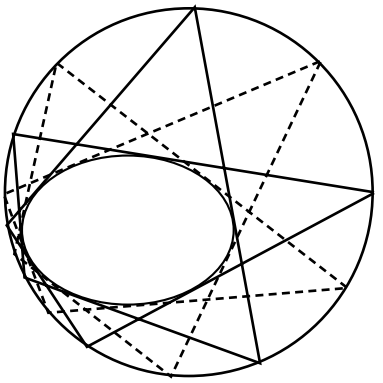

FIGURE 1. Two heptagons inscribed in a conic and circumscribed about another one

Let us present now one of the formulations of the Poncelet Theorem, with an example shown on Figure 1.

Theorem 1.1 (The Poncelet Theorem)**.** *Let $\mathcal{C}$ and $\mathcal{D}$ be two conics in the plane. Suppose that there is a polygon inscribed in $\mathcal{C}$ and circumscribed about $\mathcal{D}$. Then there are infinitely many such polygons, and all of them have the same number of sides. Moreover, each point of $\mathcal{C}$ is a vertex of such a polygonal line.*

Later on, in 1828, Jacobi gave another proof of the theorem using the addition theorem for elliptic functions (see [Jac1884]). Essentially, the Poncelet Theorem is equivalent to the addition theorems for the elliptic curves and the Poncelet proof represents a synthetic way of deriving group structure on an elliptic curve.

An important question is how do we find an analytical condition that determines, for two given conics, if an n-polygon, inscribed in one conic and circumscribed about the second, exists. In 1853 such a condition was derived by Cayley, who used the theory of Abelian integrals [Cay1854]. He was dealing with the Poncelet porism in a number of other papers [Cay1853, Cay1855, Cay1857, Cay1858, Cay1861]. Cayley's work served as an inspiration for another great mathematician, Lebesgue, who translated Cayley's proof into geometric language. He derived his proof of Cayley's condition using methods of projective geometry and algebra; see the remarkable book *Les coniques* [Leb1942]. In modern settings, Griffiths and Harris derived Cayley's theorem by finding an analytical condition for points of finite order on an elliptic curve [GH1978].

We have to emphasize that Poncelet originally proved a statement that is much more general than the theorem formulated above (see [Ber1987a, Ber1987b, Pon1822]); he derived the latter as a corollary. Namely, he considered $n+1$ conics of a pencil in the projective plane. If there exists an n-polygon with vertices lying on the first of these conics and each side touching one of the other n conics, then infinitely many such polygons exist. We shall refer to this statement as *the Full Poncelet Theorem* and call such polygons *the Poncelet polygons*.

A nice historical overview of the Poncelet Theorem, together with modern proofs and remarks is given in [BKOR1987]. Various classical theorems of Poncelet type with short modern proofs are reviewed in [BB1996], while the algebro-geometrical

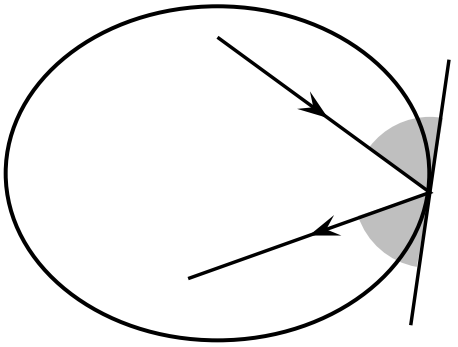

FIGURE 2. Billiard reflection

approach to families of the Poncelet polygons via modular curves is given in [BM1993, Jak1993]. There are also two recent books on the subject [Fla2009, DR2011].

The Poncelet Theorem has an important mechanical interpretation. *The elliptical billiard* [KT1991, Koz2003, Tab2005] is a dynamical system where a material point of the unit mass is moving under inertia, or in other words, with a constant velocity inside an ellipse and obeying the reflection law at the boundary, i.e. having congruent impact and reflection angles with a tangent line to the ellipse at any bouncing point (see Figure 2). It is also assumed that the reflection is absolutely elastic and that friction is neglected.

It is well known that any segment of a given elliptical billiard trajectory is tangent to the same conic, confocal with the boundary [CCS1993] (see Figure 3). If a trajectory becomes closed after n reflections, then the Poncelet Theorem implies that any trajectory of the billiard system, which shares the same caustic curve, is also periodic with period n.

Moreover, for any given pair of conics, there is a projective transformation of coordinates, such that the conics become confocal in the new coordinates. Then, polygonal lines inscribed in one of the conics and circumscribed about the other conic will become billiard trajectories.

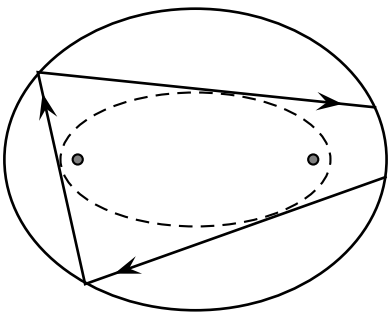

FIGURE 3. Caustic of the billiard trajectory

The Full Poncelet Theorem also has a mechanical meaning. The configuration dual to a pencil of conics in the plane is a family of confocal second order curves [Arn1978]. Let us consider the following, slightly unusual billiard. Suppose n confocal conics are given. A particle is bouncing on each of these n conics respectively. All segments of such a trajectory are tangent to one conic confocal with the given n curves. If the motion becomes closed after n reflections, then, by the Full Poncelet Theorem, any such trajectory with the same caustic is also closed.

The statement dual to the Full Poncelet Theorem can be generalized to the d-dimensional space [CCS1993] (see also [Pre1999, Pre2002]). Suppose vertices of the polygon $x_1x_2\cdots x_n$ are placed on confocal quadric hypersurfaces $\mathcal{Q}_1$, $\mathcal{Q}_2$, …, $\mathcal{Q}_n$, respectively, in the d-dimensional Euclidean space, with the consecutive sides obeying the reflection law at the corresponding hypersurface. Then all sides are tangent to some quadrics $\mathcal{Q}^1$, …, $\mathcal{Q}^{d-1}$ confocal with $\{\mathcal{Q}_i\}$; for the hypersurfaces $\{\mathcal{Q}_i, \mathcal{Q}^j\}$, an infinite family of polygons with the same properties exist. Systematic exposition of this higher-dimensional theory has been presented in a survey paper [DR2010] and in the book [DR2011].

But more than a century before these quite recent results, in 1870, Darboux proved the generalization of the Poncelet Theorem for a billiard within an ellipsoid in three-dimensional space [Dar1870]. It seems that his work on this topic was completely forgotten until very recently; see [DR2011].

An interesting generalization of the Poncelet Theorem concerning polyhedra that are simultaneously inscribed and circumscribed about two given quadrics in the three-dimensional space was obtained in [GH1977]. Further generalizations in that direction can be found in [DR2008, DR2011].

It is natural to search for Cayley-type conditions related to generalizations of the Poncelet Theorem. Such conditions for the billiard system inside an ellipsoid in Euclidean space of arbitrary finite dimension were derived in [DR1998a, DR1998b] using an algebro-geometric approach from [Ves1988, MV1991], where billiards within quadrics are also considered as discrete time systems. In recent papers [DR2004, DR2005, DR2006b, DR2006a], algebro-geometric conditions for existence of periodic billiard trajectories within k quadrics in the d-dimensional Euclidean space were derived.

Most of the results on the subject obtained by 2008 have been presented in the book [DR2011]. An important part of the book has been devoted to the Griffiths-Harris program of development of a synthetic approach to higher genera addition theorems. The book also offered an historical overview of the subject, and it included a detailed analysis of the results of Darboux and the contributions of Lebesgue.

About the same time, an extremely interesting book [Dui2010] appeared, which was devoted to discrete integrable systems from the point of view of the QRT maps,[2] elliptic surfaces, and elliptic fibrations. That book approaches the Poncelet Theorem as an important example of symmetric QRT maps; see [Dui2010, Chapter 10]. Connections to elliptic billiards are presented in [Dui2010, Chapter 11.2].

The present paper is devoted to the bicentennial jubilee of the celebrated Poncelet Theorem and it mostly exposes current advances of the subject—results which

[2]The QRT maps are named after Quispel, Roberts, and Thompson [QRT1988].

have been obtained in the last four years. The interrelation between geometry of pencils of quadrics and related billiard dynamics is continuing to play a crucial role.

The projective geometry nucleus of billiard dynamics is the double reflection theorem; see Theorem 2.11 below. The meaning of that theorem is that reflections off two confocal quadrics commute. Namely, there are four lines that belong to a certain linear space and which form a *double reflection configuration*: these four lines reflect to each other according to the billiard law at two confocal quadrics; see Figure 13 in Section 2.3.

The double reflection configuration is a cornerstone of a new type of integrable line congruence, so-called *double reflection nets*. In these discrete integrable systems of geometric origin, double reflection configurations play the role of quad-equations. The integrability condition is a consequence of an operational consistency of billiard algebra from [DR2008]; see *the six-pointed star theorem*, Theorem 4.1. These results are presented in Section 4.

Section 3 is devoted to pencils of quadrics in pseudo-Euclidean spaces and to related billiard dynamics and Poncelet configurations. A novelty of our approach is based on the notion of *relativistic quadrics*; see [DR2012a]. The general theory of relativistic quadrics is exposed in Section 3.2. Section 3.1 is devoted to the case of the Minkowski plane, and it serves as an introduction to the higher-dimensional cases. It also contains a detailed and quite elementary description of periodic trajectories of elliptic billiards. Generalized Cayley-type conditions for pseudo-Euclidean spaces of arbitrary dimension are derived in Section 3.3.

The last section is devoted to the billiards in the Euclidean plane with a more complex boundary, formed by arcs of conics from a confocal family; see [DR2012c].

For the case of billiard systems within confocal conics without nonconvex angles on the boundary, it is well known that the famous Poncelet porism holds:

(A) If there is a periodic billiard trajectory with one initial point of the boundary, then there are infinitely many such periodic trajectories with the same period, sharing the same caustic.
(B) Even more is true—if there is one periodic trajectory, then all trajectories sharing the same caustic are periodic with the same period.

See [DR2006a, DR2006b, DR2011] where the corresponding conditions of Cayley type were derived.

However, when nonconvex angles exist on the boundary, which is the case studied in Section 5, one sees that item (A) above is still generally true. However, item (B) is not true any more. *The Poncelet porism is true locally, but not globally.* Algebro-geometric conditions of Cayley's type in such a case provide only sufficient but not necessary conditions for periodicity. A deeper analysis of the dynamics in this case is related to a class of interval exchange transformations and to the use of a modified Keane condition.

Let us note that via the interval exchange transformations, the billiard flow in a domain bounded by arcs of confocal conics becomes equivalent to a flow on a certain translation surface. In this way, we made an analogy to the situation with billiards in polygons with rational angles, which has been one of most vivid research topics for a few decades; see [Zor2006, Via2008, MT2002, Smi] for some insight.

Section 5.5 is concluded by an explicit example of the billiard system that satisfies the Cayley type condition, but it is still not periodic since it satisfies the Keane condition as well. In Section 5.6, we show that there are infinitely many billiard tables bounded by arcs of confocal conics such that the corresponding flow will not be uniquely ergodic. In particular, Theorem 5.16 shows that the interval exchange transformation corresponding to certain tables is equivalent to the Veech example of minimal and not uniquely ergodic systems; see [Vee1969, MT2002].

2. Billiards and quadrics

As a starting point, we collect some basic notions and facts, which are going to be used in the sequel. A reader interested in a more detailed presentation of basic and not so basic geometrical notions may find the following useful: [Ber1987a, Sam1988, Har1967, DR2011, Ber1987b].

2.1. **Elliptical billiards and confocal conics in the Euclidean plane.** Billiard systems within confocal conics represent a natural mechanical setting for the Poncelet porism.

A general family of confocal conics in the plane can be represented as

$$\mathcal{C}_\lambda \ : \ \frac{x^2}{a-\lambda}+\frac{y^2}{b-\lambda}=1, \quad \lambda \in \mathbf{R}, \tag{2.1}$$

with $a > b > 0$ being constants; see Figure 4.

By the famous *Chasles theorem* [Cha1827], each segment of a given billiard trajectory is tangent to a fixed conic that is confocal to the boundary (see also [KT1991, DR2011]). This conic is called *the caustic* of the given trajectory; see Figure 3.

Now, fix a constant $\alpha_0 < b$. By the Full Poncelet Theorem, if there is a billiard trajectory with the caustic $\mathcal{C}_{\alpha_0}$ which becomes closed after successive reflections on ellipses $\mathcal{C}_{\lambda_1}, \ldots, \mathcal{C}_{\lambda_n}$, then each point of $\mathcal{C}_{\lambda_1}$ is a vertex of such a closed trajectory.

The following generalization was proved by Darboux in [Dar1914, Volume 3, Book VI, Chapter I].

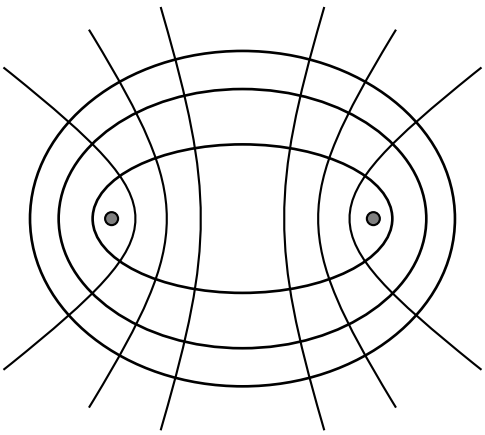

Figure 4. Family of confocal conics in the Euclidean plane

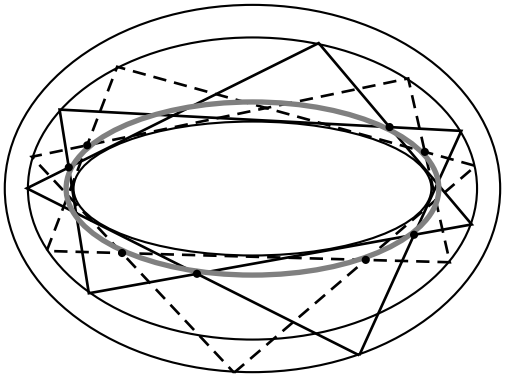

FIGURE 5. Poncelet heptagons and the Darboux grid

Theorem 2.1 (Darboux theorem on grids)**.** *Suppose that billiard trajectories with the caustic $\mathcal{C}_{\alpha_0}$ become closed after successive reflections on ellipses $\mathcal{C}_{\lambda_1}, \ldots, \mathcal{C}_{\lambda_n}$. Then, the intersection points of i-th and j-th sides of all such trajectories belong to an ellipse $\mathcal{C}_{\lambda^{ij}}$.*

Example 2.2. Consider the case when $n = 7$ and $\lambda_1 = \cdots = \lambda_6 \neq \lambda_7$. By the Darboux theorem of grids the intersection points of the first and the fourth side, the second and the fifth, the third and the sixth, as well as the third and the seventh side of each corresponding heptagon will belong to the same ellipse. In Figure 5 two such heptagons are shown, and the ellipse containing the above-mentioned intersection points is gray.

Let us note that the Darboux theorem on grids from [Dar1914] was even more general, since it related to geodesic polygons on Liouville surfaces. For discussion and the generalization of the Darboux theorem to pairs of nonclosed billiard trajectories and to the arbitrary dimension, see [DR2006b, DR2008, DR2011]. The Darboux theorem on grids has also recently been a subject of interest in [Sch2007, LT2007].

2.1.1. *The measure on a caustic of the elliptic billiard.*

Proposition 2.3. *There exist a measure μ on the conic $\mathcal{C}_{\alpha_0}$ and a function*

$$\rho : (-\infty, \alpha_0) \to \mathbf{R}$$

satisfying the following:

- *the measure μ is nonatomic, i.e., $\mu(\{X\}) = 0$ for each point X on $\mathcal{C}_{\alpha_0}$;*
- *$\mu(\ell) \neq 0$ for each open arc ℓ of $\mathcal{C}_{\alpha_0}$;*
- *for any $\lambda < \alpha_0$, and each triplet of points $X \in \mathcal{C}_\lambda$, $A \in \mathcal{C}_{\alpha_0}$, $B \in \mathcal{C}_{\alpha_0}$ such that XA, XB are tangent to $\mathcal{C}_{\alpha_0}$, the following equality holds*

$$\mu(AB) = \rho(\lambda);$$

- $\mu(\mathcal{C}_{\alpha_0}) = 1$.

Notice that the third property means that the length with respect to the measure μ of all arcs whose endpoints are on two tangents issued from a point on $\mathcal{C}_\lambda$ have the same length with respect to the measure μ; see Figure 6.

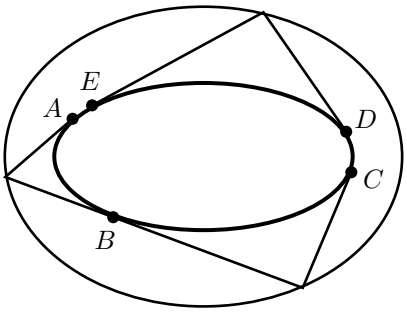

FIGURE 6. $\mu(AB) = \mu(BC) = \mu(DE)$

Proof. The space of oriented lines in the plane has a canonical area form $d\varphi \wedge dp$, where the angle φ is the direction of the line, and p is the oriented distance from the origin [Tab2005]; see also [Arn1978]. This is the only area form which is preserved by the motions of the plane. This space is in our case foliated to families of lines tangent to confocal ellipses. The area form induces a measure on each of the leaves. Since the billiard map preserves the area form and the foliation, it will preserve the measure on the corresponding caustic as well. For another construction of such a measure, see [Kin1994].

Take λ_0 such that there is a closed billiard trajectory in $\mathcal{C}_{\lambda_0}$ with the caustic $\mathcal{C}_{\alpha_0}$. There is a measure μ satisfying the first three requested properties for $\lambda = \lambda_0$; moreover, such a measure is unique up to the multiplication by constant. Thus, there is unique measure satisfying the last property as well.

Suppose the closed trajectory has n vertices. Then by Theorem 2.1 there is λ_1 such that the billiard trajectories within $\mathcal{C}_{\lambda_1}$ with the caustic $\mathcal{C}_{\alpha_0}$ become closed after $2n$ reflections and $\mathcal{C}_{\lambda_0}$ contains intersections of i-th and $(i+2)$-nd sides of those trajectories. Moreover, the measure μ will satisfy the requested properties for $\mathcal{C}_{\lambda_1}$.

By induction, we get the sequence $\mathcal{C}_{\lambda_k}$ of ellipses, such that billiard trajectories within $\mathcal{C}_{\lambda_k}$ with caustic $\mathcal{C}_{\alpha_0}$ are $2^k n$-periodic and μ satisfies the listed properties for these ellipses as well. Because of the Darboux theorem, the measure will satisfy the properties for each $\mathcal{C}_\lambda$ that has closed billiard trajectories whose period is multiples of n and the caustic $\mathcal{C}_{\alpha_0}$.

For a periodic trajectory which becomes closed after n bounces on $\mathcal{C}_\lambda$ and m windings about $\mathcal{C}_{\lambda_0}$, $\rho(\lambda) = \frac{m}{n}$. Since rational numbers are dense in the reals, μ will have the required properties for all $\lambda < \alpha_0$. □

Remark 2.4. The function ρ from Proposition 2.3 is called *the rotation function* and its values *the rotation numbers*. Note that ρ is a continuously strictly decreasing function with $\left(0, \frac{1}{2}\right)$ as the image,

$$\lim_{\lambda \to -\infty} \rho(\lambda) = \frac{1}{2}, \quad \lim_{\lambda \to \alpha_0} \rho(\lambda) = 0.$$

2.1.2. *Elliptical billiard as a Hamiltonian system.* The standard Poisson bracket for the billiard system is defined as

$$\{f,g\} = \frac{\partial f}{\partial x}\frac{\partial g}{\partial \dot{x}} - \frac{\partial f}{\partial \dot{x}}\frac{\partial g}{\partial x} + \frac{\partial f}{\partial y}\frac{\partial g}{\partial \dot{y}} - \frac{\partial f}{\partial \dot{y}}\frac{\partial g}{\partial y}.$$

Define the following functions:

$$K_\lambda(x,y,\dot{x},\dot{y}) = \frac{\dot{x}^2}{a-\lambda} + \frac{\dot{y}^2}{b-\lambda} - \frac{(\dot{x}y - \dot{y}x)^2}{(a-\lambda)(b-\lambda)}.$$

These functions represent well known first integrals of billiard systems; see [KT1991].

Proposition 2.5. *Each two functions K_λ commute,*

$$\{K_{\lambda_1}, K_{\lambda_2}\} = 0,$$

and for $\lambda_1 \neq \lambda_2$, they are functionally independent.

It is straightforward to prove the following

Proposition 2.6. *Along a billiard trajectory within any conic $\mathcal{C}_{\lambda_0}$, with the caustic $\mathcal{C}_{\alpha_0}$ and the speed of the billiard particle being equal to s, the value of each function K_λ is constant and equal to*

$$K_\lambda = \frac{\alpha_0 - \lambda}{(a-\lambda)(b-\lambda)} \cdot s^2.$$

Corollary 2.7. *Each K_λ is an integral for the billiard motion in any domain with the border composed of a few arcs of confocal conics.*

Let us recall that a Hamiltonian system on a $2n$-dimensional symplectic manifold is completely integrable if it possesses n functionally independent first integrals such that the Poisson bracket of any two of them is zero. It is well known that the Liouville–Arnold theorem (see [Arn1978]) describes regular compact leaves of a completely integrable Hamiltonian system, which are common level sets of the first integrals, as tori, with the dynamics being quasi-periodic and uniform on these invariant tori.

Although having one-sided constraints, the billiards can be seen as Hamiltonian systems. Previous considerations show that the billiard system within an ellipse can be considered as a completely integrable system, since it has $n = 2$ functionally independent and commuting first integrals. The symplectic manifold is the four-dimensional cotangent bundle of the plane. This system can be reduced to the two-dimensional symplectic manifold of lines in the plane, with the standard area form in the role of the symplectic form. The measure from Proposition 2.3 can be related to the flat structure on a one-dimensional invariant torus, represented by the caustic conic.

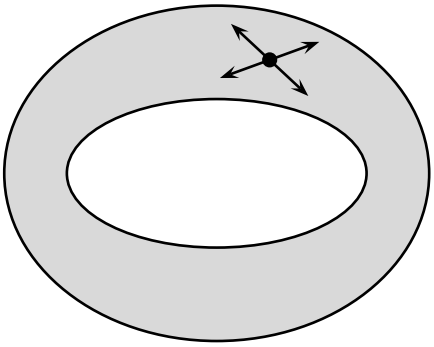

FIGURE 7. Four possible directions of motion from a given point with the fixed caustic

The invariant tori can also be viewed geometrically: the domain between the billiard border and the caustic, which is filled with corresponding trajectories, is the projection of such tori. With the fixed caustic, each point within the domain is the projection of four points from the corresponding level set of the phase space; see Figure 7.

When the caustic is an ellipse, then the ring where the trajectories are placed is the projection of two Liouville tori—each one corresponding to one direction of winding around the caustic; see Figure 8. If the caustic is a hyperbola, then the curvilinear quadrangle bounded by the branches of the hyperbola and the ellipse is the projection of a single torus; see Figure 9.

In Section 5 we will introduce a more general class of systems, *the pseudo-integrable systems*, and formulate a generalization of the Liouville–Arnold theorem, see Theorem 5.5.

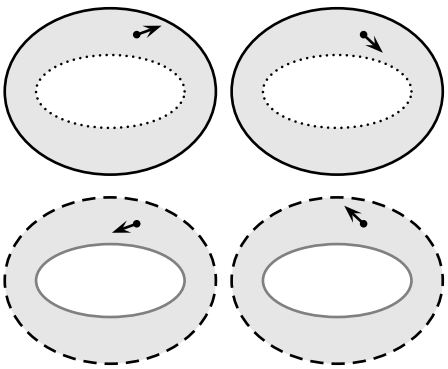

FIGURE 8. Gluing of rings along their borders that gives two tori in the phase space

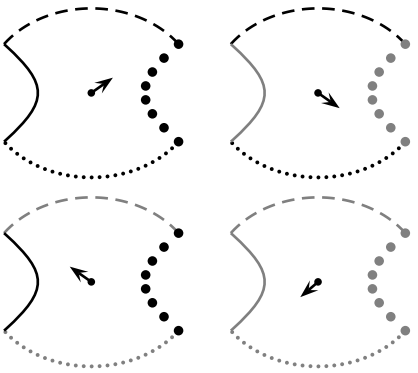

FIGURE 9. Gluing of curvilinear quadrangles rings along their borders that gives a torus in the phase space

2.2. **Confocal quadrics in the Euclidean space and billiards.** A general family of confocal quadrics in the d-dimensional Euclidean space is given by

$$\frac{x_1^2}{b_1-\lambda}+\cdots+\frac{x_d^2}{b_d-\lambda}=1, \quad \lambda\in\mathbf{R}, \tag{2.2}$$

with $b_1>b_2>\cdots>b_d>0$; see Figure 10.

Such a family has the following properties.

E1 Each point of the space $\mathbf{E}^d$ is the intersection of exactly d quadrics from (2.2); moreover, all these quadrics are of different geometrical types.

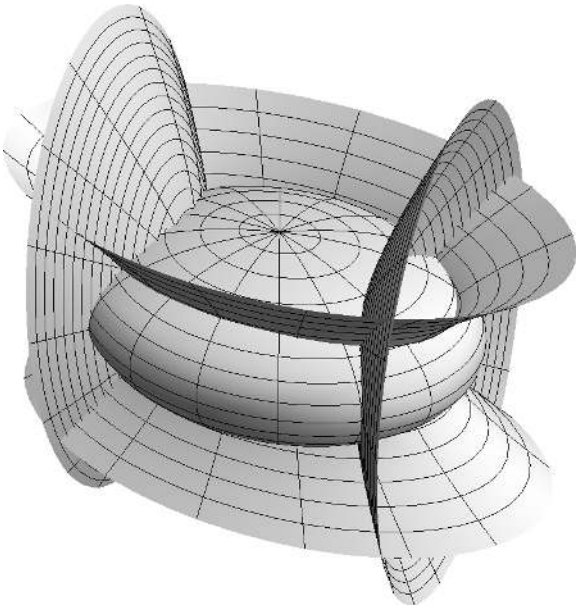

FIGURE 10. Confocal quadrics in three-dimensional Euclidean space

E2 The family (2.2) contains exactly d geometrical types of nondegenerate quadrics. Each type corresponds to one of the disjoint intervals of the parameter λ: $(-\infty, b_d)$, (b_d, b_{d-1}), $\ldots$, (b_2, b_1).

The parameters $(\lambda_1, \ldots, \lambda_d)$ corresponding to the quadrics of (2.2) that contain a given point in $\mathbf{E}^d$ are called *Jacobi coordinates*. We order them $\lambda_1 > \cdots > \lambda_d$.

Now, let us consider the motion of a billiard ball within the ellipsoid $\mathcal{E}$. Without losing generality, take the parameter corresponding to this ellipsoid to be $\lambda = 0$. Recall that, by the Chasles theorem, each line in $\mathbf{E}^d$ is touching some $d-1$ quadrics from (2.2). Moreover, for a line and its billiard reflection on a quadric from (2.2), the $d-1$ quadrics are the same. This means that each segment of a given trajectory within $\mathcal{E}$ has the same $d-1$ *caustics*. Denote their parameters by $\beta_1, \ldots, \beta_{d-1}$, and introduce

$$\{\bar{b}_1, \ldots, \bar{b}_{2d}\} = \{b_1, \ldots, b_d, 0, \beta_1, \ldots, \beta_{d-1}\},$$

such that $\bar{b}_1 \geq \bar{b}_2 \geq \cdots \geq \bar{b}_{2d}$. In this way, we will have $0 = \bar{b}_{2d} < \bar{b}_{2d-1}$, $b_1 = \bar{b}_1 > \bar{b}_2$. Moreover, it is always $\beta_i \in \{\bar{b}_{2i}, \bar{b}_{2i+1}\}$, for each $i \in \{1, \ldots, d\}$; see [Aud1994].

Now, we can summarize the main properties of the flow of the Jacobi coordinates along the billiard trajectories.

E3 Along a fixed billiard trajectory, the Jacobi coordinate λ_i $(1 \leq i \leq d)$ takes values in the segment $[\bar{b}_{2i-1}, \bar{b}_{2i}]$.

E4 Along a trajectory, each λ_i achieves local minima and maxima exactly at the touching points with the corresponding caustics, the intersection points with the corresponding coordinate hyper-planes, and, for $i = d$, at the reflection points.

E5 The values of λ_i at those points are $\bar{b}_{2i-1}$, $\bar{b}_{2i}$; between the critical points, λ_i is changed monotonously.

These properties represent the key to the algebro-geometrical analysis of the billiard flow.

2.3. **Double reflection configurations.** The billiards within pencils of quadrics induce fruitful dynamical systems in arbitrary dimension. They are meaningful in spaces with non-Euclidean metric as well and even in spaces without any metric at all.

In this section, we review a fundamental projective geometry configuration of the double reflection in the d-dimensional projective space $\mathbf{P}^d$ over an arbitrary field of characteristic not equal to 2. A detailed discussion on this matter can be found in [DR2008, DR2011] (see also [CCS1993]).

The section concludes with Proposition 2.16, where we show that the double reflection configuration can take the role of the quad-equation; that is, every line in such a configuration is determined by the remaining three. This simple observation is going to play a key role in Section 4, in particular in Section 4.2.

Let us start with recalling the notions of quadrics and confocal families in the projective space.

A quadric in $\mathbf{P}^d$ is the set given by an equation of the form

$$(Q\xi, \xi) = 0,$$

where Q is a symmetric $(d+1)\times(d+1)$ matrix, and $\xi = [\xi_0 : \xi_1 : \cdots : \xi_d]$ are homogeneous coordinates of a point in space.

Assume two quadrics are given:

$$\mathcal{Q}_1 \ : \ (Q_1\xi,\xi) = 0, \qquad \mathcal{Q}_2 \ : \ (Q_2\xi,\xi) = 0.$$

A pencil of quadrics is the family of quadrics given by equations

$$((Q_1 + \lambda Q_2)\xi,\xi) = 0, \quad \lambda \in \mathbf{P}^1.$$

A confocal system of quadrics is a family of quadrics such that its projective dual is a pencil of quadrics. For a detailed account on geometry of quadrics and their pencils, we refer the reader to [DR2011, Ber1987b].

Now, let us recall the definition of reflection off a quadric in the projective space, where metric is not defined. This definition, together with its crucial properties (the One reflection theorem and the Double reflection theorem) can be found in [CCS1993].

Denote by u the tangent plane to $\mathcal{Q}_1$ at the point x and by z the pole of u with respect to $\mathcal{Q}_2$. Suppose lines ℓ_1 and ℓ_2 intersect at x, and the plane containing these two lines meets u along ℓ; see Figure 11.

Definition 2.8. If the lines ℓ_1, ℓ_2, xz, ℓ are coplanar and harmonically conjugated, we say that ℓ_1 *is reflected to* ℓ_2 off the quadric $\mathcal{Q}_1$.

It can be proved that this definition does not depend on the choice of the quadric $\mathcal{Q}_2$ from a given confocal system [CCS1993].

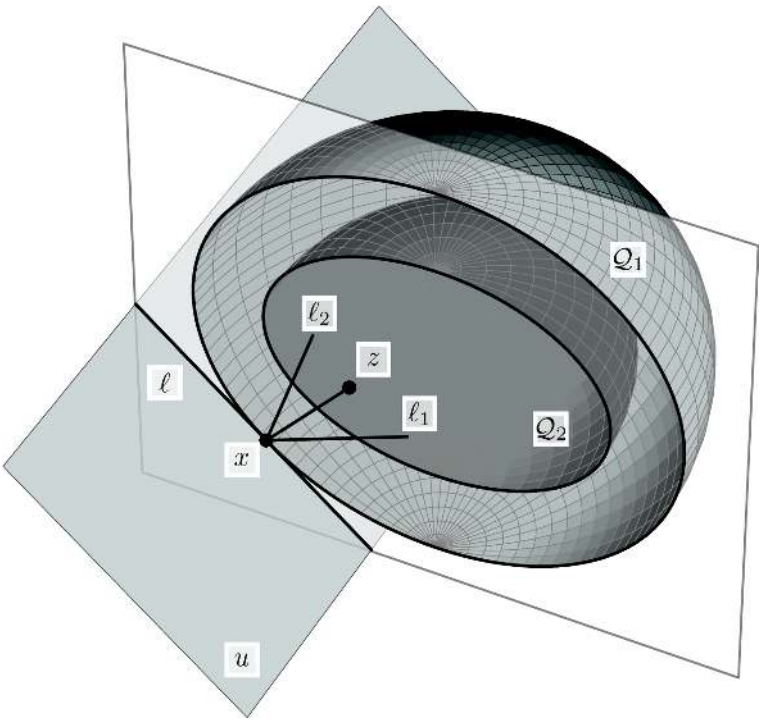

FIGURE 11. The reflection in the projective space

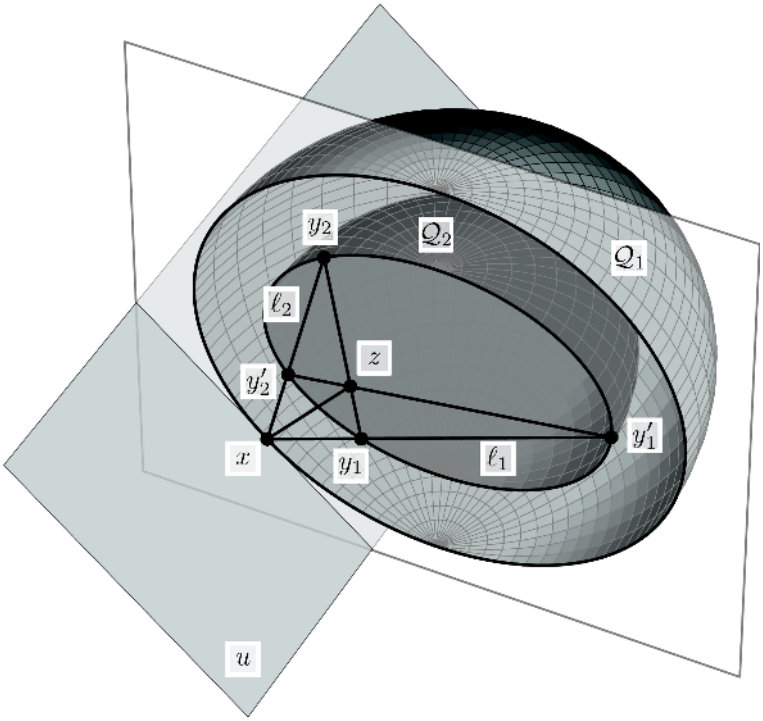

FIGURE 12. One reflection theorem

If we introduce a coordinate system in which the quadrics $\mathcal{Q}_1$ and $\mathcal{Q}_2$ are confocal in the usual sense, the reflection introduced by Definition 2.8 is the same as the standard metric one.

Theorem 2.9 (One reflection theorem)**.** *Suppose a line ℓ_1 is reflected to ℓ_2 off $\mathcal{Q}_1$ at a point x, with respect to the confocal system determined by the quadrics $\mathcal{Q}_1$ and $\mathcal{Q}_2$. Let ℓ_1 intersect $\mathcal{Q}_2$ at y_1' and y_1, let u be the tangent plane to $\mathcal{Q}_1$ at x, and let z be the pole of u with respect to $\mathcal{Q}_2$. Then the lines $y_1'z$ and y_1z contain the intersecting points y_2' and y_2, respectively, of the line ℓ_2 with $\mathcal{Q}_2$. The converse is also true; see Figure* 12.

Theorem 2.9 enables us to prove that the caustics are preserved by the reflection:

Corollary 2.10. *Let lines ℓ_1 and ℓ_2 reflect to each other off $\mathcal{Q}_1$ with respect to the confocal system determined by the quadrics $\mathcal{Q}_1$ and $\mathcal{Q}_2$. Then ℓ_1 is tangent to $\mathcal{Q}_2$ if and only if ℓ_2 is tangent to $\mathcal{Q}_2$; ℓ_1 intersects $\mathcal{Q}_2$ at two points if and only if ℓ_2 intersects $\mathcal{Q}_2$ at two points.*

The next theorem is crucial for our further considerations; its meaning is that billiard reflections off confocal quadrics commute.

Theorem 2.11 (Double reflection theorem)**.** *Suppose that $\mathcal{Q}_1$, $\mathcal{Q}_2$ are given quadrics and $x_1 \in \mathcal{Q}_1$, $y_1 \in \mathcal{Q}_2$. Let u_1 be the tangent plane of $\mathcal{Q}_1$ at x_1; z_1 the pole of u_1 with respect to $\mathcal{Q}_2$; v_1 the tangent plane of $\mathcal{Q}_2$ at y_1; and w_1 the pole of v_1 with respect to $\mathcal{Q}_1$. Denote by x_2 the intersecting point of line w_1x_1 with $\mathcal{Q}_1$, $x_2 \neq x_1$; by*

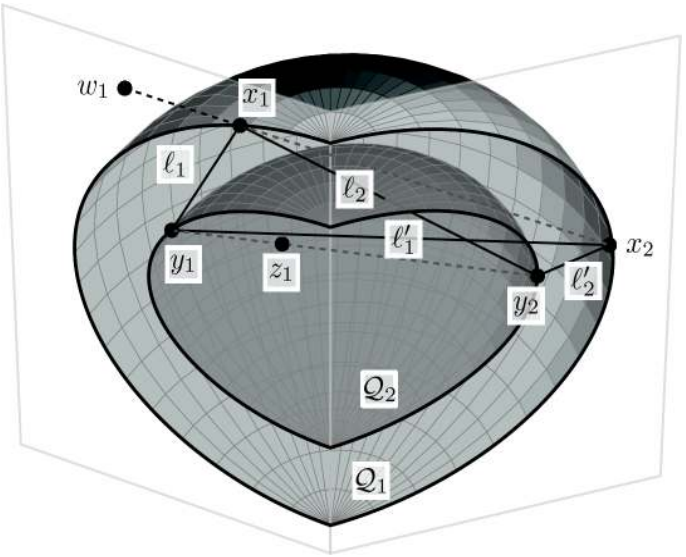

FIGURE 13. Double reflection theorem

y_2 the intersection of y_1z_1 with $\mathcal{Q}_2$, $y_2 \neq y_1$; and $\ell_1 = x_1y_1$, $\ell_2 = x_1y_2$, $\ell_1' = y_1x_2$, $\ell_2' = x_2y_2$.

Then the pair ℓ_1, ℓ_2 obeys the reflection law off $\mathcal{Q}_1$ at x_1; ℓ_1, ℓ_1' obeys the reflection law off $\mathcal{Q}_2$ at y_1; ℓ_2, ℓ_2' obeys the reflection law off $\mathcal{Q}_2$ at y_2; and ℓ_1', ℓ_2' obeys the reflection law off $\mathcal{Q}_1$ at point x_2; see Figure 13.

Let us remark that in Theorem 2.11 the four tangent planes at the reflection points belong to a pencil; see Figure 14.

Corollary 2.12. *If the line ℓ_1 is tangent to a quadric $\mathcal{Q}'$ confocal with $\mathcal{Q}_1$ and $\mathcal{Q}_2$, then ℓ_2, ℓ_1', ℓ_2' also touch $\mathcal{Q}'$.*

The following definition of virtual reflection configuration and double reflection configuration is from [DR2008], where these configurations played the central role. In Theorem 2.14, which is also proved in [DR2008], some important properties of these configurations are given.

Let points x_1, x_2 belong to $\mathcal{Q}_1$ and y_1, y_2 to $\mathcal{Q}_2$.

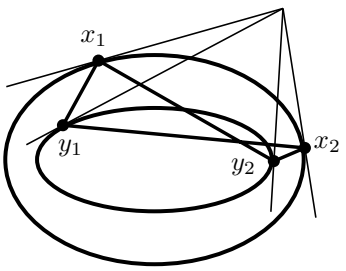

FIGURE 14. Double reflection configuration

Definition 2.13. We will say that the quadruple of points x_1, x_2, y_1, y_2 constitutes *a virtual reflection configuration* if the pairs of lines x_1y_1, x_1y_2; x_2y_1, x_2y_2; x_1y_1, x_2y_1; x_1y_2, x_2y_2 satisfy the reflection law at the points x_1, x_2 off $\mathcal{Q}_1$ and y_1, y_2 off $\mathcal{Q}_2$, respectively, with respect to the confocal system determined by $\mathcal{Q}_1$ and $\mathcal{Q}_2$.

If, additionally, the tangent planes to $\mathcal{Q}_1, \mathcal{Q}_2$ at x_1, x_2; y_1, y_2 belong to a pencil, we say that these points constitute *a double reflection configuration* (see Figure 14).

Now we list some of the basic facts about the double reflection configurations.

Theorem 2.14. *Let $\mathcal{Q}_1$, $\mathcal{Q}_2$ be two quadrics in the projective space $\mathbf{P}^d$, x_1, x_2 points on $\mathcal{Q}_1$ and y_1, y_2 on $\mathcal{Q}_2$. If the tangent hyperplanes at these points to the quadrics belong to a pencil, then x_1, x_2, y_1, y_2 constitute a virtual reflection configuration.*

Furthermore, suppose that the projective space is defined over the field of reals. Introduce a coordinate system, such that $\mathcal{Q}_1$, $\mathcal{Q}_2$ become confocal ellipsoids in the Euclidean space. If $\mathcal{Q}_2$ is placed inside $\mathcal{Q}_1$, then the sides of the quadrilateral $x_1y_1x_2y_2$ obey the real reflection from $\mathcal{Q}_1$ and the virtual reflection from $\mathcal{Q}_2$.

The statement converse to Theorem 2.14 is the following:

Proposition 2.15. *In the Euclidean space $\mathbf{E}^d$, two confocal ellipsoids $\mathcal{E}_1$ and $\mathcal{E}_2$ are given. Let points X_1, X_2 belong to $\mathcal{E}_1$, Y_1, Y_2 to $\mathcal{E}_2$, and let α_1, α_2, β_1, β_2 be the corresponding tangent planes. If a quadruple X_1, X_2, Y_1, Y_2 is a virtual reflection configuration, then planes α_1, α_2, β_1, β_2 belong to a pencil.*

The next proposition shows that three lines of a double reflection configuration uniquely determine the fourth one.

Proposition 2.16. *Let ℓ, ℓ_1, ℓ_2 be lines, and let $\mathcal{Q}_1$, $\mathcal{Q}_2$ be quadrics in the projective space. Suppose that ℓ, ℓ_1 reflect to each other off $\mathcal{Q}_1$, and ℓ, ℓ_2 off $\mathcal{Q}_2$, with respect to the confocal system determined by these two quadrics. Then there is a unique line ℓ_{12} such that four lines ℓ, ℓ_1, ℓ_2, ℓ_{12} form a double reflection configuration.*

Remark 2.17. Proposition 2.16 shows that the double reflection configuration is playing the role of the quad-equation for lines in the projective space; see Section 4.

2.4. **Pseudo-Euclidean spaces and confocal families of quadrics.** In this section, we first give a necessary account of the basic notions connected with the pseudo-Euclidean spaces and their confocal families of quadrics.

2.4.1. *Pseudo-Euclidean spaces. The pseudo-Euclidean space* $\mathbf{E}^{k,l}$ is a d-dimensional space $\mathbf{R}^d$ with *the pseudo-Euclidean scalar product*

$$\langle x, y\rangle_{k,l} = x_1y_1 + \cdots + x_ky_k - x_{k+1}y_{k+1} - \cdots - x_dy_d. \tag{2.3}$$

Here, $k, l \in \{1, \dots, d-1\}$, $k + l = d$. The pair (k, l) is called *the signature* of the space. Denote $E_{k,l} = \operatorname{diag}(1, 1, \dots, 1, -1, \dots, -1)$, with k 1's and l -1's. Then the pseudo-Euclidean scalar product is

$$\langle x, y\rangle_{k,l} = E_{k,l}x \circ y,$$

where $\circ$ is the standard Euclidean product.

The pseudo-Euclidean distance between points x, y is

$$\operatorname{dist}_{k,l}(x,y) = \sqrt{\langle x-y, x-y\rangle_{k,l}}.$$

Since the scalar product can be negative, notice that the pseudo-Euclidean distance can have imaginary values as well—between the two roots, we choose the one with the positive imaginary part.

Let ℓ be a line in the pseudo-Euclidean space, and let v be its vector. ℓ is called

- *space-like* if $\langle v, v\rangle_{k,l} > 0$;
- *time-like* if $\langle v, v\rangle_{k,l} < 0$;
- and *light-like* if $\langle v, v\rangle_{k,l} = 0$.

Two vectors x, y are *orthogonal* in the pseudo-Euclidean space if $\langle x, y\rangle_{k,l} = 0$. Note that a light-like line is orthogonal to itself.

For a given vector $v \neq 0$, consider a hyperplane $v \circ x = 0$. Vector $E_{k,l}v$ is orthogonal to the hyperplane; moreover, all other orthogonal vectors are collinear with $E_{k,l}v$. If v is light-like, then so is $E_{k,l}v$, and $E_{k,l}v$ belongs to the hyperplane.

2.4.2. *Billiard reflection in the pseudo-Euclidean space.* Let v be a vector, and let α be a hyperplane in the pseudo-Euclidean space. Decompose the vector v into the sum $v = a + n_\alpha$ of a vector n_α orthogonal to α and a belonging to α. Then vector $v' = a - n_\alpha$ is *the billiard reflection* of v on α. It is easy to see that then v is also the billiard reflection of v' with respect to α.

Moreover, let us note that the lines containing the vectors v, v', a, n_α are harmonically conjugated [KT2009].

Note that $v = v'$ if v is contained in α and $v' = -v$ if it is orthogonal to α. If n_α is light-like, which means that it belongs to α, then the reflection is not defined.

A line ℓ' is the billiard reflection of ℓ off a smooth surface $\mathcal{S}$ if their intersection point $\ell \cap \ell'$ belongs to $\mathcal{S}$ and the vectors of ℓ, ℓ' are reflections of each other with respect to the tangent plane of $\mathcal{S}$ at this point.

Remark 2.18. It can be seen directly from the definition of reflection that the type of line is preserved by the billiard reflection. Thus, the lines containing segments of a given billiard trajectory within $\mathcal{S}$ are all of the same type: they are all either space-like, time-like, or light-like.

If $\mathcal{S}$ is an ellipsoid, then it is possible to extend the reflection mapping to those points where the tangent planes contain the orthogonal vectors. At such points, a vector reflects into the opposite one, i.e., $v' = -v$ and $\ell' = \ell$. For the explanation, see [KT2009]. As follows from the explanation given there, it is natural to consider each such a reflection as two reflections.

2.4.3. *Families of confocal quadrics.* For a given set of positive constants a_1, a_2, $\ldots$, a_d, an ellipsoid is given by

$$\mathcal{E} \ : \ \frac{x_1^2}{a_1} + \frac{x_2^2}{a_2} + \cdots + \frac{x_d^2}{a_d} = 1. \tag{2.4}$$

Let us remark that an equation of any ellipsoid in the pseudo-Euclidean space can be brought into the canonical form (2.4) using transformations that preserve the scalar product (2.3).

The family of quadrics confocal with $\mathcal{E}$ is

$$\mathcal{Q}_\lambda \ : \ \frac{x_1^2}{a_1-\lambda}+\cdots+\frac{x_k^2}{a_k-\lambda}+\frac{x_{k+1}^2}{a_{k+1}+\lambda}+\cdots+\frac{x_d^2}{a_d+\lambda}=1, \qquad \lambda\in\mathbf{R}. \tag{2.5}$$

Unless stated differently, we are going to consider the nondegenerate case, when the set $\{a_1,\dots,a_k,-a_{k+1},\dots,-a_d\}$ consists of d different values,

$$a_1>a_2>\cdots>a_k>0>-a_{k+1}>\cdots>-a_d.$$

For $\lambda\in\{a_1,\dots,a_k,-a_{k+1},\dots,-a_d\}$, the quadric $\mathcal{Q}_\lambda$ is degenerate, and it coincides with the corresponding coordinate hyperplane.

It is natural to join one more degenerate quadric to the family (2.5): the one corresponding to the value $\lambda=\infty$, that is, the hyperplane at the infinity.

For each point x in the space, there are exactly d values of λ, such that the relation (2.5) is satisfied. However, not all the values are necessarily real: either all d of them are real or there are $d-2$ real and two conjugate complex values. Thus, through every point in the space, there are either d or $d-2$ quadrics from the family (2.5) [KT2009].

The line $x+tv$ ($t\in\mathbf{R}$) is tangent to quadric $\mathcal{Q}_\lambda$ if the quadratic equation

$$A_\lambda(x+tv)\circ(x+tv)=1 \tag{2.6}$$

has a double root. Here we denote

$$A_\lambda=\operatorname{diag}\left(\frac{1}{a_1-\lambda},\dots,\frac{1}{a_k-\lambda},\frac{1}{a_{k+1}+\lambda},\dots,\frac{1}{a_d+\lambda}\right).$$

Now, calculating the discriminant of (2.6), we get

$$(A_\lambda x\ \circ\ v)^2-(A_\lambda v\circ v)(A_\lambda x\ \circ\ x-1)=0, \tag{2.7}$$

which is equivalent to

$$\sum_{i=1}^{d}\frac{\varepsilon_i F_i(x,v)}{a_i-\varepsilon_i\lambda}=0, \tag{2.8}$$

where

$$F_i(x,v)=\varepsilon_i v_i^2+\sum_{j\neq i}\frac{(x_iv_j-x_jv_i)^2}{\varepsilon_j a_i-\varepsilon_i a_j} \tag{2.9}$$

with ε's given by

$$\varepsilon_i=\begin{cases}1, & 1\le i\le k,\\ -1, & k+1\le i\le d.\end{cases}$$

The equation (2.8) can be transformed to

$$\frac{\mathcal{P}(\lambda)}{\prod_{i=1}^{d}(a_i-\varepsilon_i\lambda)}=0, \tag{2.10}$$

where the coefficient of λ^{d-1} in $\mathcal{P}(\lambda)$ is equal to $\langle v,v\rangle_{k,l}$. Thus, the polynomial $\mathcal{P}(\lambda)$ is of degree $d-1$ for space-like and time-like lines, and is of a smaller degree for light-like lines. However, in the latter case, it turns out to be natural to consider the polynomial $\mathcal{P}(\lambda)$ also as of degree $d-1$, taking the corresponding roots to be equal to infinity. So, the light-like lines are characterized by being tangent to the quadric $\mathcal{Q}_\infty$.

Having this setting in mind, we note that it is proved in [KT2009] that the polynomial $\mathcal{P}(\lambda)$ has at least $d-3$ roots in $\mathbf{R}\cup\{\infty\}$.

Thus, we have

Proposition 2.19. *Any line in the space is tangent to either $d-1$ or $d-3$ quadrics of the family* (2.5). *If this number is equal to $d-3$, then there are two conjugate complex values of λ, such that the line is tangent also to these two quadrics in $\mathbf{C}^d$.*

This statement with the proof is given in [KT2009]. Let us remark that in [KT2009], it is claimed that a light-like line has only $d-2$ or $d-4$ caustic quadrics. That is because $\mathcal{Q}_\infty$ is not considered there as a member of the confocal family.

As noted in [KT2009], a line having nonempty intersection with an ellipsoid from (2.5) will be tangent to $d-1$ quadrics from the confocal family. However, the next theorem, proved in [DR2012a], will provide some more insight into the distribution of the parameters of the caustics of a given line, together with a detailed description of the distribution of the parameters of quadrics containing a given point placed inside an ellipsoid from (2.5).

Theorem 2.20. *In the pseudo-Euclidean space $\mathbf{E}^{k,l}$ consider a line intersecting ellipsoid $\mathcal{E}$* (2.4). *Then this line is touching $d-1$ quadrics from* (2.5). *If we denote their parameters by $\alpha_1,\ \ldots,\ \alpha_{d-1}$ and take*

$$\{b_1,\ \ldots,\ b_p,\ c_1,\ \ldots,\ c_q\}=\{\varepsilon_1 a_1,\ \ldots,\ \varepsilon_d a_d,\ \alpha_1,\ \ldots,\ \alpha_{d-1}\},$$
$$c_q\le\cdots\le c_2\le c_1<0<b_1\le b_2\le\cdots\le b_p,\quad p+q=2d-1,$$

we will additionally have

- *if the line is space-like, then $p=2k-1$, $q=2l$, $a_1=b_p$, $\alpha_i\in\{b_{2i-1},b_{2i}\}$ for $1\le i\le k-1$, and $\alpha_{j+k-1}\in\{c_{2j-1},c_{2j}\}$ for $1\le j\le l$;*
- *if the line is time-like, then $p=2k$, $q=2l-1$, $c_q=-a_d$, $\alpha_i\in\{b_{2i-1},b_{2i}\}$ for $1\le i\le k$, and $\alpha_{j+k}\in\{c_{2j-1},c_{2j}\}$ for $1\le j\le l-1$;*
- *if the line is light-like, then $p=2k$, $q=2l-1$, $b_p=\infty=\alpha_k$, $b_{p-1}=a_1$, $\alpha_i\in\{b_{2i-1},b_{2i}\}$ for $1\le i\le k-1$, and $\alpha_{j+k}\in\{c_{2j-1},c_{2j}\}$ for $1\le j\le l-1$.*

Moreover, for each point on ℓ inside $\mathcal{E}$, there are exactly d distinct quadrics from (2.5) *containing it. More precisely, there is exactly one parameter of these quadrics in each of the intervals*

$$(c_{2l-1},c_{2l-2}),\ \ldots,\ (c_3,c_2),\ (c_1,0),\ (0,b_1),\ (b_2,b_3),\ \ldots,\ (b_{2k-2},b_{2k-1}).$$

The analogue of Theorem 2.20 for the Euclidean space is proved in [Aud1994].

Corollary 2.21. *For each point placed inside an ellipsoid in the pseudo-Euclidean space, there are exactly two other ellipsoids from the confocal family containing this point.*

3. Pseudo-Euclidean spaces and the Poncelet Theorem

3.1. **Minkowski plane, confocal conics and billiards.**

3.1.1. *Confocal conics in the Minkowski plane.* Here, we give a review of basic properties of families of confocal conics in the Minkowski plane; see [DR2012a].

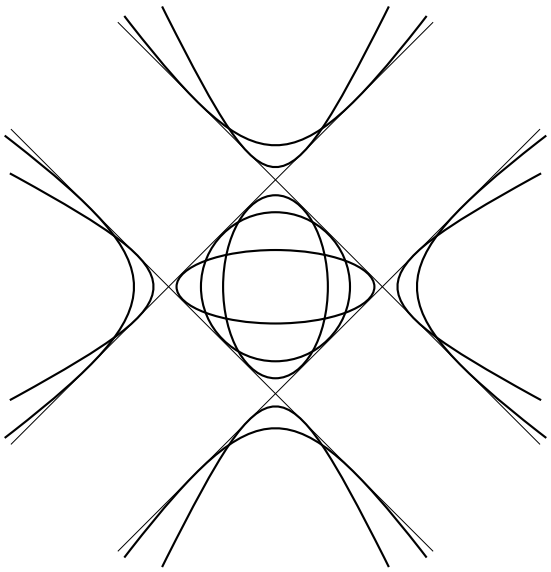

FIGURE 15. Family of confocal conics in the Minkowski plane

Denote by

$$\mathcal{E} \ : \ \frac{x^2}{a} + \frac{y^2}{b} = 1 \tag{3.1}$$

an ellipse in the plane, with a, b being fixed positive numbers.

The associated family of confocal conics is

$$\mathcal{C}_\lambda \ : \ \frac{x^2}{a-\lambda} + \frac{y^2}{b+\lambda} = 1, \quad \lambda \in \mathbf{R}. \tag{3.2}$$

The family is shown on Figure 15. We may distinguish the following three subfamilies in the family (3.2):

- for $\lambda \in (-b, a)$, the conic $\mathcal{C}_\lambda$ is an ellipse;
- for $\lambda < -b$, the conic $\mathcal{C}_\lambda$ is a hyperbola with x-axis as the major one;
- for $\lambda > a$, it is a hyperbola again, but now its major axis is y-axis.

In addition, there are three degenerated quadrics, $\mathcal{C}_a$, $\mathcal{C}_b$, $\mathcal{C}_\infty$, corresponding to y-axis, x-axis, and the line at the infinity, respectively. Note the three pairs of foci $F_1(\sqrt{a+b}, 0)$, $F_2(-\sqrt{a+b}, 0)$; $G_1(0, \sqrt{a+b})$, $G_2(0, -\sqrt{a+b})$; and $H_1(1 : -1 : 0)$, $H_2(1 : 1 : 0)$ on the line at infinity.

We notice four distinguished lines,

$$x + y = \sqrt{a+b}, \quad x + y = -\sqrt{a+b},$$
$$x - y = \sqrt{a+b}, \quad x - y = -\sqrt{a+b}.$$

These lines are common tangents to all conics from the confocal family.

Some geometric properties of conics in the Minkowski plane are analogous to the Euclidean ones. For example, for each point on the conic $\mathcal{C}_\lambda$, either the sum or the difference of its Minkowski distances from the foci F_1 and F_2 is equal to $2\sqrt{a-\lambda}$;

either the sum or the difference of the distances from the other pair of foci G_1, G_2 is equal to $2\sqrt{-b-\lambda}$ [DR2012a].

We invite the reader to make further comparisons of the confocal families of conics in the Minkowski and Euclidean planes (see Figures 4 and 15).

3.1.2. *Relativistic conics.* Since a family of confocal conics in the Minkowski plane contains three geometric types of conics, it is natural to introduce relativistic conics, which are suggested in [BM1962]. In this section, we give a brief account of related analysis.

Consider the points $F_1(\sqrt{a+b},0)$ and $F_2(-\sqrt{a+b},0)$ in the plane.

For a given constant $c \in \mathbf{R}^+ \cup i\mathbf{R}^+$, *a relativistic ellipse* is the set of points X satisfying

$$\operatorname{dist}_{1,1}(F_1,X)+\operatorname{dist}_{1,1}(F_2,X)=2c,$$

while *a relativistic hyperbola* is the union of the sets given by the equations:

$$\operatorname{dist}_{1,1}(F_1,X)-\operatorname{dist}_{1,1}(F_2,X)=2c,$$
$$\operatorname{dist}_{1,1}(F_2,X)-\operatorname{dist}_{1,1}(F_1,X)=2c.$$

The relativistic conics can be described as follows.

- $0<c<\sqrt{a+b}$**:** The corresponding relativistic conics lie on ellipse $\mathcal{C}_{a-c^2}$ from family (3.2). The ellipse $\mathcal{C}_{a-c^2}$ is split into four arcs by touching points with the four common tangent lines. Thus, the relativistic ellipse is the union of the two arcs intersecting the y-axis, while the relativistic hyperbola is the union of the other two arcs.
- $c>\sqrt{a+b}$**:** The relativistic conics lie on $\mathcal{C}_{a-c^2}$—a hyperbola with x-axis as the major one. Each branch of the hyperbola is split into three arcs by touching points with the common tangents. Thus, the relativistic ellipse is the union of the two finite arcs, while the relativistic hyperbola is the union of the four infinite ones.
- c **is imaginary:** The relativistic conics lie on hyperbola $\mathcal{C}_{a-c^2}$—a hyperbola with y-axis as the major one. As in the previous case, the branches are split into six arcs in total by common points with the four tangents. The relativistic ellipse is the union of the four infinite arcs, while the relativistic hyperbola is the union of the two finite ones.

The conics are shown on Figure 16.

Notice that all relativistic ellipses are disjoint with each other, as well as all relativistic hyperbolas. Moreover, at the intersection point of a relativistic ellipse which is a part of the geometric conic $\mathcal{C}_{\lambda_1}$ from the confocal family (3.2) and a relativistic hyperbola belonging to $\mathcal{C}_{\lambda_2}$, it is always $\lambda_1<\lambda_2$.

3.1.3. *Periodic trajectories of an elliptical billiard.* Analytic conditions for the existence of closed polygonal lines inscribed in one conic and circumscribed about another one in the projective plane are derived by Cayley [Cay1854, Cay1861]. They can be applied to the billiard trajectories within ellipses in the Minkowski plane as well, since each such trajectory has a caustic among confocal conics. In this section, we shall analyze in more detail some particular properties related to Minkowski geometry.

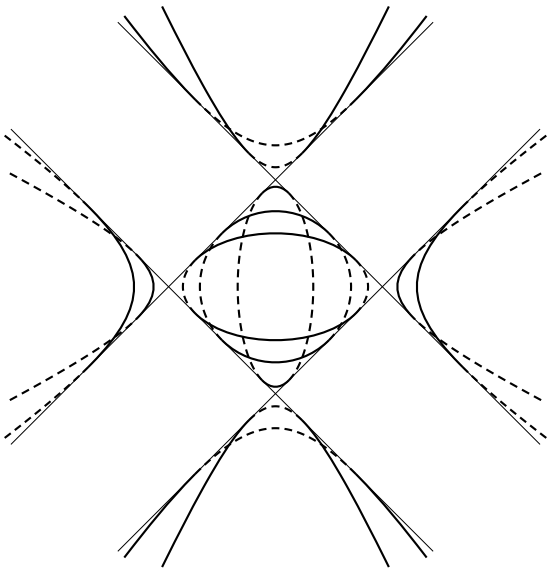

FIGURE 16. Relativistic conics in the Minkowski plane: relativistic ellipses are represented by full lines, and hyperbolas by dashed ones

Theorem 3.1. *In the Minkowski plane, consider a billiard trajectory $\mathcal{T}$ within ellipse $\mathcal{E}$ given by equation* (3.1)*. The trajectory is periodic with period $n = 2m$ if and only if the following condition is satisfied:*

$$\det \begin{pmatrix} B_3 & B_4 & \dots & B_{m+1} \\ B_4 & B_5 & \dots & B_{m+2} \\ \dots & \dots & \dots & \dots \\ B_{m+1} & B_{m+2} & \dots & B_{2m-1} \end{pmatrix} = 0. \tag{3.3}$$

The trajectory $\mathcal{T}$ is periodic with period $n = 2m + 1$ if and only if $\mathcal{C}_\alpha$ is an ellipse and the following condition is satisfied:

$$\det \begin{pmatrix} B_3 & B_4 & \dots & B_{m+2} \\ \dots & \dots & \dots & \dots \\ B_{m+1} & B_{m+2} & \dots & B_{2m} \\ C_{m+1} & C_{m+2} & \dots & C_{2m} \end{pmatrix} = 0. \tag{3.4}$$

Here

$$\sqrt{(a-t)(b+t)(\alpha-t)} = B_0 + B_1 t + B_2 t^2 + \cdots,$$

$$\sqrt{\frac{(a-t)(b+t)}{\alpha-t}} = C_0 + C_1 t + C_2 t^2 + \cdots$$

are the Taylor expansions around $t = 0$.

Proof. Each point inside $\mathcal{E}$ is the intersection of exactly two ellipses $\mathcal{C}_{\lambda_1}$ and $\mathcal{C}_{\lambda_2}$ from (3.2). The parameters λ_1, λ_2 are generalized Jacobi coordinates. Take $\lambda_1 < \lambda_2$.

Consider first the case when $\mathcal{C}_\alpha$ is a hyperbola. Then along $\mathcal{T}$ those coordinates will take values in segments $[-b, 0]$ and $[0, a]$, respectively, with the endpoints of the

segments as the only local extrema. λ_1 achieves the value $-b$ at the intersections of $\mathcal{T}$ with the x-axis, while λ_2 achieves a at the intersections with the y-axis. At each reflection point, one of the coordinates achieves the value 0. They can both be equal to 0 only at the points where $\mathcal{E}$ has a light-like tangent, and there reflection is counted twice.

This means that on a closed trajectory the number of reflections is equal to the number of intersection points with the coordinate axes. Notice that a periodic trajectory crosses each of the coordinate axes an even number of times.

The condition on $\mathcal{T}$ to become closed after n reflections on $\mathcal{E}$, n_1 crossings over x-axis, and n_2 over y-axis is that the equality

$$n_1 P_a + n_2 P_{-b} = nP_0$$

holds on the elliptic curve

$$s^2 = (a-t)(b+t)(\alpha - t),$$

where by P_β we denote a point on the curve corresponding to $t = \beta$, and P_∞ is taken to be the neutral for the elliptic curve group.

From the previous discussion $n_1 + n_2 = n$, and all three numbers are even. P_a and P_{-b} are branching points of the curve, thus $2P_a = 2P_{-b} = 2P_\infty$, so the condition becomes $nP_0 = nP_\infty$, which is equivalent to (3.3).

Now suppose $\mathcal{C}_\alpha$ is an ellipse. The generalized Jacobi coordinates take values in the segments $[-b, 0]$, $[0, \alpha]$ or in $[\alpha, 0]$, $[0, a]$, depending on the sign of α. Since both cases proceed in a similar way, we assume $\alpha < 0$.

The coordinate λ_1 has the extrema on $\mathcal{T}$ at the touching points with the caustic and some of the reflection points, while λ_2 has the extrema at the crossing points with y-axis and some of the reflection points.

The condition on $\mathcal{T}$ to become closed after n reflections on $\mathcal{E}$, with n_1 crossings over the y-axis, and n_2 touching points with the caustic is

$$n_1 P_a + n_2 P_\alpha = nP_0,$$

with $n_1 + n_2 = n$ and n_1 even.

Thus, for n even we get (3.3) in the same manner as for a hyperbola as the caustic.

For n odd, the condition is equivalent to $nP_0 = (n-1)P_\infty + P_\alpha$. Notice that one basis of the space $\mathcal{L}((n-1)P_\infty + P_\alpha)$ is

$$1, t, \dots, t^m, s, ts, \dots, t^{m-2}s, \frac{s}{t-\alpha}.$$

Using this basis, as it is shown in [DR2006a, DR2011], we obtain (3.4). □

Example 3.2 (3-periodic trajectories)**.** Let us find all 3-periodic trajectories within the ellipse $\mathcal{E}$ given by (3.1) in the Minkowski plane, i.e., all conics $\mathcal{C}_\alpha$ from the confocal family (3.2) corresponding to such trajectories.

The condition is

$$C_2 = \frac{3a^2b^2 + 2a^2b\alpha - 2ab^2\alpha - a^2\alpha^2 - 2ab\alpha^2 - b^2\alpha^2}{8(ab)^{3/2}\alpha^{5/2}} = 0,$$

which gives the following solutions for the parameter α of the caustic:

$$\alpha_1 = \frac{ab}{(a+b)^2}(a-b-2\sqrt{a^2+ab+b^2}),$$
$$\alpha_2 = \frac{ab}{(a+b)^2}(a-b+2\sqrt{a^2+ab+b^2}).$$

Notice that $-b < \alpha_1 < 0 < \alpha_2 < a$, so both caustics $\mathcal{C}_{\alpha_1}$, $\mathcal{C}_{\alpha_2}$ are ellipses.

Example 3.3 (4-periodic trajectories)**.** By Theorem 3.1, the condition is $B_3 = 0$. Since

$$B_3 = \frac{(-ab-a\alpha+b\alpha)(-ab+a\alpha+b\alpha)(ab+a\alpha+b\alpha)}{16(ab\alpha)^{5/2}},$$

we obtain the following solutions:

$$\alpha_1 = \frac{ab}{b-a}, \quad \alpha_2 = \frac{ab}{a+b}, \quad \alpha_3 = -\frac{ab}{a+b}.$$

Since $\alpha_1 \notin (-b,a)$ and $\alpha_2, \alpha_3 \in (-b,a)$, conic $\mathcal{C}_{\alpha_1}$ is a hyperbola, while $\mathcal{C}_{\alpha_2}$, $\mathcal{C}_{\alpha_3}$ are ellipses.

Example 3.4 (5-periodic trajectories)**.** The condition is

$$\det \begin{pmatrix} B_3 & B_4 \\ C_3 & C_4 \end{pmatrix} = 0.$$

Taking $a = b = 1$, we get that this is equivalent to $64\alpha^6 - 16\alpha^4 - 52\alpha^2 + 5 = 0$. This equation has four solutions in $\mathbf{R}$, all four contained in $(-1,1)$, and two conjugated solutions in $\mathbf{C}$.

3.1.4. *Light-like trajectories of an elliptical billiard.* In this section we consider in more detail light-like trajectories of the elliptical billiard; see Figure 17 for an example of such a trajectory. We are going to review results from [DR2012a] and illustrate them by some examples.

Periodic light-like trajectories. Let us first notice that the successive segments of light-like billiard trajectories are orthogonal to each other (see Figure 17). Thus a trajectory can close only after an even number of reflections.

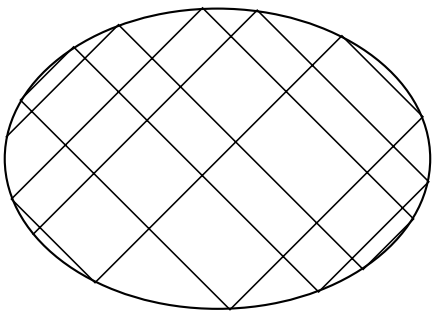

FIGURE 17. Light-like billiard trajectory

The analytic condition for n-periodicity of a light-like billiard trajectory within the ellipse $\mathcal{E}$ given by equation (3.1) can be derived as in Theorem 3.1. We get the condition stated in (3.3), with $\alpha = \infty$, i.e., (B_i) are coefficients in the Taylor expansion around $t = 0$ of $\sqrt{(a-t)(b+t)} = B_0 + B_1 t + B_2 t^2 + \cdots$.

Now we are going to derive the analytic condition for periodic light-like trajectories in another way, which will lead to a more compact form of (3.3).

By applying affine transformations, one can transform an ellipse into a circle, and the billiard map on the light-like lines becomes conjugated to a rotation of the circle. A computation of the angle of rotation gives the following.

Theorem 3.5. *A light-like billiard trajectory within ellipse $\mathcal{E}$ is periodic with period n, where n is an even integer if and only if*

$$\operatorname{arc\,tan}\sqrt{\frac{a}{b}} \in \left\{ \frac{k\pi}{n} \;\middle|\; 1 \le k < \frac{n}{2},\ \left(k, \frac{n}{2}\right) = 1 \right\}. \tag{3.5}$$

As an immediate consequence, we get

Corollary 3.6. *For a given even integer n, the number of different ratios of the axes of ellipses having n-periodic light-like billiard trajectories is equal to*

$$\begin{cases} \varphi(n)/2 & \text{if } n \text{ is not divisible by } 4, \\ \varphi(n)/4 & \text{if } n \text{ is divisible by } 4, \end{cases}$$

where φ is Euler's totient function, i.e., the number of positive integers not exceeding n that are relatively prime to n.

Remark 3.7. There are four points on $\mathcal{E}$ where the tangents are light-like. Those points cut four arcs on $\mathcal{E}$. An n-periodic trajectory within $\mathcal{E}$ hits each one of a pair of opposite arcs exactly k times, and $\frac{n}{2} - k$ times the arcs from the other pair.

Example 3.8 (10-perodic light-like trajectories)**.** For $n = 10$, condition (3.3) is

$$\det \begin{pmatrix} B_3 & B_4 & B_5 & B_6 \\ B_4 & B_5 & B_6 & B_7 \\ B_5 & B_6 & B_7 & B_8 \\ B_6 & B_7 & B_8 & B_9 \end{pmatrix} = \frac{(a+b)^{20}(5a^2 - 10ab + b^2)(a^2 - 10ab + 5b^2)}{(4ab)^{22}} = 0.$$

From here, we get that light-like billiard trajectories are 10-periodic in ellipses with the ratio of the axes equal to either $\sqrt{1 + \frac{2}{\sqrt{5}}}$ or $\sqrt{5 + 2\sqrt{5}}$.

From condition (3.5), we get

$$\sqrt{\frac{a}{b}} \in \left\{ \tan\frac{\pi}{10}, \tan\frac{2\pi}{10}, \tan\frac{3\pi}{10}, \tan\frac{4\pi}{10} \right\}.$$

Since

$$\tan\frac{\pi}{10} = \sqrt{1 - \frac{2}{\sqrt{5}}} = \frac{1}{\sqrt{5 + 2\sqrt{5}}} = \frac{1}{\tan\frac{4\pi}{10}},$$

$$\tan\frac{3\pi}{10} = \sqrt{1 + \frac{2}{\sqrt{5}}} = \frac{1}{\sqrt{5 - 2\sqrt{5}}} = \frac{1}{\tan\frac{2\pi}{10}},$$

both conditions give the same result.

A few of such trajectories are shown in Figures 18 and 19.

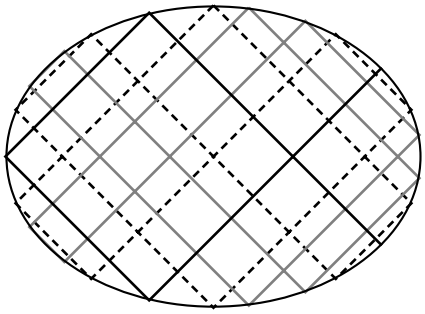

FIGURE 18. Light-like billiard trajectories with period 10 in the ellipse satisfying $a = (1 + 2/\sqrt{5})b$

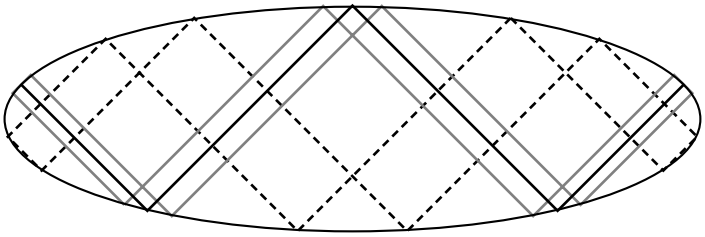

FIGURE 19. Light-like billiard trajectories with period 10 in the ellipse satisfying $a = (5 + 2\sqrt{5})b$

Light-like trajectories in ellipses and rectangular billiards. The next statement is akin to the claim that the billiard flow in a rectangle in a given direction is equivalent to a rotation of a circle.

Proposition 3.9. *The flow of the light-like billiard trajectories within ellipse $\mathcal{E}$ is trajectorially equivalent to the flow of those billiard trajectories within a rectangle whose angle with the sides is $\frac{\pi}{4}$. The ratio of the sides of the rectangle is equal to*

$$\frac{\pi}{2 \arctan \sqrt{\dfrac{a}{b}}} - 1.$$

Remark 3.10. The flow of the light-like billiard trajectories within a given oval in the Minkowski plane will be trajectorially equivalent to the flow of certain trajectories within a rectangle whenever an invariant measure m on the oval exists such that $m(AB) = m(CD)$ and $m(BC) = m(AD)$, where A, B, C, D are the points on the oval where the tangents are light-like. Some results and discussion regarding this situation are given in [GKT2007].

3.2. **Relativistic quadrics.** The aim of this section is to present the relativistic quadrics—a very recent object, which has been a main tool in our study of billiard dynamics (see [DR2012a]). First, we study geometrical types of quadrics in a

confocal family in three-dimensional Minkowski space. Then we analyze the tropic curves on quadrics in the three-dimensional case, and we introduce the important notion of discriminant sets $\Sigma^{\pm}$ corresponding to a confocal family. We present the main facts about discriminant sets in Propositions 3.11, 3.13, 3.15, 3.17. We study curved tetrahedra $\mathcal{T}^{\pm}$, which represent singularity sets of $\Sigma^{\pm}$, and we collect related results in Proposition 3.12. As the next important step, we introduce decorated Jacobi coordinates for three-dimensional Minkowski space, and we give a detailed description of the colouring into three colours. Each colour corresponds to a relativistic type, and we describe decomposition of a geometric quadric of each of the four geometric types into relativistic quadrics. This appears to be a rather involved combinatorial-geometric problem, and we solve it by using the previous analysis of the discriminant surfaces. We give a complete description of all three relativistic types of quadrics. At the end, we generalize the definition of the decorated Jacobi coordinates to an arbitrary dimension. And finally in Proposition 3.27 we prove properties PE1 and PE2.

3.2.1. *Confocal quadrics in three-dimensional Minkowski space and their geometrical types.* Let us start with the three-dimensional Minkowski space $\mathbf{E}^{2,1}$. A general confocal family of quadrics in this space is given by

$$\mathcal{Q}_\lambda \ : \ \frac{x^2}{a-\lambda}+\frac{y^2}{b-\lambda}+\frac{z^2}{c+\lambda}=1, \quad \lambda\in\mathbf{R}, \tag{3.6}$$

with $a>b>0$, $c>0$, see Figure 20.

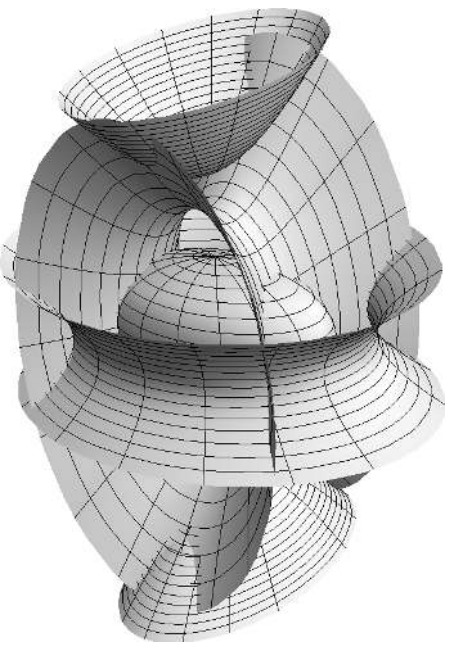

FIGURE 20. Confocal quadrics in three-dimensional Minkowski space

The family (3.6) contains four geometrical types of quadrics:

- 1-sheeted hyperboloids oriented along the z-axis, for $\lambda \in (-\infty, -c)$;
- ellipsoids, corresponding to $\lambda \in (-c, b)$;
- 1-sheeted hyperboloids oriented along the y-axis, for $\lambda \in (b, a)$;
- 2-sheeted hyperboloids, for $\lambda \in (a, +\infty)$—these hyperboloids are oriented along the z-axis.

In addition, there are four degenerated quadrics, $\mathcal{Q}_a$, $\mathcal{Q}_b$, $\mathcal{Q}_{-c}$, $\mathcal{Q}_\infty$, that is, the planes $x = 0$, $y = 0$, $z = 0$, and the plane at infinity, respectively. In the coordinate planes, we single out the following conics:

- the hyperbola $\mathcal{C}_a^{yz} \ : \ -\frac{y^2}{a-b} + \frac{z^2}{c+a} = 1$ in the plane $x = 0$,
- the ellipse $\mathcal{C}_b^{xz} \ : \ \frac{x^2}{a-b} + \frac{z^2}{c+b} = 1$ in the plane $y = 0$,
- the ellipse $\mathcal{C}_{-c}^{xy} \ : \ \frac{x^2}{a+c} + \frac{y^2}{b+c} = 1$ in the plane $z = 0$.

Notice that a confocal family of quadrics in three-dimensional Euclidean space contains only three types of quadrics; see Figure 10.

3.2.2. *Tropic curves on quadrics in three-dimensional Minkowski space and discriminant sets* $\Sigma^{\pm}$. On each quadric, notice the *tropic curves*—the set of points where the induced metrics on the tangent plane is degenerate.

Since the tangent plane at the point (x_0, y_0, z_0) of $\mathcal{Q}_\lambda$ is given by the equation

$$\frac{xx_0}{a-\lambda} + \frac{yy_0}{b-\lambda} + \frac{zz_0}{c+\lambda} = 1,$$

and the induced metric is degenerate if and only if the parallel plane that contains the origin is tangent to the light-like cone $x^2 + y^2 - z^2 = 0$, i.e.,

$$\frac{x_0^2}{(a-\lambda)^2} + \frac{y_0^2}{(b-\lambda)^2} - \frac{z_0^2}{(c+\lambda)^2} = 0,$$

we get that the tropic curves on $\mathcal{Q}_\lambda$ are the intersection of the quadric with the cone

$$\frac{x^2}{(a-\lambda)^2} + \frac{y^2}{(b-\lambda)^2} - \frac{z^2}{(c+\lambda)^2} = 0;$$

see [KT2009].

Now, consider the set of the tropic curves on all quadrics of the family (3.6).

Proposition 3.11. *The union of the tropic curves on all quadrics of* (3.6) *is the union of two ruled surfaces* Σ^+ *and* Σ^- *which can be parametrically represented as*

$$\Sigma^+ \ : \quad x = \frac{a-\lambda}{\sqrt{a+c}}\cos t, \quad y = \frac{b-\lambda}{\sqrt{b+c}}\sin t, \quad z = (c+\lambda)\sqrt{\frac{\cos^2 t}{a+c} + \frac{\sin^2 t}{b+c}},$$

$$\Sigma^- \ : \quad x = \frac{a-\lambda}{\sqrt{a+c}}\cos t, \quad y = \frac{b-\lambda}{\sqrt{b+c}}\sin t, \quad z = -(c+\lambda)\sqrt{\frac{\cos^2 t}{a+c} + \frac{\sin^2 t}{b+c}},$$

with $\lambda \in \mathbf{R}$, $\quad t \in [0, 2\pi)$.

The intersection of these two surfaces is an ellipse in the xy*-plane*

$$\Sigma^+ \cap \Sigma^- \ : \ \frac{x^2}{a+c} + \frac{y^2}{b+c} = 1, \ z = 0.$$

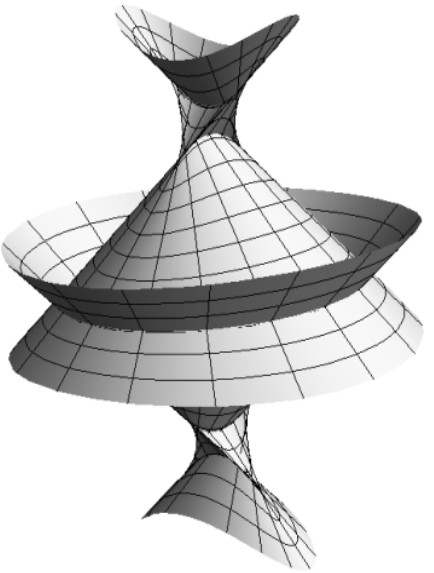

FIGURE 21. The union of all tropic curves of a confocal family

The two surfaces Σ^+, Σ^- are developable as embedded into Euclidean space. Moreover, their generatrices are all light-like.

Surfaces Σ^+ and Σ^- from Proposition 3.11 are represented on Figure 21.

In [Pei1999], a generalization of the Gauss map to the surfaces in three-dimensional Minkowski space is introduced. Namely, the *pseudo vector product* is introduced as

$$\mathbf{x}\wedge\mathbf{y} = \begin{vmatrix} x_1 & x_2 & x_3 \\ y_1 & y_2 & y_3 \\ e_1 & e_2 & -e_3 \end{vmatrix} = (x_2y_3-x_3y_2,\ x_3y_1-x_1y_3,\ -(x_1y_2-x_2y_1)) = E_{2,1}(\mathbf{x}\times\mathbf{y}).$$

It is easy to check that $\langle \mathbf{x}\wedge\mathbf{y}, \mathbf{x}\rangle_{2,1} = \langle \mathbf{x}\wedge\mathbf{y}, \mathbf{y}\rangle_{2,1} = 0$.

Then, for the surface $S : U \to \mathbf{E}^{2,1}$, with $U \subset \mathbf{R}^2$, *the Minkowski Gauss map* is defined as

$$\mathcal{G} \ : \ U \to \mathbf{RP}^2, \quad \mathcal{G}(x_1, x_2) = \mathbf{P}\left(\frac{\partial S}{\partial x_1} \wedge \frac{\partial S}{\partial x_2}\right),$$

where $\mathbf{P} : \mathbf{R}^3 \setminus \{(0,0,0)\} \to \mathbf{RP}^2$ is the usual projectivization.

Since $\mathbf{r}_\lambda \wedge \mathbf{r}_t$ is light-like for all λ and t, the Minkowski Gauss map of the surfaces $\Sigma^\pm$ is singular at all points.

The pseudo-normal vectors to $\Sigma^\pm$ are all light-like, thus these surfaces are *light-like developable*, as defined in [CI2010]. There, a classification of such surfaces is

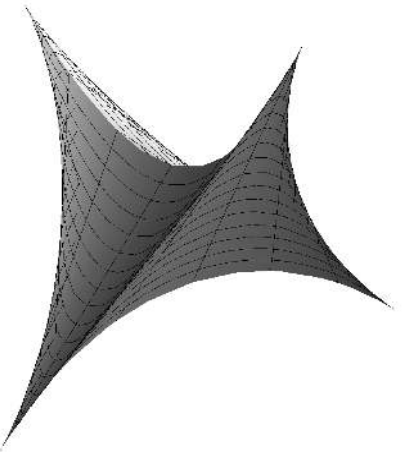

FIGURE 22. Curved tetrahedron $\mathcal{T}^+$: the union of all tropic curves on Σ^+ corresponding to $\lambda \in (b, a)$

given—each one is contained part-by-part in the following:

- a light-like plane,
- a light-like cone,
- a tangent surface of a light-like curve.

Since Σ^+ and Σ^- are contained neither in a plane nor in a cone, we expect that they will be tangent surfaces of some light-like curve, which is going to be shown in the sequel; see Corollary 3.16 later in this section.

On each of the surfaces Σ^+, Σ^-, we can notice that tropic lines corresponding to 1-sheeted hyperboloids oriented along y-axis form one curved tetrahedron; see Figure 21. Denote the tetrahedra by $\mathcal{T}^+$ and $\mathcal{T}^-$, respectively; they are symmetric with respect to the xy-plane. In Figure 22, the tetrahedron $\mathcal{T}^+ \subset \Sigma^+$ is shown.

Let us summarize the properties of these tetrahedra.

Proposition 3.12. *Consider the subset $\mathcal{T}^+$ of Σ^+ determined by the condition $\lambda \in [b, a]$. This set is a curved tetrahedron with the following properties:*

- *its vertices are*

$$V_1\left(\frac{a-b}{\sqrt{a+c}},\ 0,\ \frac{b+c}{\sqrt{a+c}}\right), \quad V_2\left(-\frac{a-b}{\sqrt{a+c}},\ 0,\ \frac{b+c}{\sqrt{a+c}}\right),$$
$$V_3\left(0,\ \frac{a-b}{\sqrt{b+c}},\ \frac{a+c}{\sqrt{b+c}}\right), \quad V_4\left(0,\ -\frac{a-b}{\sqrt{b+c}},\ \frac{a+c}{\sqrt{b+c}}\right);$$

- *the shorter arcs of the conics $\mathcal{C}_b^{xz}$ and $\mathcal{C}_a^{yz}$ determined by V_1, V_2 and V_3, V_4, respectively, are two edges of the tetrahedron;*
- *those two edges represent a self-intersection of Σ^+;*
- *other four edges are determined by the relation $-a-b+2\lambda+(a-b)\cos 2t = 0$;*
- *those four edges are cuspidal edges of Σ^+;*
- *thus, at each vertex of the tetrahedron, a swallowtail singularity of Σ^+ occurs.*

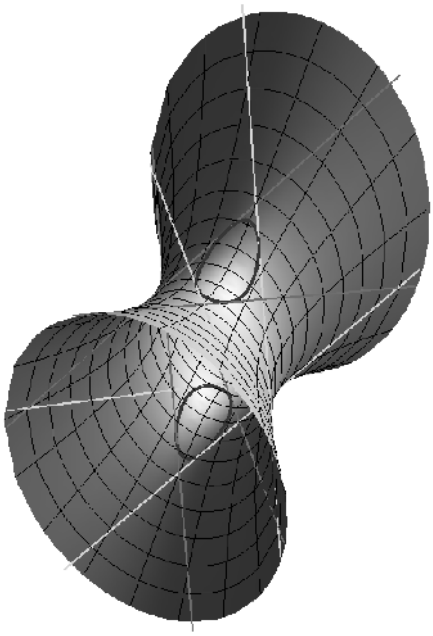

FIGURE 23. The tropic curves and its light-like tangents on a hyperboloid

It can be proved that the tropic curves of the quadric $\mathcal{Q}_{\lambda_0}$ represent exactly the locus of points (x, y, z), where equation

$$\frac{x^2}{a-\lambda} + \frac{y^2}{b-\lambda} + \frac{z^2}{c+\lambda} = 1 \tag{3.7}$$

has λ_0 as a multiple root.

Proposition 3.13. *A tangent line to a tropic curve of a nondegenerate quadric of the family* (3.6) *is always space-like, except on a* 1*-sheeted hyperboloid oriented along the y-axis.*

The tangent lines of a tropic on 1*-sheeted hyperboloids oriented along the y-axis are light-like at exactly four points, while at other points of the tropic curve the tangents are space-like.*

Moreover, a tangent line to the tropic of a quadric from (3.6) *belongs to the quadric if and only if it is light-like.*

Remark 3.14. In other words, the only quadrics of the family (3.6) that may contain a tangent to its tropic curve are 1-sheeted hyperboloids oriented along the y-axis, and those tangents are always light-like. The tropic curves and their light-like tangents on such a hyperboloid are shown on Figure 23.

Further considerations lead to

Proposition 3.15. *Each generatrix of* Σ^+ *and* Σ^- *is contained in a* 1*-sheeted hyperboloid oriented along the y-axis from* (3.6)*. Moreover, such a generatrix is touching at the same point one of the tropic curves of the hyperboloid and one of the cusp-like edges of the corresponding curved tetrahedron.*

Corollary 3.16. *The surfaces Σ^+ and Σ^- are tangent surfaces of the cuspidal edges of the tetrahedra $\mathcal{T}^+$ and $\mathcal{T}^-$, respectively.*

In the next propositions, we give a further analysis of the light-like tangents to the tropic curves on a 1-sheeted hyperboloid oriented along the y-axis.

Proposition 3.17. *For a fixed $\lambda_0 \in (b,a)$, consider a hyperboloid $\mathcal{Q}_{\lambda_0}$ from* (3.6) *and an arbitrary point (x,y,z) on $\mathcal{Q}_{\lambda_0}$. Equation* (3.7) *has, along with λ_0, two other roots in $\mathbf{C}$; denote them by λ_1 and λ_2. Then $\lambda_1{=}\lambda_2$ if and only if (x,y,z) is placed on a light-like tangent to a tropic curve of $\mathcal{Q}_{\lambda_0}$.*

Proof. This follows from the fact that the light-like tangents are contained in $\Sigma^+ \cup \Sigma^-$; see Propositions 3.11 and 3.15. □

Proposition 3.18. *Two light-like lines on a 1-sheeted hyperboloid oriented along the y-axis from* (3.6) *are either skew or intersect each other on a degenerate quadric from* (3.6).

Proof. This follows from the fact that the hyperboloid is symmetric with respect to the coordinate planes. □

Lemma 3.19. *Consider a nondegenerate quadric $\mathcal{Q}_{\lambda_0}$, which is not a hyperboloid oriented along the y-axis, i.e., $\lambda_0 \notin [b,a] \cup \{-c\}$. Then each point of $\mathcal{Q}_{\lambda_0}$ which is not on one of the tropic curves is contained in two additional distinct quadrics from the family* (3.6).

Consider two points A, B of $\mathcal{Q}_{\lambda_0}$, which are placed in the same connected component bounded by the tropic curves, and denote by λ'_A, λ''_A and λ'_B, λ''_B the solutions, different than λ_0, of equation (3.7) *corresponding to A and B, respectively. Then, if λ_0 is smaller than (resp. bigger than, between) λ'_A, λ''_A, it is also smaller than (resp. bigger than, between) λ'_B, λ''_B.*

Lemma 3.20. *Let $\mathcal{Q}_{\lambda_0}$ be a hyperboloid oriented along the y-axis, let $\lambda_0 \in (b,a)$, and let A, B be two points of $\mathcal{Q}_{\lambda_0}$, which are placed in the same connected component bounded by the tropic curves and light-like tangents. Then, if A is contained in two more quadrics from the family* (3.6), *the same is true for B.*

In this case, denote by λ'_A, λ''_A and λ'_B, λ''_B the real solutions, different than λ_0, of equation (3.7) *corresponding to A and B, respectively. Then, if λ_0 is smaller than (resp. bigger than, between) λ'_A, λ''_A, it is also smaller than (resp. bigger than, between) λ'_B, λ''_B.*

On the other hand, if A is not contained in any other quadric from (3.6), *then the same is true for all points of its connected component.*

Proof. The proof of both Lemmae 3.19 and 3.20 follows from the fact that the solutions of (3.7) are continuously changed through the space and that two of the solutions coincide exactly on the tropic curves and their light-like tangents. □

3.2.3. *Generalized Jacobi coordinates and relativistic quadrics in three-dimensional Minkowski space.*

Definition 3.21. *The generalized Jacobi coordinates* of point (x,y,z) in the three-dimensional Minkowski space $\mathbf{E}^{2,1}$ is the unordered triplet of solutions of equation (3.7).

Note that any of the following cases may occur:

- the generalized Jacobi coordinates are real and different;
- only one generalized Jacobi coordinate is real;
- the generalized Jacobi coordinates are real, but two of them coincide;
- all three generalized Jacobi coordinates are equal.

Lemmae 3.19 and 3.20 will help us define the relativistic types of quadrics in three-dimensional Minkowski space. For the quadrics from (3.6), consider their connected components bounded by the tropic curves and, for the 1-sheeted hyperboloids oriented along the y-axis, by their light-like tangent lines as well. Each connected component will represent *a relativistic quadric*.

Definition 3.22. A component of the quadric $\mathcal{Q}_{\lambda_0}$ is *of relativistic type* E if, at each of its points, λ_0 is smaller than the other two generalized Jacobi coordinates.

A component of quadric $\mathcal{Q}_{\lambda_0}$ is *of relativistic type* H^1 if, at each of its points, λ_0 is between the other two generalized Jacobi coordinates.

A component of quadric $\mathcal{Q}_{\lambda_0}$ is *of relativistic type* H^2 if, at each of its points, λ_0 is bigger than the other two generalized Jacobi coordinates.

A component of quadric $\mathcal{Q}_{\lambda_0}$ is *of relativistic type* 0 if, at each of its points, λ_0 is the only real generalized Jacobi coordinate.

Lemmae 3.19 and 3.20 guarantee that the relativistic types are well defined, i.e., that to each such quadric a unique type E, H^1, H^2, or 0 can be assigned.

Definition 3.23. Suppose (x, y, z) is a point of the three-dimensional Minkowski space $\mathbf{E}^{2,1}$ where equation (3.7) has real and different solutions. *The decorated Jacobi coordinates* of that point is the ordered triplet of pairs

$$(E, \lambda_1), \quad (H^1, \lambda_2), \quad (H^2, \lambda_3)$$

of the generalized Jacobi coordinates and the corresponding types of relativistic quadrics.

Now, we are going to analyze the arrangement of the relativistic quadrics. Let us start with their intersections with the coordinate planes.

3.2.4. *Intersection with the xy-plane.* In the xy-plane, the Minkowski metrics is reduced to the Euclidean one. The family (3.6) is intersecting that plane by the following family of confocal conics

$$\mathcal{C}^{xy}_{\lambda} \ : \ \frac{x^2}{a-\lambda} + \frac{y^2}{b-\lambda} = 1; \tag{3.8}$$

see Figure 24.

We conclude that the xy-plane is divided by the ellipse $\mathcal{C}^{xy}_{-c}$ into two relativistic quadrics:

- the region within $\mathcal{C}^{xy}_{-c}$ is a relativistic quadric of E-type;
- the region outside this ellipse is of H^1-type.

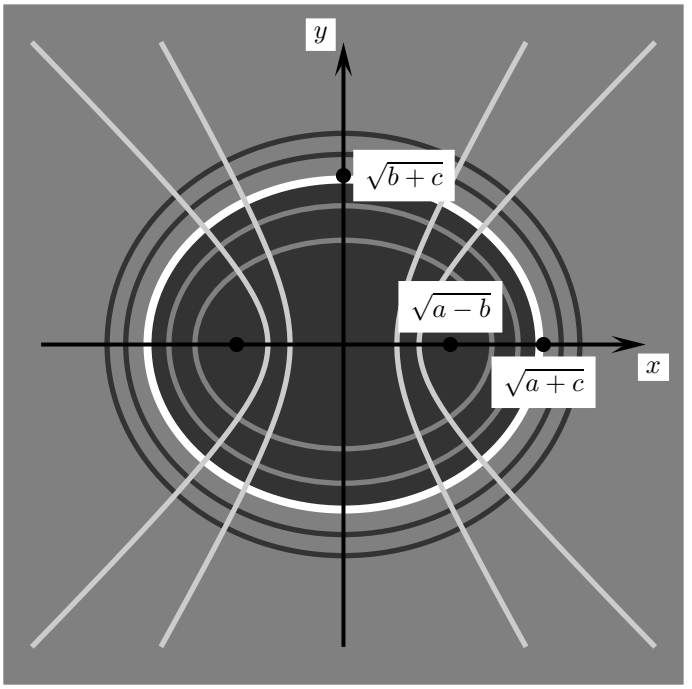

FIGURE 24. Intersection of relativistic quadrics with the xy-plane

Moreover, the types of relativic quadrics intersecting the xy-plane are

- the components of the ellipsoids are of H^1-type;
- the components of the 1-sheeted hyperboloids oriented along the y-axis are of H^2-type;
- the components of the 1-sheeted hyperboloids oriented along the z-axis are of E-type.

In Figure 24, the types E, H^1, H^2 quadrics are coloured in dark gray, medium gray, and light gray, respectively. The same colouring rule is applied in Figures 25–27.

3.2.5. *Intersection with the xz-plane.* In the xz-plane, the reduced metric is the Minkowski one. The intersection of family (3.6) with that plane is the family of confocal conics

$$\mathcal{C}_\lambda^{xz} \ : \ \frac{x^2}{a-\lambda} + \frac{z^2}{c+\lambda} = 1; \tag{3.9}$$

see Figure 25.

The plane is divided by the ellipse $\mathcal{C}_b^{xz}$ and the four joint tangents of (3.9) into 13 parts:

- the part within $\mathcal{C}_b^{xz}$ is a relativistic quadric of H^1-type;
- the four parts placed outside of $\mathcal{C}_b^{xz}$ that have a nonempty intersection with the x-axis are of H^2-type;

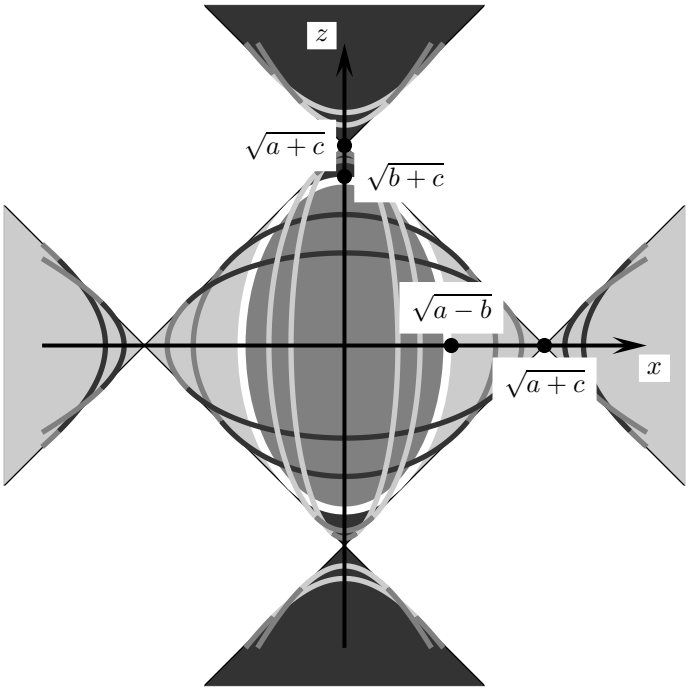

FIGURE 25. Intersection of relativistic quadrics with the xz-plane

- the four parts placed outside of $\mathcal{C}_b^{xz}$ that have a nonempty intersection with the z-axis are of E-type;
- the four remaining parts are of the 0-type, and no quadric from the family (3.6), except the degenerated $\mathcal{Q}_b$, is passing through any of their points.

3.2.6. *Intersection with the yz-plane.* As in the previous case, in the yz-plane the reduced metric is the Minkowski one. The intersection of family (3.6) with that plane is the family of confocal conics

$$\mathcal{C}_\lambda^{yz} \ : \ \frac{y^2}{b-\lambda} + \frac{z^2}{c+\lambda} = 1; \tag{3.10}$$

see Figure 26.

The plane is divided by the hyperbola $\mathcal{C}_a^{yz}$ and the joint tangents of (3.10) into 15 parts:

- the two convex parts determined by $\mathcal{C}_a^{yz}$ are relativistic quadrics of H^1-type;
- the five parts placed outside of $\mathcal{C}_a^{yz}$ that have a nonempty intersection with the coordinate axes are of H^2-type;
- the four parts, each one placed between $\mathcal{C}_a^{yz}$, and one of the joint tangents of (3.10) are of E-type;
- through the points of the four remaining parts no quadric from the family (3.6), except the degenerated $\mathcal{Q}_a$, is passing.

The intersection of relativistic quadrics with the coordinate planes is shown in Figure 27.

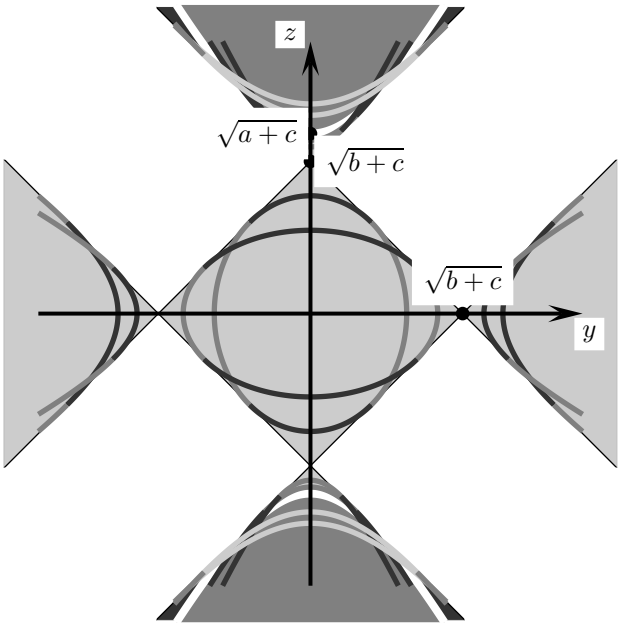

FIGURE 26. Intersection of the relativistic quadrics with the yz-plane

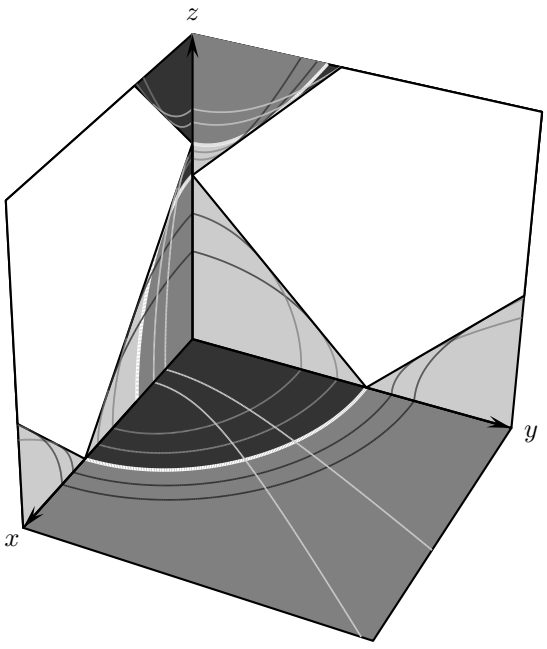

FIGURE 27. Intersection of the relativistic quadrics with the coordinate planes

Let us notice that from the above analysis, using Lemmae 3.19 and 3.20, we can determine the type of each relativistic quadric with a nonempty intersection with some of the coordinate hyperplanes.

1-*sheeted hyperboloids oriented along the z-axis:* $\lambda \in (-\infty, -c)$. Such a hyperboloid is divided by its tropic curves into three connected components—two of them are unbounded and mutually symmetric with respect to the xy-plane, while the third one is the bounded annulus placed between them. The two symmetric ones are of H^1-type, while the third one is of E-type.

Ellipsoids: $\lambda \in (-c, b)$. An ellipsoid is divided by the tropic curves into three bounded connected components—two of them are mutually symmetric with respect to the xy-plane, while the third one is the annulus placed between them. In this case, the symmetric components represent relativistic quadrics of E-type. The annulus is of H^1-type.

1-*sheeted hyperboloids oriented along the y-axis:* $\lambda \in (b, a)$. The decomposition of those hyperboloids into the relativistic quadrics is more complicated and more interesting interesting than for the other types of quadrics from (3.6). By its two tropic curves and their eight light-like tangent lines, such a hyperboloid is divided into 28 connected components:

- the two bounded components placed inside the tropic curves are of H^1-type;
- the four bounded components placed between the tropic curves and the light-like tangents, such that they have nonempty intersections with the xz-plane are of H^2-type;
- the four bounded components placed between the tropic curves and the light-like tangents, such that they have nonempty intersections with the yz-plane are of E-type;
- the two bounded components, each limited by four light-like tangents, are of H^2-type;
- the four unbounded components, each limited by two light-like tangents, such that they have nonempty intersections with the xy-plane, are of H^2-type;
- four unbounded components, each limited by two light-like tangents, such that they have nonempty intersections with the yz-plane, are of E-type;
- the eight unbounded components, each limited by four light-like tangents, are sets of points not contained in any other quadric from (3.6).

2-*sheeted hyperboloids:* $\lambda \in (a, +\infty)$. Such a hyperboloid is divided into four connected components by its tropic curves: two bounded ones are of H^2-type, while the two unbounded are of H^1-type.

3.2.7. *Decorated Jacobi coordinates and relativistic quadrics in d-dimensional pseudo-Euclidean space.* Now we are going to introduce the relativistic quadrics and their types in the confocal family (2.5) in the d-dimensional pseudo-Euclidean space $\mathbf{E}^{k,l}$.

Definition 3.24. *The generalized Jacobi coordinates* of a point x in the d-dimensional pseudo-Euclidean space $\mathbf{E}^{k,l}$ is the unordered d-tuple of solutions λ of the

equation

$$\frac{x_1^2}{a_1-\lambda}+\cdots+\frac{x_k^2}{a_k-\lambda}+\frac{x_{k+1}^2}{a_{k+1}+\lambda}+\cdots+\frac{x_d^2}{a_d+\lambda}=1. \tag{3.11}$$

As already mentioned in Section 2.4, this equation has either d or $d-2$ real solutions. Besides, some of the solutions may be multiple.

The set Σ_d of points x in $\mathbf{R}^d$ where equation (3.11) has multiple solutions is an algebraic hypersurface. Σ_d divides each quadric from (2.5) into several connected components. We call these components *the relativistic quadrics*.

Since the generalized Jacobi coordinates depend continuously on x, the following definition can be made:

Definition 3.25. We say that a relativistic quadric placed on $\mathcal{Q}_{\lambda_0}$ is *of type* E if, at each of its points, λ_0 is smaller than the other $d-1$ generalized Jacobi coordinates.

We say that a relativistic quadric placed on $\mathcal{Q}_{\lambda_0}$ is *of type* H^i $(1<i<d-1)$ if, at each of its points, λ_0 is greater than i other generalized Jacobi coordinates and smaller than $d-i-1$ of them.

We say that a relativistic quadric placed on $\mathcal{Q}_{\lambda_0}$ is *of the type* 0^i $(0<i<d-2)$ if, at each of its points, λ_0 is greater than other i real generalized Jacobi coordinates, and smaller than $d-i-2$ of them.

It would be interesting to analyze properties of the discriminant manifold Σ_d, as well as the combinatorial structure of the arrangement of the relativistic quadrics, as is done for $d=3$. Remark that this description would have $[d/2]$ substantially different cases in each dimension, depending upon the choice of k and l.

Definition 3.26. Suppose $(x_1,\dots,x_d)$ is a point of the d-dimensional Minkowski space $\mathbf{E}^{k,l}$ where equation (3.11) has real and different solutions. The *decorated Jacobi coordinates* of that point is the ordered d-tuplet of pairs

$$(E,\lambda_1),\quad (H^1,\lambda_2),\quad \dots,\quad (H^{d-1},\lambda_d),$$

of the generalized Jacobi coordinates and the corresponding types of the relativistic quadrics.

Since we will consider the billiard system within ellipsoids in pseudo-Euclidean space, it is of interest to analyze the behaviour of the decorated Jacobi coordinates inside an ellipsoid.

Proposition 3.27. *Let $\mathcal{E}$ be the ellipsoid in $\mathbf{E}^{k,l}$ given by* (2.4). *We have:*

PE1 *each point inside $\mathcal{E}$ is the intersection of exactly d quadrics from* (2.5)*; moreover, all these quadrics are of different relativistic types;*

PE2 *the types of these quadrics are E, H^1, …, H^{d-1}—each type corresponds to one of the disjoint intervals of the parameter λ,*

$$(-a_d,-a_{d-1}),(-a_{d-1},-a_{d-2}),\dots,\ (-a_{k+1},0),(0,a_k),(a_k,a_{k-1}),\dots,(a_2,a_1).$$

Proof. The function given by the left-hand side of (3.11) is continuous and strictly monotonous in each interval $(-a_d,-a_{d-1})$, $(-a_{d-1},-a_{d-2})$, …, $(-a_{k+2},-a_{k+1})$, $(a_k,a_{k-1}),\dots,(a_2,a_1)$ with infinite values at their endpoints. Thus, equation (3.11) has one solution in each of them. On the other hand, in $(-a_{k+1},a_k)$, the function is tending to $+\infty$ at the endpoints and has only one extreme value—the minimum.

Since the value of the function for $\lambda = 0$ is less than 1 for a point inside $\mathcal{E}$, it follows that equation (3.11) will have two solutions in $(-a_{k+1}, a_k)$—one positive and one negative. □

3.3. **Billiards within quadrics and their periodic trajectories.** In this section, we are first going to derive further properties of ellipsoidal billiards in pseudo-Euclidean spaces. We find in Theorem 3.28 a simple and effective criterion for determining the type of a billiard trajectory, knowing its caustics. Then we derive properties PE3–PE5 in Proposition 3.29. After that, we prove the generalization of Poncelet Theorem for the ellipsoidal billiards in the pseudo-Euclidean spaces and derive the corresponding Cayley-type conditions, giving a complete analytical description of the periodic billiard trajectories in arbitrary dimension. These results are contained in Theorems 3.30 and 3.31.

3.3.1. *Ellipsoidal billiards.* The billiard motion within an ellipsoid in pseudo-Euclidean space is a motion which is uniformly straightforward inside the ellipsoid and which obeys the reflection law on the boundary. Further, we will consider the billiard motion within the ellipsoid $\mathcal{E}$, given by equation (2.4), in $\mathbf{E}^{k,l}$. The family of quadrics confocal with $\mathcal{E}$ is (2.5).

Since functions F_i given by (2.9) are integrals of billiard motion (see [Mos1980, Aud1994, KT2009]), we have that for each zero λ of the equation (2.8) the corresponding quadric $\mathcal{Q}_\lambda$ is a caustic of the billiard motion, i.e., it is tangent to each segment of the billiard trajectory passing through point x with velocity vector v.

Note that, according to Theorem 2.20, for a point placed inside $\mathcal{E}$, there are d real solutions of equation (3.11). In other words, there are d quadrics from the family (2.5) containing such a point, although some of them may be multiple. Also, by Proposition 2.19 and Theorem 2.20, a billiard trajectory within an ellipsoid will always have $d-1$ caustics.

According to Remark 2.18, all segments of a billiard trajectory within $\mathcal{E}$ will be of the same type. Now, we can apply the reasoning from Section 2.4 to the billiard trajectories:

Theorem 3.28. *In the d-dimensional pseudo-Euclidean space $\mathbf{E}^{k,l}$, consider a billiard trajectory within ellipsoid $\mathcal{E} = \mathcal{Q}_0$, and let quadrics $\mathcal{Q}_{\alpha_1}, \dots, \mathcal{Q}_{\alpha_{d-1}}$ from the family* (2.5) *be its caustics. Then all billiard trajectories within $\mathcal{E}$ sharing the same caustics are of the same type: space-like, time-like, or light-like, as the initial trajectory. Moreover, the type is determined as follows:*

- *if $\infty \in \{\alpha_1, \dots, \alpha_{d-1}\}$, the trajectories are light-like;*
- *if $(-1)^l \cdot \alpha_1 \cdot \ldots \cdot \alpha_{d-1} > 0$, the trajectories are space-like;*
- *if $(-1)^l \cdot \alpha_1 \cdot \ldots \cdot \alpha_{d-1} < 0$, the trajectories are time-like.*

Proof. Since values of the functions F_i given by (2.9) are preserved by the billiard reflection and

$$\sum_{i=1}^{d} F_i(x, v) = \langle v, v \rangle_{k,l},$$

the type of billiard trajectory depends on the sign of the sum $\sum_{i=1}^{d} F_i(x, v)$. From the equivalence of relations (2.8) and (2.10), it follows that the sum depends only on the roots of $\mathcal{P}$, i.e., on the parameters $\alpha_1, \dots, \alpha_{d-1}$ of the caustics.

Notice that the product $\alpha_1 \cdot \ldots \cdot \alpha_{d-1}$ is changed continuously on the variety of lines in $\mathbf{E}^{k,l}$ that intersect $\mathcal{E}$, with the infinite singularities at the light-like lines. Besides, the subvariety of the light-like lines divides the variety of all lines into the subsets of space-like and time-like ones. When passing through the light-like lines, one of the parameters α_i will pass through infinity from the positive to the negative part of the reals or vice versa. Thus, a change of sign of the product occurs simultaneously with a change of the type of line.

Now, take $\alpha_j = -a_{k+j}$ for $1 \le j \le l$, and notice that all lines placed in the k-dimensional coordinate subspace $\mathbf{E}^k \times \mathbf{0}^l$ will have corresponding degenerate caustics. The reduced metrics is Euclidean in this subspace, thus such lines are space-like. Since $\alpha_1, \ldots, \alpha_k$ are positive for those lines of $\mathbf{E}^k \times \mathbf{0}^l$ that intersect $\mathcal{E}$, the statement is proved. □

Let us note that, in general, for fixed $d-1$ quadrics from the confocal family, there can be found joint tangents of different types, which makes Theorem 3.28 in a way unexpected. However, it turns out that, when the caustics are fixed, only lines having one type may have the intersection with a given ellipsoid—and only these lines give rise to the billiard trajectories.

Next, we are going to investigate the behaviour of the decorated Jacobi coordinates along ellipsoidal billiard trajectories.

Proposition 3.29. *Let $\mathcal{T}$ be a trajectory of the billiard within the ellipsoid $\mathcal{E}$ in the pseudo-Euclidean space $\mathbf{E}^{k,l}$. Denote by $\alpha_1, \ldots, \alpha_{d-1}$ the parameters of the caustics from the confocal family* (2.5) *of $\mathcal{T}$, and take $b_1, \ldots, b_p$, $c_1, \ldots, c_q$ as in Theorem* 2.20. *Then we have:*

PE3 *along $\mathcal{T}$, each generalized Jacobi coordinate takes values in exactly one of the segments,*

$$[c_{2l-1}, c_{2l-2}],\ \ldots,\ [c_2, c_1],\ [c_1, 0],\ [0, b_1],\ [b_2, b_3],\ \ldots,\ [b_{2k-2}, b_{2k-1}];$$

PE4 *along $\mathcal{T}$, each generalized Jacobi coordinate can achieve local minima and maxima only at the touching points with the corresponding caustics, the intersection points with the corresponding coordinate hyperplanes, and at the reflection points;*

PE5 *the values of generalized Jacobi coordinates at the critical points are* 0, $b_1, \ldots, b_{2k-1}, c_1, \ldots, c_{2l-1}$*; between the critical points, the coordinates are changed monotonously.*

Proof. Property PE3 follows from Theorem 2.20. Along each line, the generalized Jacobi coordinates are changed continuously. Moreover, they are monotonous at all points where the line has a transversal intersection with a nondegenerate quadric. Thus, the critical points on a line are exactly the touching points with the corresponding caustics and the intersection points with the corresponding coordinate hyperplanes.

Note that the reflection points of $\mathcal{T}$ are also points of the transversal intersection with all quadrics containing those points, except with $\mathcal{E}$. Thus, at such points, 0 will be a critical value of the corresponding generalized Jacobi coordinate, and all other coordinates are monotonous. This proves PE4 and PE5. □

The properties we obtained are pseudo-Euclidean analogs of properties E3–E5, which are true for ellipsoidal billiards in Euclidean spaces.

3.3.2. *Analytic conditions for periodic trajectories.* Now, we are going to derive the corresponding analytic conditions of Cayley's type for periodic trajectories of ellipsoidal billiards in pseudo-Euclidean space, and therefore to obtain the generalization of the Poncelet Theorem to pseudo-Euclidean spaces.

Theorem 3.30 (Generalized Cayley-type conditions)**.** *In the pseudo-Euclidean space* $\mathbf{E}^{k,l}$ $(k+l=d)$*, consider a billiard trajectory* $\mathcal{T}$ *within the ellipsoid* $\mathcal{E}$ *given by equation* (2.4)*. Let* $\mathcal{Q}_{\alpha_1}, \ldots, \mathcal{Q}_{\alpha_{d-1}}$ *from the confocal family* (2.5) *be the caustics of* $\mathcal{T}$*. Then* $\mathcal{T}$ *is periodic with period* n *if and only if the following conditions are satisfied:*

- *for* $n = 2m$*:*

$$\operatorname{rank}\begin{pmatrix} B_{d+1} & B_{d+2} & \ldots & B_{d+m-1} \\ B_{d+2} & B_{d+3} & \ldots & B_{d+m} \\ \ldots & \ldots & \ldots & \ldots \\ B_{m+1} & B_{m+2} & \ldots & B_{2m-1} \end{pmatrix} < m-d+1 \quad \textit{or}$$

$$\operatorname{rank}\begin{pmatrix} B_{d+1} & B_{d+2} & \ldots & B_{d+m} \\ \ldots & \ldots & \ldots & \ldots \\ B_m & B_{m+1} & \ldots & B_{2m-1} \\ C_m & C_{m+1} & \ldots & C_{2m-1} \\ D_m & D_{m+1} & \ldots & D_{2m-1} \end{pmatrix} < m-d+2;$$

- *for* $n = 2m+1$*:*

$$\operatorname{rank}\begin{pmatrix} B_{d+1} & B_{d+2} & \ldots & B_{d+m} \\ B_{d+2} & B_{d+3} & \ldots & B_{d+m+1} \\ \ldots & \ldots & \ldots & \ldots \\ B_{m+1} & B_{m+2} & \ldots & B_{2m} \\ C_{m+1} & C_{m+2} & \ldots & C_{2m} \end{pmatrix} < m-d+2 \quad \textit{or}$$

$$\operatorname{rank}\begin{pmatrix} B_{d+1} & B_{d+2} & \ldots & B_{d+m} \\ B_{d+2} & B_{d+3} & \ldots & B_{d+m+1} \\ \ldots & \ldots & \ldots & \ldots \\ B_{m+1} & B_{m+2} & \ldots & B_{2m} \\ D_{m+1} & D_{m+2} & \ldots & D_{2m} \end{pmatrix} < m-d+2.$$

Here, (B_i)*,* (C_i)*,* (D_i) *are the coefficients in the Taylor expansions around* $\lambda = 0$ *of the functions* $f(\lambda) = \sqrt{(\alpha_1-\lambda)\cdot\ldots\cdot(\alpha_{d-1}-\lambda)\cdot(a_1-\varepsilon_1\lambda)\cdot\ldots\cdot(a_d-\varepsilon_d\lambda)}$*,* $\frac{f(\lambda)}{b_1-\lambda}$*,* $\frac{f(\lambda)}{c_1-\lambda}$*, respectively.*

Proof. Denote

$$\mathcal{P}_1(\lambda) = (\alpha_1-\lambda)\cdot\ldots\cdot(\alpha_{d-1}-\lambda)\cdot(a_1-\varepsilon_1\lambda)\cdot\ldots\cdot(a_d-\varepsilon_d\lambda).$$

Following Jacobi [Jac1884], along a given billiard trajectory, we consider the integrals

$$\sum_{s=1}^{d}\int\frac{d\lambda_s}{\sqrt{\mathcal{P}_1(\lambda_s)}}, \quad \sum_{s=1}^{d}\int\frac{\lambda_s d\lambda_s}{\sqrt{\mathcal{P}_1(\lambda_s)}}, \quad \ldots, \quad \sum_{s=1}^{d}\int\frac{\lambda_s^{d-2}d\lambda_s}{\sqrt{\mathcal{P}_1(\lambda_s)}}. \tag{3.12}$$

By PE3 of Proposition 3.29, we may suppose that

$$\lambda_1 \in [0, b_1],\ \lambda_i \in [b_{2i-2}, b_{2i-1}] \text{ for } 2 \le i \le k;$$
$$\lambda_{k+1} \in [c_1, 0],\ \lambda_{k+j} \in [c_{2j-1}, c_{2j-2}] \text{ for } 2 \le j \le l.$$

Along a billiard trajectory, by PE4 and PE5 of Proposition 3.29, each λ_s will pass through the corresponding interval monotonously from one endpoint to another and vice versa alternately. Notice also that values $b_1, \ldots, b_{2k-1}, c_1, \ldots, c_{2l-1}$ correspond to the branching points of the hyperelliptic curve

$$\mu^2 = \mathcal{P}_1(\lambda). \tag{3.13}$$

Thus, calculating the integrals (3.12), we get that the billiard trajectory is closed after n reflections if and only if, for some n_1, n_2 such that $n_1 + n_2 = n$,

$$n\mathcal{A}(P_0) \equiv n_1\mathcal{A}(P_{b_1}) + n_2\mathcal{A}(P_{c_1}),$$

on the Jacobian of curve (3.13). Here, $\mathcal{A}$ is the Abel–Jacobi map and P_t is a point on the curve corresponding to $\lambda = t$. Further, in the same manner as in [DR1998b], we obtain the conditions as stated in the theorem. □

As an immediate consequence, we get

Theorem 3.31 (Generalized Poncelet Theorem)**.** *In the pseudo-Euclidean space* $\mathbf{E}^{k,l}$ $(k + l = d)$*, consider a billiard trajectory* $\mathcal{T}$ *within the ellipsoid* $\mathcal{E}$*.*

If $\mathcal{T}$ *is periodic and becomes closed after* n *reflections on the ellipsoid, then any other trajectory within* $\mathcal{E}$ *having the same caustics as* $\mathcal{T}$ *is also periodic with the period* n*.*

Remark 3.32. The generalization of the Full Poncelet Theorem from [CCS1993] to pseudo-Euclidean spaces is obtained in [WFS+2009]. However, only space-like and time-like trajectories were discussed there. A Poncelet-type theorem for the light-like geodesics on the ellipsoid in three-dimensional Minkowski space is proved in [GKT2007].

Remark 3.33. Theorems 3.30 and 3.31 will also hold in symmetric and degenerated cases, that is when some of the parameters $\varepsilon_i a_i$, α_j coincide, or in the case of the light-like trajectories, when $\infty \in \{\alpha_j \mid 1 \le j \le d-1\}$. In such cases, we need to apply the desingularization of the corresponding curve, as explained in detail in our works [DR2006b, DR2008].

When we consider light-like trajectories, then the factor containing the infinite parameter is omitted from the polynomial $\mathcal{P}_1$.

4. Integrable line congruences and double reflection nets

As a modern scientific discipline, discrete differential geometry emerged quite recently (see [BS2008]) within the study of lattice geometry. So-called integrability conditions for quad-graphs have a fundamental role there. On the other hand, geodesics on an ellipsoid are one of the most important and exciting examples of classical differential geometry. Billiard systems within quadrics are known to be seen as natural discretizations of systems of geodesics on ellipsoids. In the sequel we are going to present them as a part of the building blocks of the foundations of discrete differential geometry.

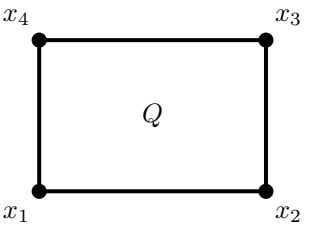

FIGURE 28. Quad-equation $Q(x_1, x_2, x_3, x_4) = 0$

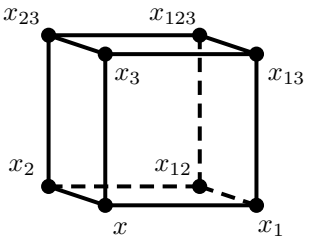

FIGURE 29. 3D-consistency

The main elements of the systems on the quad-graphs are the equations of the form $Q(x, x_1, x_2, x_{12}) = 0$ on quadrilaterals, where Q is a multi-affine polynomial, that is, a polynomial of degree one in each argument. Such equations are called *quad-equations*. The field variables x_i are assigned to the vertices of a quadrilateral as in Figure 28. The quad-equation can be solved for each variable, and the solution is a rational function of the other three variables. Following [ABS2009], we consider the idea of integrability as consistency; see Figure 29. We assign six quad-equations to the faces of a coordinate cube. The system is said to be *3D-consistent* if the three values for x_{123} obtained from the equations on right, back, and top faces coincide for arbitrary initial data.

We will be interested here in a geometric version of integrable quad-graphs, with lines in $\mathbf{P}^d$ playing the role of vertex fields. We will denote by $\mathcal{L}^d$ the Grassmannian $\mathrm{Gr}(2, d+1)$ of the two-dimensional vector subspaces of the $(d+1)$-dimensional vector space, $d \geq 2$.

4.1. **Billiard algebra and quad-graphs.** This section is devoted to a quad-graph interpretation from [DR2012b] of some results obtained previously using billiard algebra.

Let us start with a theorem on confocal families of quadrics from [DR2008]:

Theorem 4.1 (Six-pointed star theorem)**.** *Let $\mathcal{F}$ be a family of confocal quadrics in $\mathbf{P}^3$. There exist configurations consisting of twelve planes in $\mathbf{P}^3$ with the following properties:*

- *The planes may be organized in eight triplets, such that each plane in a triplet is tangent to a different quadric from $\mathcal{F}$, and the three touching points are collinear. Every plane in the configuration is a member of two triplets.*

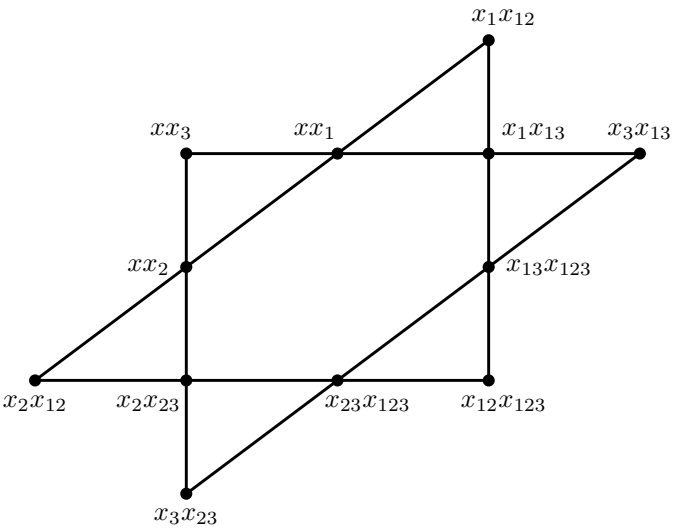

FIGURE 30. A configuration of planes from Theorem 4.1

- *The planes may be organized in six quadruplets, such that the planes in each quadruplet belong to a pencil and are tangent to two different quadrics from $\mathcal{F}$. Every plane in the configuration is a member of two quadruplets.*

Moreover, such a configuration is determined by three planes tangent to three different quadrics from $\mathcal{F}$, with collinear touching points.

Such a configuration of planes in the dual space $\mathbf{P}^{3*}$ is shown in Figure 30; each plane corresponds to a vertex of the polygonal line.

To understand the notation used in Figure 30, let us recall the construction leading to the configurations from Theorem 4.1. Take $\mathcal{Q}_1$, $\mathcal{Q}_2$, $\mathcal{Q}_3$ to be quadrics from $\mathcal{F}$, and α, β, γ, respectively, their tangent planes such that the touching points A, B, C are collinear. Denote by x the line containing these three points, and by x_1, x_2, x_3 the lines obtained from x by the reflections off $\mathcal{Q}_1$, $\mathcal{Q}_2$, $\mathcal{Q}_3$ at A, B, C, respectively.

Now, as in Proposition 2.16, determine lines x_{12}, x_{13}, x_{23}, x_{123} such that they complete the triplets $\{x, x_1, x_2\}$, $\{x, x_1, x_3\}$, $\{x, x_2, x_3\}$, $\{x_3, x_{13}, x_{23}\}$, respectively, to the double reflection configurations.[3]

Notice the following objects in Figure 30:

twelve vertices: to each vertex, a plane tangent to one of the three quadrics $\mathcal{Q}_1$, $\mathcal{Q}_2$, $\mathcal{Q}_3$ and a pair of lines are assigned—the lines of any pair are reflected to each other off the quadric at the touching point with the assigned plane;

eight triangles: in any triangle, the planes assigned to the vertices are touching the corresponding quadrics at three collinear points—thus to each triangle, the line containing these points is naturally assigned;

[3]Let us note that in [DR2008], the lines x, x_1, x_2, x_3, x_{12}, x_{13}, x_{23}, x_{123} were denoted by $\mathcal{O}$, p, q, s, $-x$, p_1, q_1, $x + s$, respectively, where the addition is defined in the billiard algebra introduced in that paper.

six edges: each edge contains four vertices—four planes assigned to these vertices are in the same pencil; thus a double reflection configuration corresponds to each edge.

Now, we are ready to prove the 3D-consistency of the quad-relation introduced via double reflection configurations. The meaning of the following theorem is that reflections on three quadrics commute.

Theorem 4.2. *Let x, x_1, x_2, x_3 be lines in the projective space, such that x_1, x_2, x_3 are obtained from x by reflections off confocal quadrics $\mathcal{Q}_1$, $\mathcal{Q}_2$, $\mathcal{Q}_3$, respectively. Introduce lines x_{12}, x_{13}, x_{23}, x_{123} such that the following quadruplets are double reflection configurations:*

$$\{x, x_1, x_{12}, x_2\}, \quad \{x, x_1, x_{13}, x_3\}, \quad \{x, x_2, x_{23}, x_3\}, \quad \{x_1, x_{12}, x_{123}, x_{13}\}.$$

Then the following quadruplets are also double reflection configurations:

$$\{x_2, x_{12}, x_{123}, x_{23}\}, \quad \{x_3, x_{13}, x_{123}, x_{23}\}.$$

Proof. Let us remark that the configuration described in Theorem 4.1 has obviously a combinatorial structure of the cube, with the planes corresponding to the edges of the cube. In this way, lines x, x_1, x_2, x_3, x_{12}, x_{13}, x_{23}, x_{123} will correspond to the vertices of the cube as shown in Figure 29. A pair of lines is represented by endpoints of an edge if they reflect to each other off the plane joined to this edge. Faces of the cube represent double reflection configurations. Notice also that planes joined to parallel edges of the cube are tangent to a same quadric. The statement follows from Theorem 4.1 and the construction given after; see Figure 30. □

4.2. **Double reflection nets.** Assume a family of confocal quadrics is given in $\mathbf{P}^d$. Notice that, by the Chasles theorem [Cha1827], every line in $\mathbf{P}^d$ touches $d-1$ quadrics from the family.

Moreover, by Corollary 2.12, these $d-1$ quadrics are preserved by the billiard reflection. The confocal quadrics touched by a line are called *the caustics* of that line, or consequently, the caustics of the billiard trajectory that contains the line.

Now, fix $d-1$ quadrics from the pencil, and take $\mathcal{A} \subset \mathcal{L}^d$ to be the set of all lines touching these $d-1$ quadrics.

Definition 4.3. *A double reflection net* is a map

$$\varphi \ : \ \mathbf{Z}^m \to \mathcal{A}, \tag{4.1}$$

such that there exist m quadrics $\mathcal{Q}_1, \ldots, \mathcal{Q}_m$ from the confocal pencil, satisfying the following conditions:

(1) the sequence $\{\varphi(\mathbf{n}_0 + i\mathbf{e}_j)\}_{i\in\mathbf{Z}}$ represents a billiard trajectory within $\mathcal{Q}_j$, for each $j \in \{1, \ldots, m\}$ and $\mathbf{n}_0 \in \mathbf{Z}^m$;
(2) the lines $\varphi(\mathbf{n}_0)$, $\varphi(\mathbf{n}_0 + \mathbf{e}_i)$, $\varphi(\mathbf{n}_0 + \mathbf{e}_j)$, $\varphi(\mathbf{n}_0 + \mathbf{e}_i + \mathbf{e}_j)$ form a double reflection configuration, for all $i, j \in \{1, \ldots, m\}$, $i \neq j$ and $\mathbf{n}_0 \in \mathbf{Z}^m$.

In other words, for each edge in $\mathbf{Z}^m$ of direction $\mathbf{e}_i$, the lines corresponding to its vertices meet at $\mathcal{Q}_i$, while the four tangent planes at the intersection points, associated to an elementary quadrilateral, belong to a pencil.

The image $\varphi(\mathbf{Z}^m)$ can be also described as the set of images of a given line ℓ obtained by all possible sequences of reflections off quadrics $\mathcal{Q}_1, \ldots, \mathcal{Q}_m$. All

images of ℓ lie on a leaf of the Lagrangian foliation $\mathcal{A}$ consisting of the lines that are tangent to the same confocal quadrics as ℓ.

In the following subsections, we describe some examples of double reflection nets. After that, we construct F-transformations of double reflection nets and conclude this section by establishing a connection with Grassmannian Darboux nets from [ABS2009].

4.2.1. *Example of a double reflection net in Minkowski space.* Consider the three-dimensional Minkowski space $\mathbf{E}^{2,1}$. In this space, let a general confocal family be given by (3.6).

Fix $\lambda_0 \in (b, a)$, and consider the hyperboloid $\mathcal{Q}_{\lambda_0}$. Denote by a_1, a_2, a_3, a_4, b_1, b_2, b_3, b_4 the light-like generatrices of $\mathcal{Q}_{\lambda_0}$, in the following way (see Figure 31):

- the lines a_i belong to one family, and b_i to the other, of the generatrices of $\mathcal{Q}_{\lambda_0}$; that is, a_i and a_j are always skew for $i \neq j$, while a_i and b_j are coplanar for all i, j;
- a_1, a_2, b_3, b_4 are tangent to the tropic curve contained in the half-space $z > 0$, while a_3, a_4, b_1, b_2 are touching the other tropic curve;
- a_i is parallel to b_i for each i;

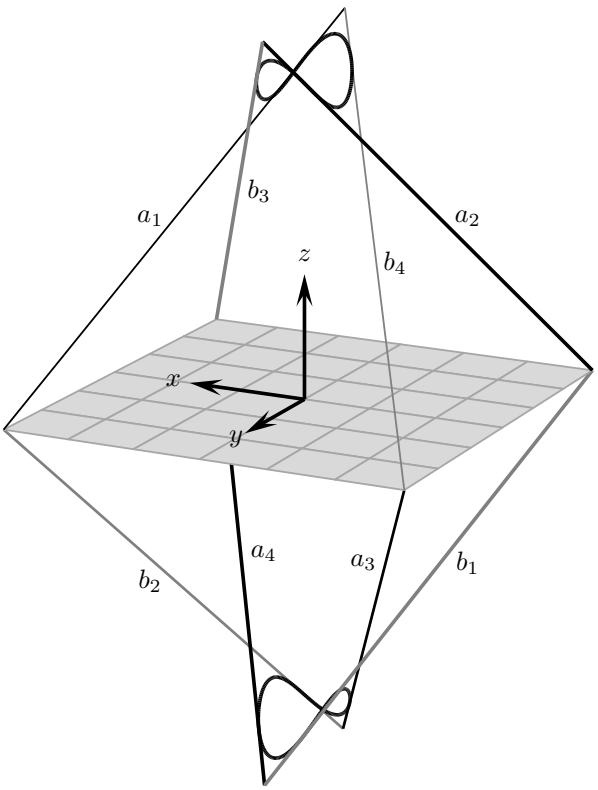

FIGURE 31. The tropic curves of $\mathcal{Q}_{\lambda_0}$ and their light-like tangents

- the pairs (a_1, b_2), (a_2, b_1), (a_3, b_4), (a_4, b_3) have intersection points in the xy-plane;
- the pairs (a_1, b_3), (a_2, b_4), (a_3, b_1), (a_4, b_2) have intersection points in the xz-plane;
- the pairs (a_1, b_4), (a_2, b_3), (a_3, b_2), (a_4, b_1) have intersection points in the yz-plane.

Take $\mathcal{A}$ to be the set of all generatrices of the hyperboloid $\mathcal{Q}_{\lambda_0}$, i.e., the set of all lines having $\mathcal{Q}_{\lambda_0}$ as a double caustic. In particular, $\mathcal{A}$ contains all lines a_i, b_i.

It is possible to define a map

$$\varphi_M \ : \ \mathbf{Z}^4 \to \mathcal{A}$$

such that the image of φ_M is the set $\{a_1, a_2, a_3, a_4, b_1, b_2, b_3, b_4\}$, and for each $\mathbf{n} \in \mathbf{Z}^4$ lines $\varphi_M(\mathbf{n} + \mathbf{e}_1)$, $\varphi_M(\mathbf{n} + \mathbf{e}_2)$, $\varphi_M(\mathbf{n} + \mathbf{e}_3)$, $\varphi_M(\mathbf{n} + \mathbf{e}_4)$ are obtained from $\varphi_M(\mathbf{n})$ by the reflection off $\mathcal{Q}_a$, $\mathcal{Q}_b$, $\mathcal{Q}_{-c}$, $\mathcal{Q}_\infty$, respectively.

More precisely, φ_M will be periodic with period 2 in each coordinate and:

$$\begin{aligned}
&\varphi_M(0,0,0,0) = \varphi_M(1,1,1,1) = a_1, \quad \varphi_M(1,1,0,0) = \varphi_M(0,0,1,1) = a_2,\\
&\varphi_M(1,0,1,0) = \varphi_M(0,1,0,1) = a_3, \quad \varphi_M(0,1,1,0) = \varphi_M(1,0,0,1) = a_4,\\
&\varphi_M(0,0,0,1) = \varphi_M(1,1,1,0) = b_1, \quad \varphi_M(1,1,0,1) = \varphi_M(0,0,1,0) = b_2,\\
&\varphi_M(1,0,1,1) = \varphi_M(0,1,0,0) = a_3, \quad \varphi_M(0,1,1,1) = \varphi_M(1,0,0,0) = b_4.
\end{aligned}$$

It is shown in Figure 32 how vertices of the unit tesseract in $\mathbf{Z}^4$ are mapped by φ_M.

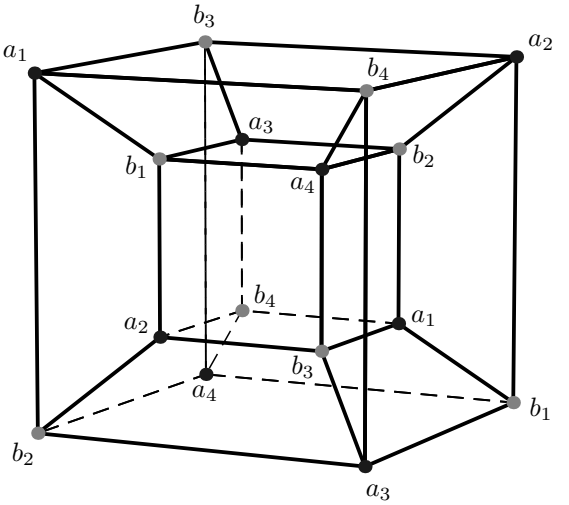

FIGURE 32. Mapping φ_M on the unit tesseract

It is straightforward to prove the following

Proposition 4.4. *φ_M is a double reflection net.*

4.2.2. *Poncelet–Darboux grids and double reflection nets.* Let $\mathcal{E}$ be an ellipse in the Euclidean plane

$$\mathcal{E} \ : \ \frac{x^2}{a} + \frac{y^2}{b} = 1, \quad a > b > 0,$$

and let $(a_i)_{i\in\mathbf{Z}}$ be a billiard trajectory within $\mathcal{E}$.

As is well known, all lines a_i are touching the same conic $\mathcal{C}$ confocal with $\mathcal{E}$; see Section 2.1. Here, we will additionally suppose that $\mathcal{C}$ is an ellipse. Denote by $\mathcal{A}$ the set of tangents of $\mathcal{C}$. Fix m positive integers $k_1, \ldots, k_m$, and define the mapping

$$\varphi_D \ : \ \mathbf{Z}^m \to \mathcal{A}, \quad \varphi_D(n_1, \ldots, n_m) = a_{n_1k_1+\cdots+n_mk_m}.$$

Proposition 4.5. *Map φ_D is a double reflection net.*

Proof. Since $\varphi_D(\mathbf{n} + i\mathbf{e}_j) = a_{n_1k_1+\cdots+n_mk_m+ik_j}$, $(\mathbf{n} = (n_1, \ldots, n_m))$, it follows by [DR2011, Theorem 18] that the sequence $(\varphi_D(\mathbf{n} + i\mathbf{e}_j))_{i\in\mathbf{Z}}$ represents a billiard trajectory within some ellipse $\mathcal{E}_j$, confocal with $\mathcal{E}$ and $\mathcal{C}$.

Immediately, by Definition 2.13, lines $\varphi(\mathbf{n}_0)$, $\varphi(\mathbf{n}_0 + \mathbf{e}_i)$, $\varphi(\mathbf{n}_0 + \mathbf{e}_j)$, $\varphi(\mathbf{n}_0 + \mathbf{e}_i + \mathbf{e}_j)$ form a virtual reflection configuration for each $\mathbf{n}_0 \in \mathbf{Z}^m$, $i, j \in \{1, \ldots, m\}$. Moreover, by Proposition 2.15, they also form a double reflection configuration. □

Remark 4.6. It is interesting to consider only those nets where the m ellipses $\mathcal{E}_j$ appearing in the proof of Proposition 4.5 are distinct. If some of them coincide, then we may consider the corresponding subnet.

Suppose that (a_i) is a nonperiodic trajectory. Then, choosing any m and any set of distinct positive numbers $k_1, \ldots, k_m$, we get substantially different double reflection nets.

For (a_i) being n-periodic, it is enough to consider the case where $k_i = i$, $i \in \{1, \ldots, [n/2]\}$, $(m = [n/2])$.

Example 4.7. Suppose (a_i) is a 5-periodic billiard trajectory within $\mathcal{E}$; see Figure 33. The corresponding double reflection net is

$$\varphi_D \ : \ \mathbf{Z}^2 \to \mathcal{A}, \quad \varphi_D(n_1, n_2) = a_{n_1+2n_2}.$$

4.2.3. *s-skew lines and double reflection nets.* Now, let us consider a family of confocal quadrics in $\mathbf{E}^d$ $(d \geq 3)$ and fix its $d-1$ quadrics. As usual, $\mathcal{A}$ is the set of all lines tangent to the fixed quadrics.

It is shown in [DR2008] that, from a line in $\mathcal{A}$, we can obtain any other line from that set in at most $d-1$ reflections on quadrics from the confocal family. We called lines a, b from $\mathcal{A}$ *s-skew* if s is the smallest number such that they can be obtained by $s+1$ such reflections.

Now, suppose lines a, b are s-skew $(s \geq 1)$, and let $\mathcal{Q}_1, \ldots, \mathcal{Q}_{s+1}$ be the corresponding quadrics from the confocal family.

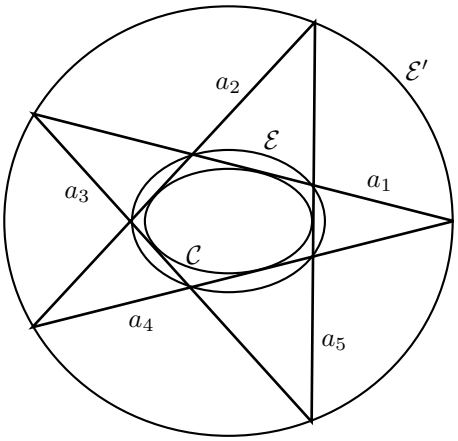

FIGURE 33. A Poncelet pentagon

Theorem 4.8. *There is a unique double reflection net*

$$\varphi_s \ : \ \mathbf{Z}^{s+1} \to \mathcal{A},$$

which satisfies the following:

- $\varphi_s(0,\dots,0) = a$*;*
- $\varphi_s(1,\dots,1) = b$*;*
- $\{\varphi(\mathbf{n}_0 + i\mathbf{e}_j)\}_{i\in\mathbf{Z}}$ *represents a billiard trajectory within* $\mathcal{Q}_j$*, for each* $j \in \{1,\dots,s+1\}$ *and* $\mathbf{n}_0 \in \mathbf{Z}^{s+1}$*.*

Proof. First, we are going to define a mapping φ_s on $\{0,1\}^{s+1}$.

For a permutation $\mathbf{p} = (p_1,\dots,p_{s+1})$ of the set $\{1,\dots,s+1\}$, we take a sequence of lines $(\ell_0^{\mathbf{p}},\dots,\ell_{s+1}^{\mathbf{p}})$ such that $\ell_0^{\mathbf{p}} = a$, $\ell_s^{\mathbf{p}} = b$, and $\ell_{i-1}^{\mathbf{p}}$, $\ell_i^{\mathbf{p}}$ satisfy the reflection law off $\mathcal{Q}_{p_i}$ for each $i \in \{1,\dots,s+1\}$. Such a sequence exists and is unique. Moreover, if $k \in \{1,\dots,s+1\}$ is given and permutations $\mathbf{p}$, $\mathbf{p}'$ coincide in the first k coordinates, then $\ell_i^{\mathbf{p}} = \ell_i^{\mathbf{p}'}$ for $i \le k$. Take $\{i_1,\dots,i_k\}$ to be a subset of $\{1,\dots,s+1\}$, and $\mathbf{p}$ any permutation of set $\{1,\dots,s+1\}$ with $p_1 = i_1$, …, $p_k = i_k$. We define

$$\varphi_s(\chi(1),\dots,\chi(s+1)) = \ell_k^{\mathbf{p}},$$

where $\chi = \chi_{\{i_1,\dots,i_k\}}$ is the corresponding characteristic function on $\{1,\dots,s+1\}$:

$$\chi \ : \ \{1,\dots,s+1\} \to \{0,1\}, \quad \chi(j) = \begin{cases} 1, & j \in \{i_1,\dots,i_k\}; \\ 0, & j \notin \{i_1,\dots,i_k\}. \end{cases}$$

In this way, we have constructed φ_s on $\{0,1\}^{s+1}$.

Subsequently, φ_s can be extended to the rest of $\mathbf{Z}^{s+1}$, so that $\{\varphi_s(\mathbf{n}_0 + i\mathbf{e}_j)\}_{i\in\mathbf{Z}}$ will represent billiard trajectories within $\mathcal{Q}_j$.

This construction is correct and unique due to Theorem 4.2. □

4.2.4. *Construction of double reflection nets.* Let $\mathcal{Q}_1,\dots,\mathcal{Q}_m$ be distinct quadrics belonging to a confocal family, and let ℓ be a line in $\mathbf{P}^d$. Let us choose lines ℓ_i satisfying with ℓ the reflection law off $\mathcal{Q}_i$, $1 \le i \le m$.

Theorem 4.9. *There is a unique double reflection net $\varphi : \mathbf{Z}^m \to \mathcal{A}_\ell$, with the following properties:*

- $\varphi(0,\dots,0) = \ell$;
- $\varphi(\mathbf{e}_i) = \ell_i$, *for each* $i \in \{1,\dots,m\}$.

By $\mathcal{A}_\ell$, we denote the set of all lines in $\mathbf{P}^d$ touching the same $d-1$ quadrics from the confocal family as ℓ.

Proof. First we define φ on $\{0,1\}^m$ from the condition that lines corresponding to each 2-face of the unit cube need to form a double reflection configuration. This construction is unique because of Proposition 2.16, and it is correct due to the 3D-consistency property proved in Theorem 4.2.

At all other points of $\mathbf{Z}^m$, φ is uniquely defined from the request that $\{\varphi(\mathbf{n}_0 + i\mathbf{e}_j)\}_{i\in\mathbf{Z}}$ will be the billiard trajectories within $\mathcal{Q}_j$.

Consistency of the construction follows again from Theorem 4.2. □

4.2.5. *Focal nets and F-transformations of double reflection nets.* Let $\varphi : \mathbf{Z}^m \to \mathcal{A}$ be a double reflection net. Its *i-th focal net* is the map $F^{(i)} : \mathbf{Z}^m \to \mathbf{P}^d$ defined by $F^{(i)}(\mathbf{n}) = \varphi(\mathbf{n}) \cap \varphi(\mathbf{n} + \mathbf{e}_i)$ [BS2008].

For given $\mathbf{n}_0 \in \mathbf{Z}^m$ and distinct indices $i, j, k \in \{1,\dots m\}$, consider the following points of its i-th focal net:

$$F_i = F^{(i)}(\mathbf{n}_0) = \varphi(\mathbf{n}_0) \cap \varphi(\mathbf{n}_0 + \mathbf{e}_i),$$
$$F_{ij} = F^{(i)}(\mathbf{n}_0 + \mathbf{e}_j) = \varphi(\mathbf{n}_0 + \mathbf{e}_j) \cap \varphi(\mathbf{n}_0 + \mathbf{e}_j + \mathbf{e}_i),$$
$$F_{ik} = F^{(i)}(\mathbf{n}_0 + \mathbf{e}_k) = \varphi(\mathbf{n}_0 + \mathbf{e}_k) \cap \varphi(\mathbf{n}_0 + \mathbf{e}_k + \mathbf{e}_i),$$
$$F_{ijk} = F^{(i)}(\mathbf{n}_0 + \mathbf{e}_j + \mathbf{e}_k) = \varphi(\mathbf{n}_0 + \mathbf{e}_j + \mathbf{e}_k) \cap \varphi(\mathbf{n}_0 + \mathbf{e}_j + \mathbf{e}_k + \mathbf{e}_i).$$

Proposition 4.10. *Points F_i, F_{ij}, F_{ik}, F_{ijk} are coplanar.*

Proof. This is a consequence of the theorem of focal nets from [BS2008]. However, we will show the direct proof, from configurations considered in Section 4.1.

The four points belong to quadric $\mathcal{Q}_i$. The tangent planes to $\mathcal{Q}_i$ at these points, divided into two pairs, determine two pencils of planes. According to Theorem 4.1, the two pencils are coplanar; thus they intersect. As a consequence, the lines of poles with respect to the quadric $\mathcal{Q}_i$, which correspond to these two pencils of planes, also intersect. It follows that the four points are coplanar. □

Two double reflection nets $\varphi, \varphi^+ : \mathbf{Z}^m \to \mathcal{A}$ are said to be *related by an F-transformation* if for every $\mathbf{n} \in \mathbf{Z}^m$ the corresponding lines $\varphi(\mathbf{n})$ and $\varphi^+(\mathbf{n})$ intersect [BS2008].

We are going to construct an F-transformation of the double reflection net.

First, we select a quadric $\mathcal{Q}_\delta$ from the confocal family and introduce a line ℓ' which satisfies with $\varphi(\mathbf{n}_0)$ the reflection law off $\mathcal{Q}_\delta$.

By Theorem 4.9, it is possible to construct a double reflection net $\bar\varphi : \mathbf{Z}^{m+1} \to \mathcal{A}$, such that:

- $\bar\varphi(\mathbf{n}, 0) = \varphi(\mathbf{n})$;
- $\bar\varphi(\mathbf{n}_0, 1) = \ell'$.

Now, we define

$$\varphi^+ \ : \ \mathbf{Z}^m \to \mathcal{A}, \quad \varphi^+(\mathbf{n}) = \bar{\varphi}(\mathbf{n}, 1).$$

Proposition 4.11. *Map φ^+ is an F-transformation of φ.*

Proof. Lines $\varphi^+(\mathbf{n})$ and $\varphi(\mathbf{n})$ meet, since they satisfy the reflection law off $\mathcal{Q}_\delta$. □

In other words, the double reflection nets φ, φ^+ are obtained from each other by reflecting the corresponding lines off a single quadric, $\mathcal{Q}_\delta$.

4.2.6. *Double reflection nets and Grassmannian Darboux nets.* Let us recall the definition of a Grassmannian Darboux net from [ABS2009]: a map from the edges of a regular square lattice $\mathbf{Z}^m$ to the Grassmannian $\mathbf{G}_r^d$ of the r-dimensional projective subspaces of the d-dimensional projective space is *a Grassmannian Darboux net* if the four r-spaces of an elementary quadrilateral belong to a $(2r+1)$-space. For $r = 0$, the ordinary Darboux nets from [Sch2003] are obtained, where the four points of intersection associated to a quadrilateral belong to a line.

Now, consider the general double reflection net (4.1).

To each edge $(\mathbf{n_0}, \mathbf{n_0} + \mathbf{e}_i)$ of $\mathbf{Z}^m$, we can associate the plane which is tangent to $\mathcal{Q}_i$ at point $\varphi(\mathbf{n_0}) \cap \varphi(\mathbf{n_0} + \mathbf{e}_i)$. Since the lines corresponding to the vertices of a face form a double reflection configuration, the four planes associated to the edges belong to a pencil.

In this way, we see that a double reflection net induces a map

$$E(\mathbf{Z}^m) \to \mathbf{G}_{d-1}^d,$$

where $E(\mathbf{Z}^m)$ is the set of all edges of the integer lattice $\mathbf{Z}^m$. Thus the double reflection nets induce a subclass of dual Darboux nets.

It was shown in [Sch2003] how to associate discrete integrable hierarchies to the Darboux nets.

4.3. **Yang–Baxter map.** *A Yang–Baxter map* is a map $R : \mathcal{X} \times \mathcal{X} \to \mathcal{X} \times \mathcal{X}$, satisfying the Yang–Baxter equation,

$$R_{23} \circ R_{13} \circ R_{12} = R_{12} \circ R_{13} \circ R_{23},$$

where $R_{ij} : \mathcal{X} \times \mathcal{X} \times \mathcal{X} \to \mathcal{X} \times \mathcal{X} \times \mathcal{X}$ acts as R on the i-th and j-th factor in the product and as the identity on the remaining one; see [ABS2004] and references therein.

Here, we are going to construct an example of the Yang–Baxter map associated to the confocal families of quadrics. To begin, we fix a family of confocal quadrics in $\mathbf{CP}^n$:

$$\mathcal{Q}_\lambda \ : \ \frac{z_1^2}{a_1 - \lambda} + \cdots + \frac{z_d^2}{a_d - \lambda} = z_{n+1}^2, \tag{4.2}$$

where $a_1, \ldots, a_d$ are constants in $\mathbf{C}$, and $[z_1 : z_2 : \cdots : z_{n+1}]$ are the homogeneous coordinates in $\mathbf{CP}^n$.

Take $\mathcal{X}$ to be the space $\mathbf{CP}^{n*}$ dual to the n-dimensional projective space, i.e., the variety of all hyperplanes in $\mathbf{CP}^n$. Note that a general hyperplane in the space is tangent to exactly one quadric from family (4.2). Besides, in a general pencil of hyperplanes, there are exactly two of them tangent to a fixed general quadric.

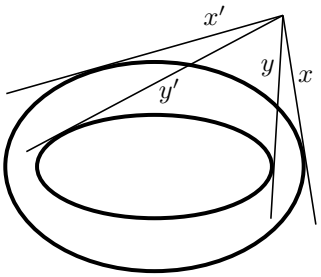

FIGURE 34. $R(x, y) = (x', y')$

Now, consider a pair x, y of hyperplanes. They are touching, respectively, unique quadrics $\mathcal{Q}_\alpha$, $\mathcal{Q}_\beta$ from (4.2). Besides, these two hyperplanes determine a pencil of hyperplanes. This pencil contains unique hyperplanes x', y', other than x, y, that are tangent to $\mathcal{Q}_\alpha$, $\mathcal{Q}_\beta$, respectively; as shown on Figure 34.

We define $R : \mathbf{CP}^{n*} \times \mathbf{CP}^{n*} \to \mathbf{CP}^{n*} \times \mathbf{CP}^{n*}$, in such a way that $R(x, y) = (x', y')$ if (x', y') are obtained from (x, y) as just described, see Figure 34.

Maps

$$R_{12},\ R_{13},\ R_{23}\ :\ \mathbf{CP}^{n*} \times \mathbf{CP}^{n*} \times \mathbf{CP}^{n*} \to \mathbf{CP}^{n*} \times \mathbf{CP}^{n*} \times \mathbf{CP}^{n*}$$

are then defined as follows

$$\begin{aligned} R_{12}(x, y, z) &= (x', y', z) \quad \text{for} \quad (x', y') = R(x, y), \\ R_{13}(x, y, z) &= (x', y, z') \quad \text{for} \quad (x', z') = R(x, z), \\ R_{23}(x, y, z) &= (x, y', z') \quad \text{for} \quad (y', z') = R(y, z). \end{aligned}$$

To prove the Yang–Baxter equation for the map R, we will need

Lemma 4.12. *Let $\mathcal{Q}_\alpha$, $\mathcal{Q}_\beta$, $\mathcal{Q}_\gamma$ be three nondegenerate quadrics from family* (4.2) *and x, y, z, respectively, their tangent hyperplanes. Take*

$$(x_2, y_1) = R(x, y), \quad (x_3, z_1) = R(x, z), \quad (y_3, z_2) = R(y, z).$$

Let x_{23}, y_{13}, z_{12} be the joint hyperplanes of pencils determined by the pairs (x_3, y_3) and (x_2, z_2), (x_3, y_3) and (y_1, z_1), and (y_1, z_1) and (x_2, z_2), respectively. Then x_{23}, y_{13}, z_{12} touch the quadrics $\mathcal{Q}_\alpha$, $\mathcal{Q}_\beta$, $\mathcal{Q}_\gamma$, respectively.

Proof. This statement, formulated for the dual space in dimension $n = 2$, is proved as [ABS2004, Theorem 5].

Consider the dual situation in an arbitrary dimension n. The dual quadrics $\mathcal{Q}^*_\alpha$, $\mathcal{Q}^*_\beta$, $\mathcal{Q}^*_\gamma$ belong to a linear pencil, and points x^*, y^*, z^*, dual to the hyperplanes x, y, z, are respectively placed on these quadrics. Take the two-dimensional plane containing these three points. The intersection of the pencil of quadrics with that, and any other plane as well, represents a pencil of conics. Thus, Theorem 5 from [ABS2004] will remain true in any dimension.

This lemma is dual to that theorem, thus the proof is complete. □

Theorem 4.13. *The map R satisfies the Yang–Baxter equation.*

Proof. Let x, y, z be hyperplanes in $\mathbf{CP}^n$. We want to prove that

$$R_{23} \circ R_{13} \circ R_{12}(x, y, z) = R_{12} \circ R_{13} \circ R_{23}(x, y, z).$$

Denote by $\mathcal{Q}_\alpha$, $\mathcal{Q}_\beta$, $\mathcal{Q}_\gamma$ the quadrics from (4.2) touching x, y, z, respectively.

Let

$$(x, y, z) \xrightarrow{R_{12}} (x_2, y_1, z) \xrightarrow{R_{13}} (x_{23}, y_1, z_1) \xrightarrow{R_{23}} (x_{23}, y_{13}, z_{12}),$$

$$(x, y, z) \xrightarrow{R_{23}} (x, y_3, z_2) \xrightarrow{R_{13}} (x_3, y_3, z'_{12}) \xrightarrow{R_{12}} (x'_{23}, y'_{13}, z'_{12}).$$

Now, apply Lemma 4.12 to the hyperplanes x, y, z_2. Since

$$(x_2, y_1) = R(x, y), \quad (x_3, z'_{12}) = R(x, z_2), \quad (y_3, z) = R(y, z_2),$$

we have that the joint hyperplane of the pencils (x_3, y_3) and (x_2, z) is touching $\mathcal{Q}_\alpha$; therefore, this plane must coincide with x_{23} and x'_{23}, i.e., $x_{23} = x'_{23}$. Also, the joint hyperplane of the pencils (y_1, z'_{12}) and (x_2, z) is touching $\mathcal{Q}_\gamma$; therefore, this is z_1 and $z_{12} = z'_{12}$. Finally, the joint hyperplane of pencils (x_3, y_3) and (y_1, z'_{12}) is tangent to $\mathcal{Q}_\beta$. It follows this is $y_{13} = y'_{13}$, which completes the proof. □

Remark 4.14. Instead of defining R to act on the whole space $\mathbf{CP}^{n*} \times \mathbf{CP}^{n*}$, we can restrict it to the product of two nondegenerate quadrics from (4.2), namely,

$$R(\alpha, \beta) \ : \ \mathcal{Q}^*_\alpha \times \mathcal{Q}^*_\beta \to \mathcal{Q}^*_\alpha \times \mathcal{Q}^*_\beta,$$

where a pair (x, y) of tangent hyperplanes is mapped into a pair (x_1, y_1) in such a way that x, y, x_1, y_1 belong to the same pencil.

The corresponding Yang–Baxter equation is

$$R_{23}(\beta, \gamma) \circ R_{13}(\alpha, \gamma) \circ R_{12}(\alpha, \beta) = R_{12}(\alpha, \beta) \circ R_{13}(\alpha, \gamma) \circ R_{23}(\alpha, \beta),$$

where both sides of the equation represent maps from $\mathcal{Q}^*_\alpha \times \mathcal{Q}^*_\beta \times \mathcal{Q}^*_\gamma$ to itself.

In [ABS2004], for irreducible algebraic varieties $\mathcal{X}_1$ and $\mathcal{X}_2$, *a quadrirational mapping* $F \ : \ \mathcal{X}_1 \times \mathcal{X}_2 \to \mathcal{X}_1 \times \mathcal{X}_2$ is defined. For such a map F and any fixed pair $(x, y) \in \mathcal{X}_1 \times \mathcal{X}_2$, except from some closed subvarieties of codimension bigger or equal to 1, the graph $\Gamma_F \subset \mathcal{X}_1 \times \mathcal{X}_2 \times \mathcal{X}_1 \times \mathcal{X}_2$ intersects each of the sets $\{x\} \times \{y\} \times \mathcal{X}_1 \times \mathcal{X}_2$, $\mathcal{X}_1 \times \mathcal{X}_2 \times \{x\} \times \{y\}$, $\mathcal{X}_1 \times \{y\} \times \{x\} \times \mathcal{X}_2$, $\{x\} \times \mathcal{X}_2 \times \mathcal{X}_1 \times \{y\}$ at exactly one point (see [ABS2004, Definition 3]). In other words, Γ_F is the graph of four rational maps, F, F^{-1}, $\bar{F}$, $\bar{F}^{-1}$.

The following proposition is a generalization of [ABS2004, Proposition 4].

Proposition 4.15. *The map $R(\alpha, \beta) \ : \ \mathcal{Q}^*_\alpha \times \mathcal{Q}^*_\beta \to \mathcal{Q}^*_\alpha \times \mathcal{Q}^*_\beta$ is quadrirational. It is an involution, and it coincides with its companion $\bar{R}(\alpha, \beta)$.*

5. Pseudo-integrable billiards and the local Poncelet Theorem

5.1. **Billiards in domains bounded by a few confocal conics.** In this section we analyze the billiard dynamics in a domain bounded by arcs of a few confocal conics, such that there are reflex angles on the boundary. In order to describe some phenomena appearing in such systems, let us consider the domain $\mathcal{D}_0$ bounded by two confocal ellipses from family (2.1) and two segments placed on the smaller axis of theirs, as shown in Figure 35.

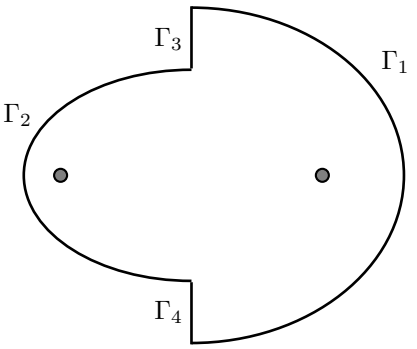

FIGURE 35. Domain bounded by two confocal ellipses and two segments on the y-axis

More precisely, we fix parameters β_1, β_2 such that $\beta_1 < \beta_2 < b$, and take the border of $\mathcal{D}_0$ to be

$$\begin{aligned}
\partial\mathcal{D}_0 &= \Gamma_1 \cup \Gamma_2 \cup \Gamma_3 \cup \Gamma_4,\\
\Gamma_1 &= \{(x,y) \in \mathcal{C}_{\beta_1} \mid x \geq 0\},\\
\Gamma_2 &= \{(x,y) \in \mathcal{C}_{\beta_2} \mid x \leq 0\},\\
\Gamma_3 &= \{(0,y) \mid \sqrt{b-\beta_2} \leq y \leq \sqrt{b-\beta_1}\},\\
\Gamma_4 &= \{(0,y) \mid -\sqrt{b-\beta_1} \leq y \leq -\sqrt{b-\beta_2}\}.
\end{aligned}$$

Notice that segments Γ_3, Γ_4 are lying on the the degenerate conic $\mathcal{C}_a$ of family (2.1).

By the Chasles theorem [Cha1827], as we have already mentioned in Section 2.1, each line in the plane is touching exactly one conic from a given confocal family; moreover, this conic remains the same after the reflection off any conic from the family. Thus, each billiard trajectory in a domain bounded by arcs of several confocal conics has a caustic from the confocal family.

Consider the billiard trajectories within domain $\mathcal{D}_0$ whose caustic is an ellipse, and denote it by $\mathcal{C}_{\alpha_0}$. In addition, we assume that $\mathcal{C}_{\alpha_0}$ is completely placed inside the billiard table, i.e., $\beta_2 < \alpha_0 < b$. An example of such a trajectory is shown in Figure 36.

Such billiard trajectories fill out the ring $\mathcal{R}$ placed between the billiard border and the caustic, see Figure 37.

Let us examine the leaf of the phase space composed by those trajectories. The leaf is naturally decomposed into four rings equal to $\mathcal{R}$, which are glued to each other along the border arcs. We describe the gluing in detail:

- $\mathcal{R}_1$ This ring contains the points in the phase space that correspond to the billiard particle moving away from the caustic and the clockwise direction around the coordinate centre.
- $\mathcal{R}_2$ Corresponds to the motion away from the caustic in the counterclockwise direction.
- $\mathcal{R}_3$ Corresponds to the motion towards the caustic in the counterclockwise direction.
- $\mathcal{R}_4$ Corresponds to the motion towards the caustic in the clockwise direction.

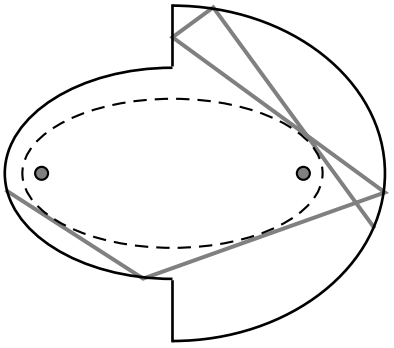

FIGURE 36. A billiard trajectory in $\mathcal{D}_0$ with an ellipse as caustic

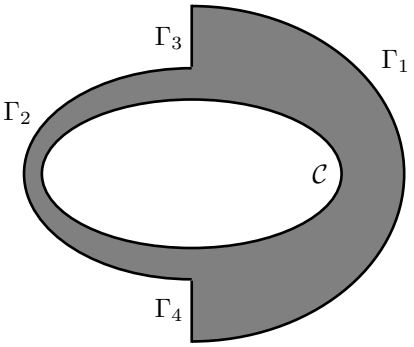

FIGURE 37. Ring $\mathcal{R}$

Notice that the reflection off the two ellipse arcs contained in the billiard boundary changes the direction of the particle motion with respect to the caustic, but it preserves the direction of the motion around the centre. The same holds for passing through the tangency points with the caustic. On the other hand, the reflection off the axis changes the direction of motion around the centre, but preserves the direction with respect to the caustic. Thus, the four rings are glued to each other according to the following scheme.

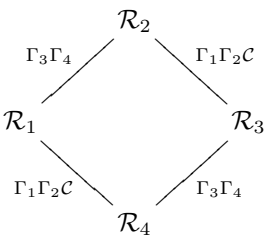

Let us represent all the rings in Figures 38 and 39.

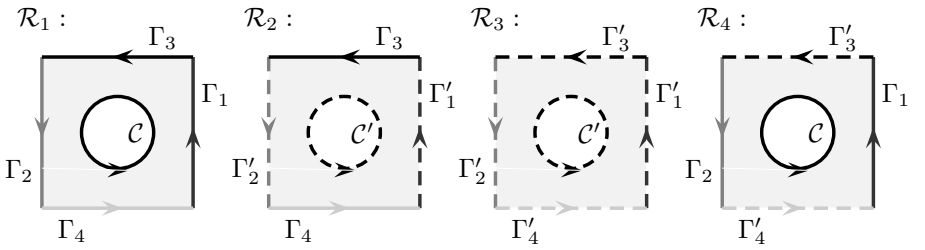

FIGURE 38. Rings $\mathcal{R}_1$, $\mathcal{R}_2$, $\mathcal{R}_3$, $\mathcal{R}_4$

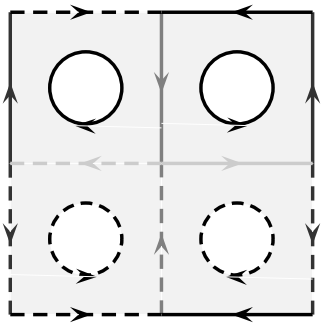

FIGURE 39. Gluing rings $\mathcal{R}_1$, $\mathcal{R}_2$, $\mathcal{R}_3$, $\mathcal{R}_4$

Now, we have

Proposition 5.1. *All the billiard trajectories within domain $\mathcal{D}_0$ with the fixed caustic $\mathcal{C}_{\alpha_0}$ form an orientable surface of genus* 3.

In contrast, notice that the leaves for the billiard within an ellipse are tori (see Figures 8 and 9 from Section 2).

5.2. **Topological estimates.** Now we consider a more general billiard desk shape. Let $\mathcal{D}$ be a bounded domain in the plane such that its boundary $\Gamma = \partial\mathcal{D}$ is the union of finitely many arcs of confocal conics from the family (2.1). Any trajectory of that billiard has a caustic, which will be a conic from (2.1) touching all lines containing the segments of the trajectory. Let us fix $\mathcal{C}_{\lambda_0}$ as the caustic.

Notice that all tangent lines of a conic fill out an infinite domain in the plane: if the conic is an ellipse, the domain is its exterior; for a hyperbola, it is the part of the plane between its branches.

Denote by $\mathcal{D}_{\lambda_0}$ the intersection of $\mathcal{D}$ with the domain containing the tangent lines of caustic $\mathcal{C}_{\lambda_0}$. All billiard trajectories with the caustic $\mathcal{C}_{\lambda_0}$ are placed within $\mathcal{D}_{\lambda_0}$, which is a bounded set whose boundary $\Gamma_{\lambda_0} = \partial\mathcal{D}_{\lambda_0}$ is the union of finitely many arcs of conics from (2.1). We assume that $\mathcal{D}_{\lambda_0}$ is connected as well; otherwise, we consider its connected component.

All billiard trajectories in the domain $\mathcal{D}$ with the caustic $\mathcal{C}_{\lambda_0}$ will correspond to a certain compact leaf $\mathcal{M}(\lambda_0)$ in the phase space. $\mathcal{M}_{\lambda_0}$ is obtained by gluing four copies of $\mathcal{D}_{\lambda_0}$ along the corresponding arcs of the boundary $\Gamma_{\lambda_0} = \partial\mathcal{D}_{\lambda_0}$, similarly as it is explained in Section 5.1.

On $\mathcal{M}_{\lambda_0}$ the singular points of the billiard flow correspond to vertices of reflex angles on the boundary of $\mathcal{D}_{\lambda_0}$. Since confocal conics are orthogonal to each other at the points of intersection, only two types of such angles may appear: full angles and angles of 270°. The vertex of a full angle is the projection of two singular points from the phase space, each one having four separatrices. On the other hand, a vertex of 270° is the projection of only one singular point, which has six separatrices.

Using the Euler–Poincaré formula, as in [Via2008], we get the following estimate for the total number $N = N(\mathcal{M}_{\lambda_0})$ of saddle-connections:

Proposition 5.2. *The total number $N = N(\mathcal{M}_{\lambda_0})$ of saddle-connections is bounded from above:*

$$N(\mathcal{M}_{\lambda_0}) \leq \frac{1}{2}\sum_{i=1}^{k} s_i = k - \chi(\mathcal{M}_{\lambda_0}),$$

where k is the number of singular points of the flow on $\mathcal{M}_{\lambda_0}$ and $s_1, \ldots, s_k$ are the numbers of separatrices at each singular point.

As a corollary, we get

Proposition 5.3. *Consider the billiard within $\mathcal{D}$ with the caustic $\mathcal{C}_{\lambda_0}$. If the corresponding subdomain $\mathcal{D}_{\lambda_0}$ has $\tilde{k}$ reflex angles on its boundary Γ_{λ_0}, then*

- $N \leq 3\tilde{k}$;
- $g(\mathcal{M}_{\lambda_0}) = \tilde{k} + 1$.

Notice that the genus of surface $\mathcal{M}_{\lambda_0}$ depends only on the number of reflex angles on the boundary of $\mathcal{D}_{\lambda_0}$ and not of their types. Also, $\tilde{k} \leq k$.

Example 5.4.
- If there are no reflex angles on the boundary, i.e., $k = 0$, then $\mathcal{M}_{\lambda_0}$ is a torus: $g = 1$, $N = 0$.
- If there is only one reflex angle on the boundary, we have that $g = 2$.

We finish this subsection by formulating an analogue of the Liouville–Arnold theorem for pseudo-integrable billiard systems, which is a consequence of the Maier theorem from the theory of measured foliations (see [Mai1943, Via2008]). In our case, the measured foliation is defined by the kernel of the closed 1-form

$$w = \frac{d\lambda_1}{\sqrt{(a-\lambda_1)(b-\lambda_1)(\lambda_0-\lambda_1)}} + \frac{d\lambda_2}{\sqrt{(a-\lambda_2)(b-\lambda_2)(\lambda_0-\lambda_2)}},$$

where λ_1, λ_2 are the Jacobian coordinates associated to the confocal family (2.1).

Theorem 5.5. *There exist pairwise disjoint open domains $D_1, \ldots, D_n$ on $\mathcal{M}_{\lambda_0}$, each of them being invariant under the billiard flow, such that their closures cover $\mathcal{M}_{\lambda_0}$ and for each $j \in \{1, \ldots, n\}$,*

- *either D_j consists of periodic billiard trajectories and is homeomorphic to a cylinder*
- *or D_j consists of nonperiodic trajectories all of which are dense in D_j.*

The boundary of each D_j consists of saddle-connections.

In contrast to the completely integrable Hamiltonian systems, compact leaves of our billiards could be of a genus greater than 1. Moreover, one leaf could contain several regions with periodic trajectories, each region having its own different

period, along with several regions where the motion is nonperiodic. Because of that, we call such systems *pseudo-integrable*, taking into account the fact that they possess two independent commuting first integrals, as has been shown in Section 2.1.

5.3. **The Poncelet Theorem and Cayley-type conditions.** As in Section 5.2, we consider a billiard within a bounded domain $\mathcal{D}$ whose boundary $\Gamma = \partial\mathcal{D}$ is the union of finitely many arcs of confocal conics from the family (2.1). We fix $\mathcal{C}_{\lambda_0}$ as a caustic and denote by $\mathcal{D}_{\lambda_0}$ the intersection of $\mathcal{D}$ with the domain containing tangent lines of caustic $\mathcal{C}_{\lambda_0}$. Then $\Gamma'_{\lambda_0} = \Gamma \cap \partial\mathcal{D}_{\lambda_0}$ is the union of finitely many arcs of conics from (2.1).

Theorem 5.6. *There exist subsets $\delta_1, \dots, \delta_n$ of Γ'_{λ_0}, with the properties:*

- *$\delta_1, \dots, \delta_n$ are invariant under the billiard map;*
- *$\delta_1, \dots, \delta_n$ are pairwise disjoint;*
- *each δ_i is a finite union of d_i open subarcs of Γ'_{λ_0}*

$$\delta_i = \bigcup_{j=1}^{d_i} \ell_j^i;$$

- *closure of $\delta_1 \cup \dots \cup \delta_N$ is Γ'_{λ_0},*

such that they satisfy the following.

- *If one billiard trajectory with bouncing points within δ_i is periodic, then all such trajectories are periodic with the same period n_i. Moreover, n_i is a multiple of d_i, and every such a trajectory bounces the same number $\frac{n_i}{d_i}$ of times off each arc ℓ_j^i.*
- *If the billiard trajectories having vertices in δ_i are nonperiodic, then the bouncing points of each trajectory are dense in δ_i.*

The boundary of each δ_i consists of bouncing points of saddle-connections.

This theorem is a consequence of Theorem 5.5 from the previous section. The proof follows from the fact that each of the domains D_i intersects Γ'_{λ_0} and forms $\delta_i = \Gamma'_{\lambda_0} \cap D_i$.

In [DR2004], we analyzed billiards within domains bounded by arcs of several confocal quadrics and *the billiard ordered game* within a few confocal ellipsoids; see also [DR2006a] for detailed examples. Unlike in the present article, the domains considered in [DR2004, DR2006a] did not contain reflex angles at the boundary. However, the technique used there to describe the periodic trajectories can be directly transferred to the present problems.

Before stating the Cayley-type conditions, recall that a point is being reflected off conic $\mathcal{C}_{\lambda_0}$ *from outside* if the corresponding Jacobi elliptic coordinate achieves a local maximum at the reflection point, and *from inside* if there the coordinate achieves a local minimum (see [DR2004]).

Theorem 5.7. *Consider domain $\mathcal{D}$ bounded by arcs of k ellipses $\mathcal{C}_{\beta_1}, \dots, \mathcal{C}_{\beta_k}$, l hyperbolas $\mathcal{C}_{\gamma_1}, \dots, \mathcal{C}_{\gamma_l}$, and several segments belonging to the degenerate conics from the confocal family* (2.1)

$$\beta_1, \dots, \beta_k \subset (-\infty, b),\ k \geq 1,\ \gamma_1, \dots, \gamma_l \subset (b, a),\ l \geq 0.$$

Let $\mathcal{C}_{\alpha_0}$ be an ellipse contained within all ellipses $\mathcal{C}_{\beta_1}, \ldots, \mathcal{C}_{\beta_k}$: $b > \alpha_0 > \beta_i$ for all $i \in \{1, \ldots, k\}$. A necessary condition for the existence of a billiard trajectory within $\mathcal{D}$ with the caustic $\mathcal{C}_{\alpha_0}$, such that the trajectory becomes closed after

- *n_i' reflections from inside and n_i'' reflections from outside off $\mathcal{C}_{\beta_i}$, $1 \le i \le k$;*
- *m_j' reflections from inside and m_j'' reflections from outside off $\mathcal{C}_{\gamma_j}$, $1 \le j \le l$;*
- *the total number of p intersections with the x-axis and reflections off the segments contained in the x-axis;*
- *the total number of q intersections with the y-axis and reflections off the segments contained in the y-axis;*

is

$$\sum_{i=1}^{k}(n_i' - n_i'')(\mathcal{A}(P_{\beta_i}) - \mathcal{A}(P_{\alpha_0})) + \sum_{j=1}^{l}(m_j' - m_j'')\mathcal{A}(P_{\gamma_j}) + p\mathcal{A}(P_a) - q\mathcal{A}(P_b) = 0,$$

$$m_j' - m_j'' + p - q = 0.$$

Here $\mathcal{A}$ is the Abel–Jacobi map of the elliptic curve,

$$\gamma \ : \ s^2 = \mathcal{P}(t) := (a-t)(b-t)(\alpha_0 - t),$$

and P_δ denotes the point $(\delta, \sqrt{\mathcal{P}(\delta)})$ on γ.

Proof. Following Jacobi [Jac1884] and Darboux [Dar1870], similarly as in [DR2004], we consider the sums

$$\int \frac{d\lambda_1}{\sqrt{\mathcal{P}(\lambda_1)}} + \int \frac{d\lambda_2}{\sqrt{\mathcal{P}(\lambda_2)}} \text{ and } \int \frac{\lambda_1 d\lambda_1}{\sqrt{\mathcal{P}(\lambda_1)}} + \int \frac{\lambda_2 d\lambda_2}{\sqrt{\mathcal{P}(\lambda_2)}}$$

over a billiard trajectory $A_1 \cdots A_N$. Here (λ_1, λ_2) are the Jacobi elliptic coordinates, $\lambda_1 < \lambda_2$. The second integral is equal to the length of the trajectory, while the first one is zero.

Since along any billiard trajectory, λ_1 achieves local extrema at the points of the reflection off the ellipses and the touching points with the caustic, and λ_2 at the points of the reflection off the hyperbolas and the intersection points with the coordinate axes, we obtain that $A_1 = A_N$ is equivalent to the condition stated. □

We illustrate this theorem on the example when the billiard table is $\mathcal{D}_0$, as defined in Section 5.1.

Example 5.8. A necessary condition for the existence of a billiard trajectory within $\mathcal{D}_0$ with the caustic $\mathcal{C}_{\alpha_0}$, such that the trajectory becomes closed after n_1 reflections off $\mathcal{C}_{\beta_1}$ and n_2 reflections off $\mathcal{C}_{\beta_2}$ is

$$n_1\mathcal{A}(P_{\beta_1}) + n_2\mathcal{A}(P_{\beta_2}) = (n_1 + n_2)\mathcal{A}(P_{\alpha_0}).$$

Notice that in this case the numbers p and q are always even and equal to each other. Since $2\mathcal{A}(P_a) = 2\mathcal{A}(P_b)$, the corresponding summands are cancelled out.

5.4. **Interval exchange transformation.** In this section, we are going to establish a connection of the billiard dynamics within domain $\mathcal{D}_0$ defined in Section 5.1 with interval exchange transformations. We start with the definition of such transformations, while more detail on them may be found in [Via2008, Zor2006, Kea1975, Vee1978].

5.4.1. *Interval exchange maps.* Let $I \subset \mathbf{R}$ be an interval, and let $\{I_\alpha \mid \alpha \in \mathcal{A}\}$ be its finite partition into subintervals. Here $\mathcal{A}$ is a finite set of at least two elements. We consider all intervals to be closed on the left and open on the right.

An interval exchange map is a bijection of I into itself, such that its restriction to each I_α is a translation. Such a map f is determined by the following data:

- A pair (π_0, π_1) of bijections $\mathcal{A} \to \{1, \dots, d\}$ describing the order of subintervals $\{I_\alpha\}$ in I and $\{f(I_\alpha)\}$ in $f(I) = I$. We denote
$$\pi = \begin{pmatrix} \pi_0^{-1}(1) & \pi_0^{-1}(2) & \dots & \pi_0^{-1}(d) \\ \pi_1^{-1}(1) & \pi_1^{-1}(2) & \dots & \pi_1^{-1}(d) \end{pmatrix}.$$
- A vector $\lambda = (\lambda_\alpha)_{\alpha \in \mathcal{A}}$ of the lengths of I_α.

5.4.2. *Billiard dynamics.* To each billiard trajectory, we join the sequence
$$\{(X_n, s_n)\}, \quad X_n \in \mathcal{C}_{\alpha_0}, \quad s_n \in \{+, -\},$$
where X_n are joint points of the trajectory with the caustic, while $s_n = +$ if at X_n the trajectory is winding counterclockwise and $s_n = -$ if it is winding clockwise about the caustic.

Introduce the metric μ on the caustic $\mathcal{C}_{\alpha_0}$ as in Proposition 2.3. Then we parametrize $\mathcal{C}_{\alpha_0}$ by the parameters
$$p \ : \ \mathcal{C}_{\alpha_0} \to [0, 1), \quad q \ : \ \mathcal{C}_{\alpha_0} \to [-1, 0),$$
which are natural with respect to μ such that p is oriented counterclockwise and q clockwise along $\mathcal{C}_{\alpha_0}$, and the values $p = 0$ and $q = -1$ correspond to points P_0, Q_0 respectively, as shown in Figure 40.

Consider one segment of a billiard trajectory, and let $X \in \mathcal{C}_{\alpha_0}$ be its touching point with the caustic. Suppose that the particle is moving counterclockwise on that segment. From Figure 40, we conclude

- if X is between points P_1 and P_2, then the particle is going to hit the arc $\mathcal{C}_{\lambda_2}$;
- if X is between P_2 and P_0, the particle is going to hit the arc $\mathcal{C}_{\lambda_1}$;

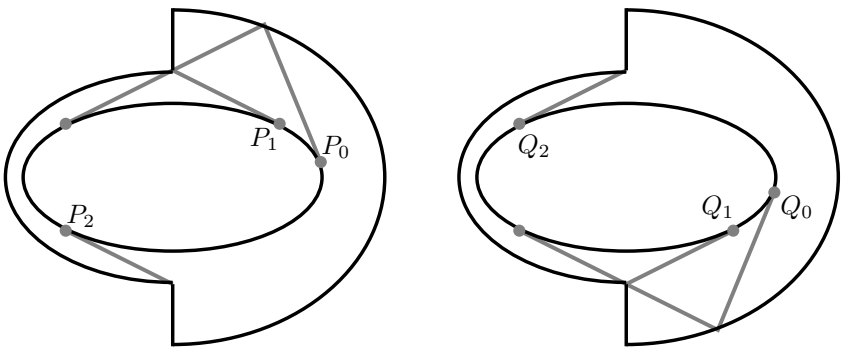

FIGURE 40. Parametrizations of the caustic

- for X between P_0 and P_1, the particle is going to hit $\mathcal{C}_{\lambda_1}$ and the upper segment before the next contact with the caustic, and the direction of motion is changed to clockwise.

Similarly, if the particle is moving in clockwise direction, we have

- if X is between points Q_1 and Q_2, then the particle is going to hit the arc $\mathcal{C}_{\lambda_2}$;
- if X is between Q_2 and Q_0, the particle is going to hit the arc $\mathcal{C}_{\lambda_1}$;
- for X between Q_0 and Q_1, the particle is going to hit $\mathcal{C}_{\lambda_1}$ and the lower segment before the next contact with the caustic, and the direction of motion is changed to counterclockwise.

To see the billiard dynamics as an interval exchange transformation, we make the identification

$$(X,+) \sim p(X), \quad (X,-) \sim q(X).$$

In other words:

- we identify the joint point X of a given trajectory with the caustic with $p(X) \in [0,1)$ if the particle is moving in a counterclockwise direction on the corresponding segment;
- for the motion in a clockwise direction, we identify X with $q(X) \in [-1,0)$.

Denote the rotation numbers $r_1 = \rho(\lambda_1)$, $r_2 = \rho(\lambda_2)$ (see Proposition 2.3).

The parametrization values for points denoted in Figure 40 are

$$p(P_0) = 0, \quad p(P_1) = r_1 - r_2, \quad p(P_2) = r_1 - r_2 + \frac{1}{2},$$
$$q(Q_0) = -1, \quad q(Q_1) = r_1 - r_2 - 1, \quad q(Q_2) = r_1 - r_2 - \frac{1}{2}.$$

Now, we distinguish three cases depending on the position of point P_0 with respect to the x-axis (see Figure 40), i.e., on the sign of $\frac{1}{4} + \frac{r_2}{2} - r_1$.

P_0 is on the x-axis: $\frac{1}{4} + \frac{r_2}{2} - r_1 = 0$. The interval exchange map is

$$\xi \mapsto \begin{cases} \xi + r_1 + \frac{3}{2}, & \xi \in [-1, -\frac{1}{2} - r_1), \\ \xi + r_2, & \xi \in [-\frac{1}{2} - r_1, -r_1), \\ \xi + r_1 - 1, & \xi \in [-r_1, 0), \\ \xi + r_1 - \frac{1}{2}, & \xi \in [0, \frac{1}{2} - r_1), \\ \xi + r_2, & \xi \in [\frac{1}{2} - r_1, 1 - r_1), \\ \xi + r_1 - 1, & \xi \in [1 - r_1, 1), \end{cases}$$

as shown in Figure 41.

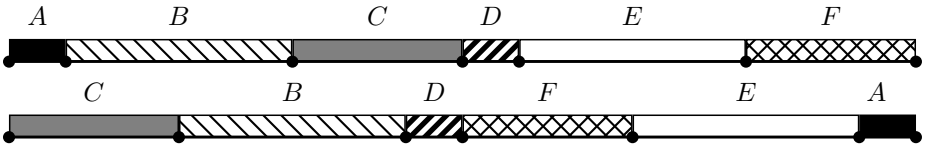

FIGURE 41. Interval exchange transformation for the case $\frac{1}{4} + \frac{r_2}{2} - r_1 = 0$

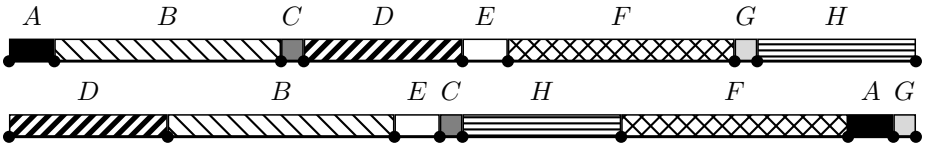

FIGURE 42. Interval exchange transformation for the case $\frac{1}{4} + \frac{r_2}{2} - r_1 > 0$

To the map, the pair (π, λ) is joined

$$\pi = \begin{pmatrix} A & B & C & D & E & F \\ C & B & D & F & E & A \end{pmatrix},$$
$$\lambda = \left(\frac{1}{2} - r_1,\ \frac{1}{2},\ r_1,\ \frac{1}{2} - r_1,\ \frac{1}{2},\ r_1\right).$$

P_0 is above the x-axis: $\frac{1}{4} + \frac{r_2}{2} - r_1 > 0$. The interval exchange map in this case is shown in Figure 42 and given by

$$\xi \mapsto \begin{cases} \xi + r_1 + \frac{3}{2}, & \xi \in [-1, r_1 - r_2 - 1), \\ \xi + r_2, & \xi \in [r_1 - r_2 - 1, r_1 - r_2 - \frac{1}{2}), \\ \xi + r_1, & \xi \in [r_1 - r_2 - \frac{1}{2}, -r_1), \\ \xi + r_1 - 1, & \xi \in [-r_1, 0), \\ \xi + r_1 - \frac{1}{2}, & \xi \in [0, r_1 - r_2), \\ \xi + r_2, & \xi \in [r_1 - r_2, r_1 - r_2 + \frac{1}{2}), \\ \xi + r_1, & \xi \in [r_1 - r_2 + \frac{1}{2}, 1 - r_1), \\ \xi + r_1 - 1, & \xi \in [1 - r_1, 1). \end{cases}$$

The map can be described by the pair (π, λ):

$$\pi = \begin{pmatrix} A & B & C & D & E & F & G & H \\ D & B & E & C & H & F & A & G \end{pmatrix},$$
$$\lambda = \left(r_1 - r_2,\ \frac{1}{2},\ r_2 - 2r_1 + \frac{1}{2},\ r_1,\ r_1 - r_2,\ \frac{1}{2},\ r_2 - 2r_1 + \frac{1}{2},\ r_1\right).$$

P_0 is below the x-axis: $\frac{1}{4} + \frac{r_2}{2} - r_1 < 0$. The interval exchange map corresponding to the billiard dynamics is

$$\xi \mapsto \begin{cases} \xi + r_1 + \frac{3}{2}, & \xi \in [-1, -\frac{1}{2} - r_1), \\ \xi + r_1 - \frac{1}{2}, & \xi \in [-\frac{1}{2} - r_1, r_1 - r_2 - 1), \\ \xi + r_2, & \xi \in [r_1 - r_2 - 1, r_1 - r_2 - \frac{1}{2}), \\ \xi + r_1 - 1, & \xi \in [r_1 - r_2 - \frac{1}{2}, 0), \\ \xi + r_1 - \frac{1}{2}, & \xi \in [0, \frac{1}{2} - r_1), \\ \xi + r_1 - \frac{3}{2}, & \xi \in [\frac{1}{2} - r_1, r_1 - r_2), \\ \xi + r_2, & \xi \in [r_1 - r_2, r_1 - r_2 + \frac{1}{2}), \\ \xi + r_1 - 1, & \xi \in [r_1 - r_2 + \frac{1}{2}, 1); \end{cases}$$

see Figure 43.

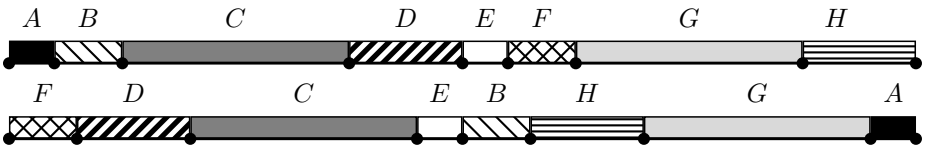

FIGURE 43. Interval exchange transformation for the case $\frac{1}{4} + \frac{r_2}{2} - r_1 < 0$

To the map, the pair (π, λ) is joined

$$\pi = \begin{pmatrix} A & B & C & D & E & F & G & H \\ F & D & C & E & B & H & G & A \end{pmatrix},$$

$$\lambda = \left(\frac{1}{2} - r_1, 2r_1 - r_2 - \frac{1}{2}, \frac{1}{2}, r_2 + \frac{1}{2} - r_1, \frac{1}{2} - r_1, 2r_1 - r_2 - \frac{1}{2}, \frac{1}{2}, r_2 + \frac{1}{2} - r_1\right).$$

Notice that in all three cases the interval exchange transformations depend only on the rotation numbers r_1, r_2. Thus, we have

Theorem 5.9. *The billiard dynamics inside the domain $\mathcal{D}_0$ with the caustic $\mathcal{C}_{\alpha_0}$ does not depend on the parameters a, b of the confocal family* (2.1) *but only on the rotation numbers r_1, r_2.*

5.4.3. *Domain bounded by the ellipses with the rotation numbers $\frac{5-\sqrt{5}}{10}$ and $\frac{\sqrt{5}}{10}$.* By Theorem 5.9 it is enough to consider the case when the confocal family is degenerate, i.e., consists of concentric circles.

In this example, there exist six saddle-connections, represented in Figure 44. Each polygonal line shown on the figure corresponds to two trajectories in the phase space, depending on the direction of the motion.

Vertices of the saddle-connections divide the billiard border into eleven parts; see Figure 45.

All trajectories in this billiard domain corresponding to the fixed caustic are periodic:

- either all bouncing points of a given trajectory are in the gray parts (in this case the billiard particle hits each gray part twice until the trajectory becomes closed and the trajectory is 14-periodic (see Figures 46 and 46c)

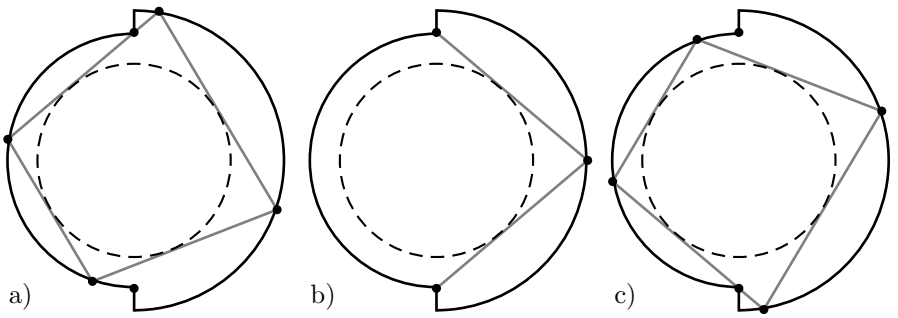

FIGURE 44. Saddle-connections corresponding to the circles with the rotation numbers $\frac{5-\sqrt{5}}{10}$ and $\frac{\sqrt{5}}{10}$.

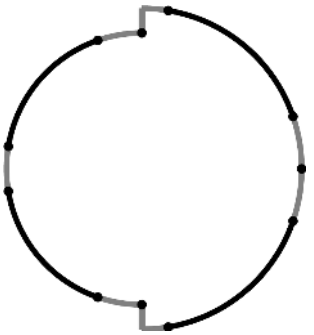

FIGURE 45. Parts of the boundary corresponding to the circles with the rotation numbers $\frac{5-\sqrt{5}}{10}$ and $\frac{\sqrt{5}}{10}$

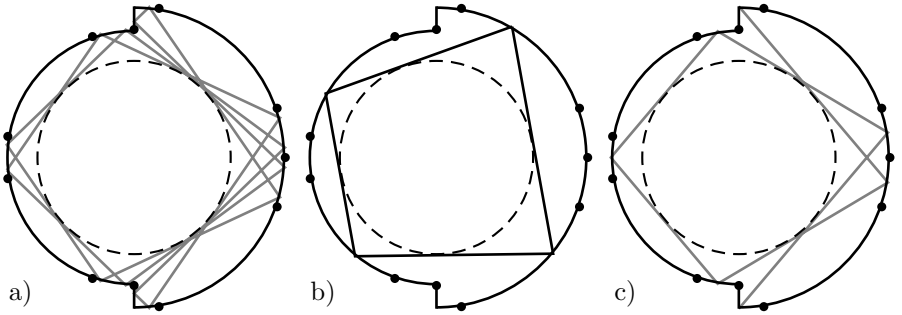

FIGURE 46. Periodic trajectories corresponding to the circles with the rotation numbers $\frac{5-\sqrt{5}}{10}$ and $\frac{\sqrt{5}}{10}$

and notice that such a trajectory bounces six times on each of the circles and once on each of the segments);

- or all bouncing points are in the black parts (the particle will hit each part once until closure and the trajectory is 4-periodic (see Figure 46b), and such a trajectory reflects twice on each of the circular arcs).

The corresponding level set in the phase space is divided into three parts by the saddle-connections:

- The part containing all 14-periodic trajectories is bounded by four saddle-connections whose projections to the configuration space is shown on Figures 44a and 44c, and the saddle-connections corresponding to Figure 44b are lying inside this part.
- Two parts containing all 4-periodic trajectories winding about the caustic in the clockwise and counterclockwise direction are bounded by the saddle-connections winding in the same direction whose projections to the configuration space is shown in Figures 44a and 44c.

5.5. **The Keane condition and minimality.** An interval exchange transformation is called *minimal* if its every orbit is dense in the whole domain. When considering pseudo-billiards, minimal interval exchange transformations will correspond

to the cases when all orbits are dense in the domain between the billiard border and the caustic.

Following [Via2008, Zor2006], we are going to formulate a sufficient condition for minimality. Let f be an interval exchange transformation of I, given by pair (π, λ). Denote by p_α the left endpoint of I_α. Then the transformation satisfies *the Keane condition* if

$$f^m(p_\alpha) \neq p_\beta \quad \text{for all } m \geq 1,\ \alpha \in \mathcal{A},\ \beta \in \mathcal{A} \setminus \{\pi_0^{-1}(1)\}.$$

Obviously, none of the transformations from Section 5.4 satisfies the Keane condition; namely, the midpoint of the interval is the left endpoint of one of I_α, and it is the image of another endpoint in the corresponding interval exchange map.

The goal of this section is to find an analogue of the Keane condition for interval exchange transformations appearing in billiard dynamics.

5.5.1. *Billiard-like transformations and the modified Keane condition.* Analysis of the examples from Section 5.4 motivates the following definitions.

Definition 5.10. An interval exchange transformation f of $I = [-1, 1)$ is *billiard-like* if the partition into subintervals satisfies the following:

- for each α, I_α is contained either in $[-1, 0)$ or $[0, 1)$;
- for each α, $f(I_\alpha)$ is contained either in $[-1, 0)$ or $[0, 1)$;
- both $[-1, 0)$ and $[0, 1)$ contain at least two intervals of the partition.

Definition 5.11. We will say that a billiard-like interval exchange transformation f satisfies *the modified Keane condition* if

$$f^m(p_\alpha) \neq p_\beta \text{ for all } m \geq 1,\ \alpha \in \mathcal{A}, \text{ and } \beta \in \mathcal{B} \text{ such that } p_\beta \notin \{-1, 0\}.$$

Lemma 5.12. *If a billiard-like interval exchange transformation satisfies the modified Keane condition, then the transformation has no periodic points.*

We say that an interval exchange transformation is *irreducible* if for no $k < |\mathcal{A}|$ the union

$$I_{\alpha_{\pi_0^{-1}(1)}} \cup \cdots \cup I_{\alpha_{\pi_0^{-1}(k)}}$$

is invariant under the transformation. The usual Keane condition implies irreducibility. However, this is not the case for the modified Keane condition—it may happen that the transformation falls apart into two irreducible transformations on $[-1, 0)$ and $[0, 1)$. On the other hand, if for a transformation satisfying the modified Keane condition there is an interval $I_\alpha \subset [-1, 0)$ such that $f(I_\alpha) \subset [0, 1)$, irreducibility will also take place.

Proposition 5.13. *If an irreducible billiard-like interval exchange transformation f satisfies the modified Keane condition, then f is minimal.*

An example. Consider billiard trajectories within domain $\mathcal{D}_0$ with caustic $\mathcal{C}_{\alpha_0}$, as described in Section 5.1. In addition, suppose the rotation numbers corresponding to the ellipses $\mathcal{C}_{\lambda_1}$ and $\mathcal{C}_{\lambda_2}$ are

$$r_1 = \frac{5}{11} + \frac{1}{22\pi}, \quad r_2 = \frac{5}{11} - \frac{1}{220\pi}.$$

With the given rotation numbers, the Cayley-type conditions from Theorem 3.30 can be rewritten in a simpler form. Namely, a necessary condition for existence

of a trajectory within $\mathcal{D}_0$ which becomes closed after n reflections of $\mathcal{C}_{\lambda_1}$ and m reflections off $\mathcal{C}_{\lambda_2}$ is

$$nr_1 + mr_2 \in \mathbf{Z}.$$

In this case, this condition is satisfied for $n = 1$ and $m = 10$:

$$r_1 + 10r_2 = 5. \tag{5.1}$$

Since $\frac{1}{4} + \frac{r_2}{2} - r_1 > 0$, the corresponding interval exchange transformation is given by

$$\Pi = \begin{pmatrix} A & B & C & D & E & F & G & H \\ D & B & E & C & H & F & A & G \end{pmatrix},$$

$$\lambda = \left(\frac{1}{20\pi},\ \frac{1}{2},\ \frac{1}{22} - \frac{21}{220\pi},\ \frac{5}{11} + \frac{1}{22\pi},\ \frac{1}{20\pi},\ \frac{1}{2},\ \frac{1}{22} - \frac{21}{220\pi},\ \frac{5}{11} + \frac{1}{22\pi} \right).$$

Proposition 5.14. *The transformation* (Π, λ) *satisfies the modified Keane condition.*

Proof. Suppose that p and p' are two endpoints of the intervals such that $p' \notin \{-1, 0\}$ and $f^k(p) = p'$ for some $k \geq 1$. Notice that

$$p = \alpha r_1 + \beta r_2 + \gamma \frac{1}{2}, \quad p' = \alpha' r_1 + \beta' r_2 + \gamma' \frac{1}{2},$$

for some $\alpha, \alpha' \in \{-1, 0, 1\}$, $\beta, \beta' \in \{-1, 0\}$, $\gamma, \gamma' \in \{-2, -1, 0, 1, 2\}$.

We have

$$p' = f^k(p) = p + k_1 r_1 + k_2 r_2 + k_3 \frac{1}{2},$$

for some integers k_1, k_2, k_3 such that $k_1 + k_2 = k$, $k_1 \geq 0$, $k_2 \geq 0$. Thus

$$(k_1 + \alpha - \alpha')r_1 + (k_2 + \beta - \beta')r_2 + (k_3 + \gamma - \gamma')\frac{1}{2} = 0. \tag{5.2}$$

Since r_1 and r_2 are irrational, equations (5.1) and (5.2) must be dependent:

$$a := k_1 + \alpha - \alpha' = \frac{1}{10}(k_2 + \beta - \beta') = -\frac{1}{10}(k_3 + \gamma - \gamma'). \tag{5.3}$$

For each $\xi \in B \cup F$, either $f(\xi)$ or $f^2(\xi)$ are not in $B \cup F$, thus

$$k_2 \leq 2k_1 + 2. \tag{5.4}$$

Combining (5.4) and (5.3) we get $8a \leq 7$. Since k_2 is nonnegative, (5.4) gives that $a = 0$, which leads to $k = k_1 + k_2 \leq 3$. By direct calculation we check that none of the partition interval endpoints is mapped into another one, different from -1 and 0 by at most three iterations. □

In this example, the Cayley-type condition for periodicity is satisfied. However, closed trajectories do not exist, and, moreover, each of the trajectories densely fills the ring between the billiard border and the caustic.

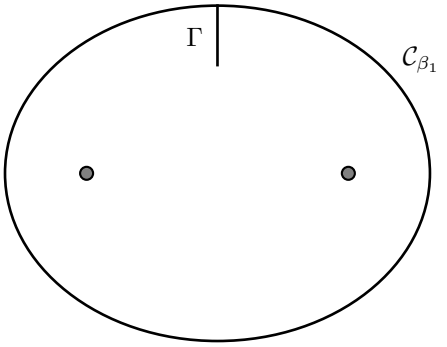

FIGURE 47. Domain $\mathcal{D}_1$ within an ellipse having a "wall" on the y-axis

5.6. **Unique ergodicity.** In this section it will be shown that there are infinitely many billiard tables bounded by arcs of the confocal conics, such that the corresponding flow will not be uniquely ergodic.

Consider the billiard table $\mathcal{D}_1$ whose boundary consists of the ellipse $\mathcal{C}_{\beta_1}$ from (2.1) and segment $\Gamma = \{(0, y) \mid \sqrt{b-\beta_2} \le y \le \sqrt{b-\beta_1}\}$, with $\beta_1 < \beta_2 < b$: $\partial\mathcal{D}_1 = \mathcal{C}_{\beta_1} \cup \Gamma$; see Figure 47.

Fix the parameter α_0: such that $\beta_2 < \alpha_0 < b$, and take $\mathcal{C}_{\alpha_0}$ to be the caustic. A corresponding billiard trajectory is shown in Figure 48.

Proposition 5.15. *The billiard flow within the domain $\mathcal{D}_1$ with the caustic $\mathcal{C}_{\alpha_0}$ is equivalent to the following exchange transformation of the interval $[-1, 1)$:*

$$\xi \mapsto \begin{cases} \xi + r_1, & \xi \in [-1, -r_1), \\ \xi + r_1 - 1, & \xi \in [-r_1, r_2 - r_1), \\ \xi + r_1, & \xi \in [r_2 - r_1, 1 - r_1), \\ \xi + r_1 - 1, & \xi \in [1 - r_1, r_2 - r_1 + 1), \\ \xi + r_1 - 2, & \xi \in [r_2 - r_1 + 1, 1), \end{cases} \tag{5.5}$$

with $r_1 = \rho(\beta_1)$, $r_2 = \rho(\beta_2)$, and ρ is the corresponding rotation function; see Proposition 2.3.

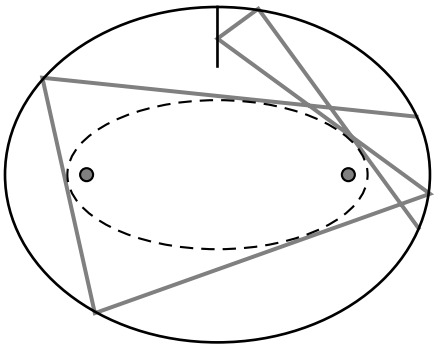

FIGURE 48. A billiard trajectory in $\mathcal{D}_1$ with an ellipse as the caustic

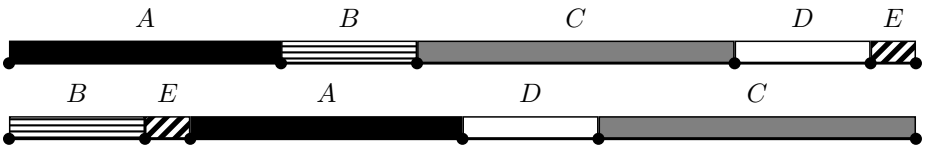

FIGURE 49. Transformation corresponding to the billiard within $\mathcal{D}_1$

Proof. The billiard flow is equivalent to the discrete dynamics of touching points of the trajectory with the caustic, with the direction of motion taken into account.

Introduce the metric μ on the caustic $\mathcal{C}_{\alpha_0}$, as in Proposition 2.3. Then, we parametrize $\mathcal{C}_{\alpha_0}$ by the parameters

$$p \,:\, \mathcal{C}_{\alpha_0} \to [0,1), \quad q \,:\, \mathcal{C}_{\alpha_0} \to [-1,0),$$

which are natural with respect to μ such that p is oriented counterclockwise and q clockwise along $\mathcal{C}_{\alpha_0}$, and the values $p=0$ and $q=-1$ correspond to touching points contained in the right half-plane and left half-plane, respectively, of tangential lines from $(0,\sqrt{b-\beta_2})$. Having in mind that reflection on the "wall" Γ changes the orientation of motion, we obtain (5.5). □

Map (5.5) is represented by the pair (π,λ)

$$\pi = \begin{pmatrix} A & B & C & D & E \\ B & E & A & D & C \end{pmatrix},$$
$$\lambda = (1-r_1,\ r_2,\ 1-r_2,\ r_2,\ r_1-r_2);$$

see also Figure 49.

Theorem 5.16. *There are billiard tables $\mathcal{D}_1$ and caustics, such that the corresponding billiard flows are minimal and not uniquely ergodic.*

Proof. The transformation (5.5) corresponds to the Veech example of minimal and not uniquely ergodic systems [Vee1969]; see also [MT2002]. Namely, choose α_0 and β_1 such that $r_1=\rho(\beta_1)$ is an irrational number with unbounded partial quotients. Then there are irrational numbers r, such that for $r_2=\rho(\beta_2)=r_1-r$, the measure μ on $\mathcal{C}_{\alpha_0}$ is not ergodic, thus not uniquely ergodic. □

ACKNOWLEDGMENTS

Vladimir Dragović is grateful to Marcelo Viana and IMPA (Rio de Janeiro, Brazil) for hospitality and support. Milena Radnović is grateful to the associateship scheme of the *The Abdus Salam* ICTP (Trieste, Italy) for its support and to Vered Rom-Kedar from The Weizmann Institute of Science (Rehovot, Israel) for hospitality and support. The authors are grateful to the referees for suggestions and comments which led to significant improvement of the exposition.

About the authors

Vladimir Dragović received a doctorate in mathematics from the University of Belgrade with Professor Boris Dubrovin. He has been a research professor and the head of the department of mechanics at the Mathematical Institute of the Serbian Academy of Sciences and Arts. Recently, he became a professor of mathematics at the University of Texas at Dallas.

Milena Radnović received a doctorate in mathematics from the University of Belgrade with Vladimir Dragović. She is an associate research professor at the Mathematical Institute of the Serbian Academy of Sciences and Arts. She is also a junior associate of the ICTP in Trieste, Italy. Recently, she joined the University of Sydney as a research fellow.

References

[ABS2004] V. E. Adler, A. I. Bobenko, and Yu. B. Suris, *Geometry of Yang–Baxter maps: pencils of conics and quadrirational mappings*, Comm. Anal. Geom. **12** (2004), no. 5, 967–1007. MR2103308 (2005i:14012)

[ABS2009] V. E. Adler, A. I. Bobenko, and Y. B. Suris, *Integrable discrete nets in Grassmannians*, Lett. Math. Phys. **89** (2009), no. 2, 131–139, DOI 10.1007/s11005-009-0328-1. MR2534880 (2010f:37130)

[Arn1978] V. Arnold, *Mathematical Methods of Classical Mechanics*, Springer Verlag, New York, 1978.

[Aud1994] M. Audin, *Courbes algébriques et systèmes intégrables: géodésiques des quadriques* (French, with English summary), Exposition. Math. **12** (1994), no. 3, 193–226. MR1295705 (95k:58068)

[BB1996] W. Barth and Th. Bauer, *Poncelet theorems*, Exposition. Math. **14** (1996), no. 2, 125–144. MR1395253 (97f:14051)

[BM1993] W. Barth and J. Michel, *Modular curves and Poncelet polygons*, Math. Ann. **295** (1993), no. 1, 25–49, DOI 10.1007/BF01444875. MR1198840 (94c:14045)

[Ber1987a] M. Berger, *Geometry. I*, Universitext, Springer-Verlag, Berlin, 1987. Translated from the French by M. Cole and S. Levy. MR882541 (88a:51001a)

[Ber1987b] M. Berger, *Geometry. II*, Universitext, Springer-Verlag, Berlin, 1987. Translated from the French by M. Cole and S. Levy. MR882916 (88a:51001b)

[BM1962] G. Birkhoff and R. Morris, *Confocal conics in space-time*, Amer. Math. Monthly **69** (1962), 1–4. MR0133039 (24 #A2875)

[BS2008] A. I. Bobenko and Y. B. Suris, *Discrete differential geometry*, Graduate Studies in Mathematics, vol. 98, American Mathematical Society, Providence, RI, 2008. Integrable structure. MR2467378 (2010f:37125)

[BKOR1987] H. J. M. Bos, C. Kers, F. Oort, and D. W. Raven, *Poncelet's closure theorem*, Exposition. Math. **5** (1987), no. 4, 289–364. MR917349 (88m:14041)

[Cay1853] A. Cayley, *Note on the porism of the in-and-circumscribed polygon*, Philosophical magazine **6** (1853), 99–102.

[Cay1854] A. Cayley, *Developments on the porism of the in-and-circumscribed polygon*, Philosophical magazine **7** (1854), 339–345.

[Cay1855] A. Cayley, *On the porism of the in-and-circumscribed triangle, and on an irrational transformation of two ternary quadratic forms each into itself*, Philosophical magazine **9** (1855), 513–517.

[Cay1857] A. Cayley, *On the porism of the in-and-circumscribed triangle*, Quarterly Mathematical Journal **1** (1857), 344–354.

[Cay1858] A. Cayley, *On the a posteriori demonstration of the porism of the in-and-circumscribed triangle*, Quarterly Mathematical Journal **2** (1858), 31–38.

[Cay1861] A. Cayley, *On the porism of the in-and-circumscribed polygon*, Philosophical Transactions of the Royal Society of London **51** (1861), 225–239.

[CCS1993] S.-J. Chang, B. Crespi, and K. J. Shi, *Elliptical billiard systems and the full Poncelet's theorem in n dimensions*, J. Math. Phys. **34** (1993), no. 6, 2242–2256, DOI 10.1063/1.530115. MR1218986 (94g:58092)

[Cha1827] Chasles, *Géométrie pure. Théorèmes sur les sections coniques confocales* (French), Ann. Math. Pures Appl. [Ann. Gergonne] **18** (1827/28), 269–276. MR1556443

[CI2010] S. Chino and S. Izumiya, *Lightlike developables in Minkowski 3-space*, Demonstratio Math. **43** (2010), no. 2, 387–399. MR2668483 (2011f:58069)

[Dar1870] G. Darboux, *Sur les polygones inscrits et circonscrits à l'ellipsoïde*, Bulletin de la Société philomathique **7** (1870), 92–94.

[Dar1914] G. Darboux, *Leçons sur la théorie générale des surfaces et les applications géométriques du calcul infinitesimal*, Vol. 2 and 3, Gauthier-Villars, Paris, 1914.

[DR1998a] V. Dragović and M. Radnović, *Conditions of Cayley's type for ellipsoidal billiard*, J. Math. Phys. **39** (1998), no. 1, 355–362, DOI 10.1063/1.532317. MR1489624 (98j:14041)

[DR1998b] V. Dragović and M. Radnović, *On periodical trajectories of the billiard systems within an ellipsoid in* $\mathbf{R}^d$ *and generalized Cayley's condition*, J. Math. Phys. **39** (1998), no. 11, 5866–5869, DOI 10.1063/1.532600. MR1653096 (99j:58158)

[DR2004] V. Dragović and M. Radnović, *Cayley-type conditions for billiards within k quadrics in* $\mathbb{R}^d$, J. Phys. A **37** (2004), no. 4, 1269–1276, DOI 10.1088/0305-4470/37/4/014. MR2043219 (2005f:37123)

[DR2005] V. Dragović and M. Radnović, *Corrigendum: "Cayley-type conditions for billiards within k quadrics in* $\mathbb{R}^d$*" [J. Phys. A* **37** *(2004), no. 4, 1269–1276; MR2043219]*, J. Phys. A **38** (2005), no. 36, 7927, DOI 10.1088/0305-4470/38/36/C01. MR2185422 (2006f:37086)

[DR2006a] V. Dragovich and M. Radnovich, *A review of the analytic description of periodic billiard trajectories* (Russian, with Russian summary), Sovrem. Mat. Prilozh. **21, Geom. Zadachi Teor. Upr.** (2004), 154–165, DOI 10.1007/s10958-006-0154-2; English transl., J. Math. Sci. (N. Y.) **135** (2006), no. 4, 3244–3255. MR2157924 (2006f:37050)

[DR2006b] V. Dragović and M. Radnović, *Geometry of integrable billiards and pencils of quadrics* (English, with English and French summaries), J. Math. Pures Appl. (9) **85** (2006), no. 6, 758–790, DOI 10.1016/j.matpur.2005.12.002. MR2236243 (2007f:37083)

[DR2008] V. Dragović and M. Radnović, *Hyperelliptic Jacobians as billiard algebra of pencils of quadrics: beyond Poncelet porisms*, Adv. Math. **219** (2008), no. 5, 1577–1607, DOI 10.1016/j.aim.2008.06.021. MR2458147 (2009k:14055)

[DR2010] V. Dragovich and M. Radnovich, *Integrable billiards and quadrics* (Russian, with Russian summary), Uspekhi Mat. Nauk **65** (2010), no. 2(392), 133–194, DOI 10.1070/RM2010v065n02ABEH004673; English transl., Russian Math. Surveys **65** (2010), no. 2, 319–379. MR2668802 (2011j:37107)

[DR2011] V. Dragović and M. Radnović, *Poncelet porisms and beyond*, Frontiers in Mathematics, Birkhäuser/Springer Basel AG, Basel, 2011. Integrable billiards, hyperelliptic Jacobians and pencils of quadrics. MR2798784 (2012j:14059)

[DR2012a] V. Dragović and M. Radnović, *Ellipsoidal billiards in pseudo-Euclidean spaces and relativistic quadrics*, Adv. Math. **231** (2012), no. 3-4, 1173–1201, DOI 10.1016/j.aim.2012.06.004. MR2964601

[DR2012b] V. Dragović and M. Radnović, *Billiard algebra, integrable line congruences, and double reflection nets*, J. Nonlinear Math. Phys. **19** (2012), no. 3, 1250019, 18, DOI 10.1142/S1402925112500192. MR2978885

[DR2012c] V. Dragović and M. Radnović, *Pseudo-integrable billiards and arithmetic dynamics* (2012), available at `arXiv:1206.0163[nlin.SI]`.

[Dui2010] J. J. Duistermaat, *Discrete integrable systems*, Springer Monographs in Mathematics, Springer, New York, 2010. QRT maps and elliptic surfaces. MR2683025 (2012g:37178)

[Fla2009] L. Flatto, *Poncelet's theorem*, American Mathematical Society, Providence, RI, 2009. Chapter 15 by S. Tabachnikov. MR2465164 (2011f:37001)

[GKT2007] D. Genin, B. Khesin, and S. Tabachnikov, *Geodesics on an ellipsoid in Minkowski space*, Enseign. Math. (2) **53** (2007), no. 3-4, 307–331. MR2455947 (2009m:37163)

[GH1977] P. Griffiths and J. Harris, *A Poncelet theorem in space*, Comment. Math. Helv. **52** (1977), no. 2, 145–160. MR0498606 (58 #16695)

[GH1978] P. Griffiths and J. Harris, *On Cayley's explicit solution to Poncelet's porism*, Enseign. Math. (2) **24** (1978), no. 1-2, 31–40. MR497281 (80g:51017)

[Har1967] R. Hartshorne, *Foundations of projective geometry*, Lecture Notes, Harvard University, vol. 1966/67, W. A. Benjamin, Inc., New York, 1967. MR0222751 (36 #5801)

[Jac1884] C. Jacobi, *Vorlesungen über Dynamic. Gesammelte Werke, Supplementband*, Berlin, 1884.

[Jak1993] B. Jakob, *Moduli of Poncelet polygons*, J. Reine Angew. Math. **436** (1993), 33–44, DOI 10.1515/crll.1993.436.33. MR1207279 (94c:14010)

[Kea1975] M. Keane, *Interval exchange transformations*, Math. Z. **141** (1975), 25–31. MR0357739 (50 #10207)

[KT2009] B. Khesin and S. Tabachnikov, *Pseudo-Riemannian geodesics and billiards*, Adv. Math. **221** (2009), no. 4, 1364–1396, DOI 10.1016/j.aim.2009.02.010. MR2518642 (2010g:53163)

[Kin1994] J. L. King, *Three problems in search of a measure*, The Americal Mathematical Monthly **101** (1994), no. 7, 609–628.

[KT1991] V. V. Kozlov and D. V. Treshchëv, *Billiardy* (Russian), Moskov. Gos. Univ., Moscow, 1991. Geneticheskoe vvedenie v dinamiku sistem s udarami. [A genetic introduction to the dynamics of systems with impacts]. MR1157370 (93k:58094b)

[Koz2003] V. V. Kozlov, *Rationality conditions for the ratio of elliptic integrals and the great Poncelet theorem* (Russian, with Russian summary), Vestnik Moskov. Univ. Ser. I Mat. Mekh. **4** (2003), 6–13, 71; English transl., Moscow Univ. Math. Bull. **58** (2003), no. 4, 1–7 (2004). MR2054501 (2005d:33030)

[Leb1942] H. Lebesgue, *Les coniques*, Gauthier-Villars, Paris, 1942.

[LT2007] M. Levi and S. Tabachnikov, *The Poncelet grid and billiards in ellipses*, Amer. Math. Monthly **114** (2007), no. 10, 895–908. MR2363055 (2009b:37044)

[Mai1943] A. G. Maier, *Trajectories on closable orientable surfaces* (Russian), Sb. Math. **12** (1943), 71–84.

[MT2002] H. Masur and S. Tabachnikov, *Rational billiards and flat structures*, Handbook of dynamical systems, Vol. 1A, North-Holland, Amsterdam, 2002, pp. 1015–1089, DOI 10.1016/S1874-575X(02)80015-7. MR1928530 (2003j:37002)

[MV1991] J. Moser and A. P. Veselov, *Discrete versions of some classical integrable systems and factorization of matrix polynomials*, Comm. Math. Phys. **139** (1991), no. 2, 217–243. MR1120138 (92g:58054)

[Mos1980] J. Moser, *Geometry of quadrics and spectral theory*, The Chern Symposium 1979 (Proc. Internat. Sympos., Berkeley, Calif., 1979), Springer, New York, 1980, pp. 147–188. MR609560 (82j:58064)

[Pei1999] D. Pei, *Singularities of* $\mathbf{R}\mathrm{P}^2$*-valued Gauss maps of surfaces in Minkowski 3-space*, Hokkaido Math. J. **28** (1999), no. 1, 97–115. MR1673482 (2000a:58097)

[Pon1822] J. V. Poncelet, *Traité des propriétés projectives des figures*, Metz, Paris, 1822.

[Pon1862] J. V. Poncelet, *Applications d'analyse et de géométrie*, Mallet-Bachelier, Paris, 1862.

[1869] *Obituary notices of fellows deceased. Jean Victor Poncelet*, Proceedings of the Royal Society of London **18** (1869).

[Pre1999] E. Previato, *Poncelet's theorem in space*, Proc. Amer. Math. Soc. **127** (1999), no. 9, 2547–2556, DOI 10.1090/S0002-9939-99-05307-1. MR1662198 (2000d:14056)

[Pre2002] E. Previato, *Some integrable billiards*, SPT 2002: Symmetry and perturbation theory (Cala Gonone), World Sci. Publ., River Edge, NJ, 2002, pp. 181–195, DOI 10.1142/9789812795403_0020. MR1976669 (2004c:37134)

[QRT1988] G. R. W. Quispel, J. A. G. Roberts, and C. J. Thompson, *Integrable mappings and soliton equations*, Phys. Lett. A **126** (1988), no. 7, 419–421, DOI 10.1016/0375-9601(88)90803-1. MR924318 (88m:58084)

[Sam1988] P. Samuel, *Projective geometry*, Undergraduate Texts in Mathematics, Springer-Verlag, New York, 1988. Translated from the French by Silvio Levy; Readings in Mathematics. MR960691 (89f:51003)

[Sch2003] W. K. Schief, *Lattice geometry of the discrete Darboux, KP, BKP and CKP equations. Menelaus' and Carnot's theorems*, J. Nonlinear Math. Phys. **10** (2003), no. suppl. 2, 194–208, DOI 10.2991/jnmp.2003.10.s2.17. MR2062279 (2005g:37136)

[Sch2007] R. E. Schwartz, *The Poncelet grid*, Adv. Geom. **7** (2007), no. 2, 157–175, DOI 10.1515/ADVGEOM.2007.010. MR2314815 (2008f:37081)

[Smi] J. Smillie, *The dynamics of billiard flows in rational polygons*, Encyclopedia of Mathematical Sciences (Yu. Sinai, ed.), Vol. 100, Springer-Verlag, 1999.

[Tab2005] S. Tabachnikov, *Geometry and billiards*, Student Mathematical Library, vol. 30, American Mathematical Society, Providence, RI, 2005. MR2168892 (2006h:51001)

[Tch1852] P. L. Tchebycheff, *Report of the Extarordinary Professor of St Petersburg University Tchebycheff about the Trip Abroad*, Complete Collected Works, Vol. 5, AN SSSR, Moscow-Leningrad, 1946, 1852, pp. 246–255.

[Vee1969] W. A. Veech, *Strict ergodicity in zero dimensional dynamical systems and the Kronecker-Weyl theorem* mod 2, Trans. Amer. Math. Soc. **140** (1969), 1–33. MR0240056 (39 #1410)

[Vee1978] W. A. Veech, *Interval exchange transformations*, J. Analyse Math. **33** (1978), 222–272, DOI 10.1007/BF02790174. MR516048 (80e:28034)

[Ves1988] A. P. Veselov, *Integrable systems with discrete time, and difference operators* (Russian), Funktsional. Anal. i Prilozhen. **22** (1988), no. 2, 1–13, 96, DOI 10.1007/BF01077598; English transl., Funct. Anal. Appl. **22** (1988), no. 2, 83–93. MR947601 (90a:58081)

[Via2008] M. Viana, *Dynamics of interval exchange maps and Teichmüller flows*, 2008. lecture notes.

[WFS+2009] Y.-X. Wang, H. Fan, K.-J. Shi, C. Wang, K. Zhang, and Y. Zeng, *Full Poncelet Theorem in Minkowski dS and AdS Spaces*, Chinese Phys. Lett. **26** (2009), no. 1, 010201.

[Zor2006] A. Zorich, *Flat surfaces*, Frontiers in number theory, physics, and geometry. I, Springer, Berlin, 2006, pp. 437–583, DOI 10.1007/978-3-540-31347-2_13. MR2261104 (2007i:37070)

Department of Mathematical Sciences, University of Texas at Dallas, Dallas, Texas; Mathematical Institute SANU, Kneza Mihaila 36, Belgrade, Serbia

E-mail address: vladimir.dragovic@utdallas.edu

Mathematical Institute SANU, Kneza Mihaila 36, Belgrade, Serbia

E-mail address: milena@mi.sanu.ac.rs